

(200)
R290
NO. 90-560

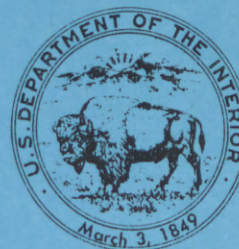
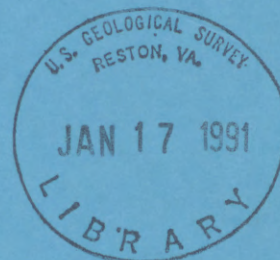
X

Conceptual Evaluation of Regional Ground-Water Flow in the Carbonate-Rock Province of the Great Basin, Nevada, Utah, and Adjacent States

U.S. GEOLOGICAL SURVEY

Open-File Report 90-560

*A product of the Regional
Aquifer-System Analysis for the
Great Basin*





Conceptual Evaluation of Regional Ground-Water Flow in the Carbonate-Rock Province of the Great Basin, Nevada, Utah, and Adjacent States

By Thomas J. Burbey and David E. Prudic

U.S. GEOLOGICAL SURVEY

Open-File Report 90-560

*A product of the Regional
Aquifer-System Analysis of the
Great Basin*



Carson City, Nevada
1991

DEPARTMENT OF THE INTERIOR

MANUEL LUJAN, JR., *Secretary*

U.S. GEOLOGICAL SURVEY

Dallas L. Peck, *Director*

Any use of trade, product, or firm names in this publication is for descriptive purposes only and does not constitute endorsement by the U.S. Government.

For additional information
write to:

U.S. Geological Survey
Room 227, Federal Building
705 North Plaza Street
Carson City, NV 89701

Copies of this report may be
purchased from:

U.S. Geological Survey
Books and Open-File Reports Section
Federal Center, Building 810
Box 25425
Denver, CO 80225

FOREWORD

This report will be published soon, in color, as U.S. Geological Survey Professional Paper 1409-D. Because of recently heightened interest in the regional hydrogeology of the Great Basin in southern and eastern Nevada, this interim open-file version, in black and white, is being released pending publication of the Professional Paper.

Carson City, Nevada
January 1991

CONTENTS

	Page		Page
Abstract	1	Simulation results—Continued	
Introduction	2	Correlation of simulated ground-water flow to regional geologic features	40
Purpose and scope	2	Distribution of flow into regions	47
Previous investigations	6	Flow regions	47
Description of the carbonate-rock province	7	Death Valley region	47
Physiography	7	Recharge	49
Climate	7	Discharge	49
Surface water	9	Flow systems	49
Acknowledgments	11	Simulation of alternative flow paths	54
Ground water in the carbonate-rock province	11	Colorado River region	56
Hydrogeology	11	Recharge	56
Occurrence and movement of ground water	13	Discharge	60
Conceptual evaluation of ground-water flow	15	White River subregion	60
General assumptions	15	Virgin River subregion	63
Model development	17	Las Vegas subregion	64
Application of finite-difference equations	17	Bonneville region	66
Model grid	17	Recharge	66
Representation as a two-layer system	19	Discharge	66
Boundary conditions	19	Description of subregions	66
Modeling approach	20	Sevier-Escalante subregion	66
Estimates of recharge	23	Fish Springs subregion	70
Initial estimates of transmissivity and leakance	27	Steptoe subregion	72
Model calibration	27	Great Salt Lake subregion	73
Algorithms used to calibrate model	27	Railroad Valley region	74
Limits of calibration	31	Upper Humboldt River region	78
Simulation results	36	Summary and conclusions	81
Computed transmissivities	36	References cited	85

ILLUSTRATIONS

	Page
FIGURE 1. Map showing location of the Great Basin and carbonate-rock province study areas	3
2. Map showing hydrographic areas	4
3. Diagram showing population growth in study area between 1900 and 1984	5
4. Map showing distribution of average annual precipitation	8
5. Map showing major rivers and lakes in the Great Basin study area	10
6. Geologic sections of Precambrian and Paleozoic rocks in carbonate-rock province study area	12
7. Map showing principal source areas for ground-water recharge, areas of evapotranspiration, and locations of regional springs	14
8. Map showing distribution of estimated ground-water withdrawals by hydrographic areas for 1975	16
9. Map showing finite-difference grid network	18
10. Diagram showing evapotranspiration and modified evapotranspiration functions incorporated into computer program	21
11-19. Maps showing:	
11. Regional spring discharge locations and discharge locations at general-head boundaries in relation to model grid	22
12. Locations where water-level measurements are available from wells tapping basin-fill deposits	24
13. Locations where water-level measurements are available from wells tapping consolidated rocks	25
14. Distribution of recharge in individual model cells and areas of recharge from general-head boundaries	26
15. Principal rock types in upper model layer and initially assigned transmissivity values	28
16. Simulated evapotranspiration rates	32
17. Distribution of observed evapotranspiration	33
18. Simulated steady-state water levels of upper and lower model layers	34
19. Computed transmissivities of upper and lower model layers	37

FIGURE 20. Histograms showing computed transmissivities in upper and lower model layers in relation to major rock types -----	Page 39
21-32. Maps showing:	
21. Selected geologic features and simulated water levels in upper and lower model layers, including areas of evapotranspiration and locations of regional springs -----	42
22. Outcrop areas of rocks that are potential barriers to ground-water flow, evapotranspiration, simulated water levels, and estimated flow regions in upper model layer -----	45
23. Metamorphic core complexes, subsurface magnetic source bodies, outcrop areas of rocks that are potential barriers to ground-water flow, distribution of regional springs, simulated water levels, and estimated flow regions in lower model layer -----	46
24. Distribution of simulated flow in areas having components of predominantly upward, downward, and horizontal flow -----	48
25. Areas of estimated recharge, simulated regional spring discharge, and simulated evapotranspiration in Death Valley region -----	50
26. Simulated flow-system boundaries, ground-water divides, and flow paths compared with those described in previous hydrologic studies for Death Valley region -----	51
27. Simulated ground-water flow paths in Colorado River region -----	57
28. Areas of estimated recharge, simulated regional spring discharge, and simulated evapotranspiration in Colorado River region -----	59
29. Areas of estimated recharge, simulated regional spring discharge, and simulated evapotranspiration in Bonneville region -----	67
30. Area boundaries and simulated ground-water flow directions in Bonneville region -----	69
31. Areas of estimated recharge and simulated regional spring discharge and evapotranspiration; approximate extent of Cortez rift; and simulated flow directions for Railroad Valley region -----	75
32. Areas of estimated recharge and simulated evapotranspiration, approximate extent of Cortez rift, and simulated flow directions in Upper Humboldt River region in relation to Humboldt River drainage basin -----	79

TABLES

TABLE		Page
1. Observed versus simulated spring discharge rates following calibration -----		30
2. Simulated ground-water flow budgets, Death Valley region -----		53
3. Simulated ground-water flow budgets, Colorado River region -----		58
4. Simulated ground-water flow budgets, Bonneville region -----		68
5. Simulated ground-water flow budget, Railroad Valley region -----		76
6. Simulated ground-water flow budget, Upper Humboldt River region -----		80
7. Simulated ground-water flow budgets of the five deep-flow regions -----		84

CONVERSION FACTORS AND ABBREVIATIONS

For readers who wish to convert measurements from the inch-pound system of units to the metric system of units, the conversion factors are listed below:

Multiply inch pound unit	By	To obtain metric units
acre-feet (acre-ft)	0.001233	cubic hectometers (hm ³)
acre-feet per year (acre-ft/yr)	0.001233	cubic hectometers per year (hm ³ /yr)
feet (ft)	0.3048	meters (m)
inches (in.)	25.40	millimeters (mm)
miles (mi)	1.609	kilometers (km)
square feet per second (ft ² /s)	0.0929	square meters per second (m ² /s)
square feet per day (ft ² /d)	0.0929	square meters per day (m ² /d)
square miles (mi ²)	2.590	square kilometers (km ²)

For temperature, degrees Fahrenheit (°F) may be converted to degrees Celsius (°C) by using the formula

$$^{\circ}\text{C} = 0.5556 (^{\circ}\text{F} - 32).$$

SEA LEVEL

In this report, "sea level" refers to the National Geodetic Vertical Datum of 1929 (NGVD of 1929)—a geodetic datum derived from a general adjustment of the first-order level net of both the United States and Canada, formerly called "Sea Level Datum of 1929."

CONCEPTUAL EVALUATION OF REGIONAL GROUND-WATER FLOW IN THE CARBONATE-ROCK PROVINCE OF THE GREAT BASIN, NEVADA, UTAH, AND ADJACENT STATES

By THOMAS J. BURBEY and DAVID E. PRUDIC

ABSTRACT

The carbonate-rock province of the Great Basin, mainly in eastern Nevada and western Utah, is characterized by a thick sequence of Paleozoic rocks. Beneath the carbonate rocks are Cambrian clastics and Precambrian basement rocks. Since deposition, however, compression, extension, intrusive and volcanic episodes, and erosion have greatly modified the distribution and thickness of the carbonate rocks and emplaced a variety of rocks and deposits within and above the carbonate rocks. The most notable features are the normal faults caused by Tertiary extension which have formed the north- to northeast-trending mountain ranges and adjacent basins that are partly filled with detritus from the mountains.

Ground-water flow in the province was conceptualized as relatively shallow flow, primarily through basin-fill deposits and adjacent mountain ranges, superimposed over deeper flow through carbonate rocks. A computer model was developed to simulate this concept. The province was divided into cells with dimensions of 5 miles by 7.5 miles containing two model layers. The upper model layer was used to simulate flow primarily through basin-fill deposits and adjacent mountain ranges to depths of several thousand feet. The lower model layer was used to simulate deep flow beneath the basin fill and mountain ranges. The actual depth to the base of deep flow is unknown. The carbonate rocks may be as much as 30,000 feet thick, and freshwater has been detected to depths of as much as 10,000 feet.

Several simplifying and necessary assumptions were made during the conceptualization and simulation of ground-water flow in the province: (1) Flow through fractures and solution openings in consolidated rocks is approximately equivalent to flow through a porous medium; (2) Darcy's Law is applicable from a regional perspective; (3) ground-water flow is in a state of equilibrium where recharge equals discharge (prior to ground-water withdrawals), and most of the recharge occurs in or near the mountain ranges; (4) areal distribution of discharge is known as well as amount of discharge from regional springs; and (5) transmissivity is homogeneous and isotropic for an area that is represented by a model cell. Although the assumptions are probably valid for parts of the province, the validity of each assumption is unknown for its entirety. Therefore, the model results should be interpreted with caution and are considered to be conceptual.

Transmissivity values in both model layers and vertical leakage between layers were adjusted during repeated simulations until computed water levels approximated the general water-level trends that were interpolated and extrapolated from measured water levels, and areas of simulated discharge approximated areas of known

discharge. Because the amount of recharge and discharge are only approximately known and because water-level data are not available for large parts of the area, the computed transmissivity and leakage values are at best approximate. Nonetheless, several inferences can be made regarding flow in the province.

Model-derived fluxes indicate that flow in the lower model layer can be divided into five deep-flow regions. These regions are named the (1) Death Valley, (2) Colorado River, (3) Bonneville, (4) Railroad Valley, and (5) Upper Humboldt River regions after the terminal sink for deep ground-water flow in each region. Superimposed over the 5 deep-flow regions are 17 shallow-flow regions as determined from model derived fluxes in the upper model layer. These regions approximately coincide with the delineations of flow systems from topography, water-level data, discharge areas, and water budgets.

In general, the simulation of flow in the eastern and northern parts of the province is from south to north toward the Great Salt Lake Desert (Bonneville region) and the Humboldt River; elsewhere, flows are north to south toward either Death Valley or the Virgin and Colorado Rivers.

Most of the ground-water discharge in the model simulation is due to evapotranspiration or springs prior to reaching the terminal sinks, particularly in the Colorado River region. This is probably due to low-permeability rocks and (or) basin fill within the area of the sinks. The estimate of recharge, as well as discharge, within the carbonate-rock province is 1.6 million acre-feet per year, which is about 3 percent of the estimated total precipitation. If local flow were included, the estimates of recharge and discharge would be considerably more.

The transmissivity and leakage values were determined independently of the geology but are based on limited water-level data and the distribution and amount of recharge and discharge. However, simulation of flow in the upper model layer is generally away from or around outcrop areas of intrusive rocks, ancient volcanoes, Precambrian basement rocks, and fine-grained basin-fill deposits. Flow in the lower model layer is generally diverted around inferred low-permeability barriers as interpreted from aeromagnetic anomalies. Such anomalies may represent Precambrian basement rocks or granitic intrusions.

Although the model simulation is entirely conceptual, this report presents estimates of the direction and magnitude of flow from recharge to discharge areas and discusses where the results agree and disagree with hypotheses and hydrologic estimates reported by other investigators.

INTRODUCTION

Ground-water flow within an area dominated by basin-fill and carbonate-rock aquifers in western Utah and eastern Nevada and small parts of Arizona, California, and Idaho was studied as part of the Great Basin Regional Aquifer-System Analysis (RASA) project. The Great Basin RASA project began in 1980 as part of a national program designed to evaluate the Nation's aquifer systems at a regional scale (Harrill and others, 1983). The primary reason for the Great Basin RASA project is an increased demand for water in an area that has limited water supplies. The increased demand for water is caused by (1) an increase in the number of people living within or near the Great Basin, (2) an increase in irrigated cropland, and (3) a number of large coal-fired powerplants that are being built or are planned to be built. Also, parts of the study area are used for underground testing of nuclear weapons and potentially for disposal and storage of nuclear and hazardous wastes. A better understanding of regional flow throughout the study area is needed to manage and develop the ground-water resource in the area.

This report presents a concept of regional ground-water flow in the carbonate-rock province of the Great Basin. Additional results of the Great Basin RASA project are described in other chapters of Professional Paper 1409 and include detailed simulations of ground-water flow in selected basins, and analyses of regional hydrogeology and geochemistry.

The area of the Great Basin RASA project is about 140,000 mi² and includes most of Nevada, the western half of Utah, and parts of California, Oregon, Idaho, and Arizona (fig. 1). Most of the ground water pumped is from unconsolidated deposits that partly fill each of the 240 hydrographic areas (Harrill and others, 1983), most of which are topographically closed or nearly closed basins (fig. 2). Most of the hydrographic areas contain a ground-water reservoir in the unconsolidated basin-fill deposits and include the drainage area of adjacent mountains. These hydrographic areas are used by State and local agencies for planning and management of water resources.

The eastern two-thirds of the Great Basin is underlain by thick sequences of Paleozoic carbonate rocks which were deposited in a shallow marine environment. The area is defined in this report as the carbonate-rock province of the Great Basin and is bounded on the east, south, and north by boundaries of the Great Basin RASA project (Harrill and others, 1983; and fig. 1). These boundaries include the Wasatch Range and the Colorado Plateau to the east, the Snake River drainage divide to the north, and the

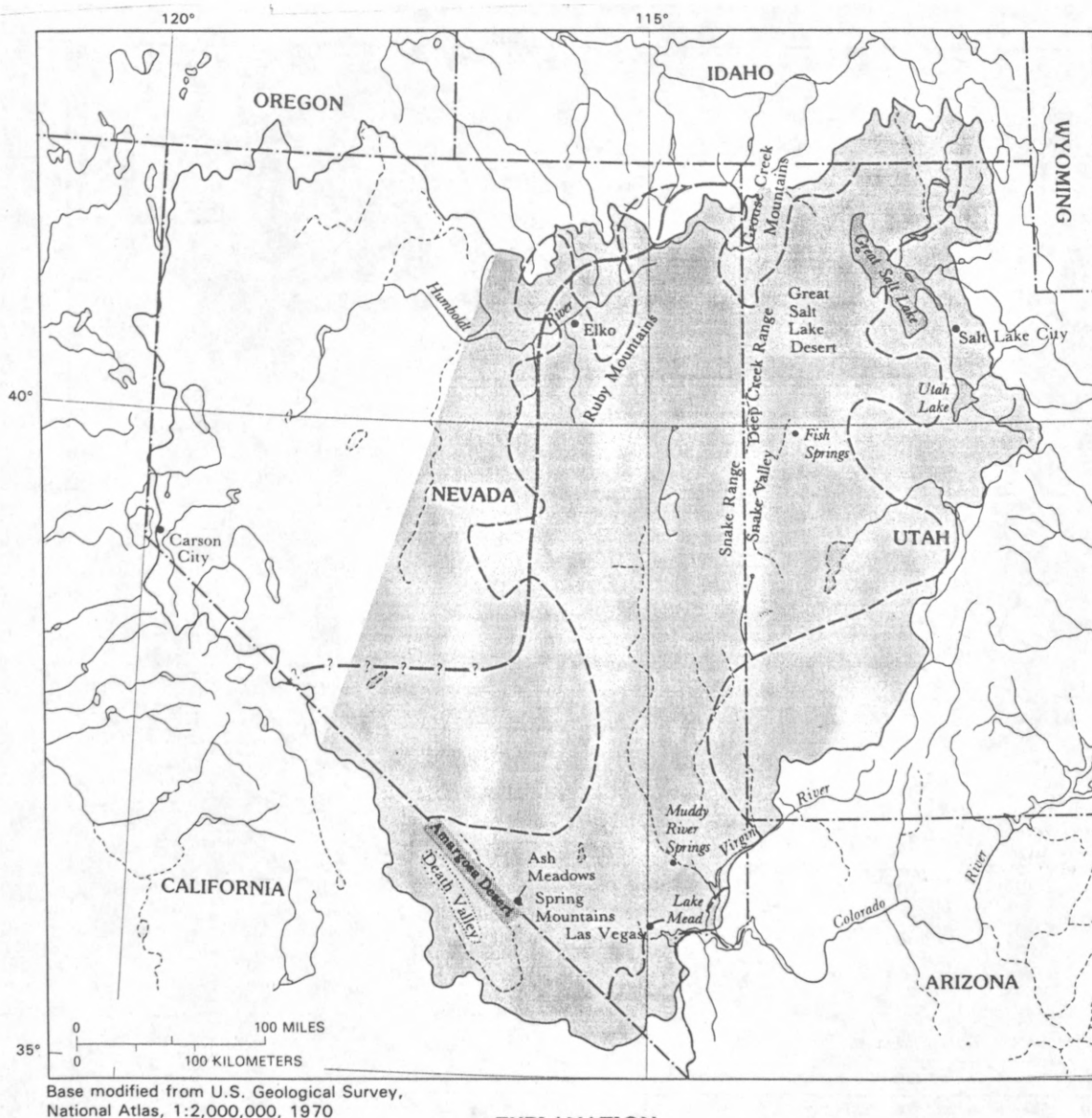
predominantly Precambrian rock exposures in the mountains to the south. The southern boundary also includes hydrologic boundaries of the Virgin and Colorado Rivers and Death Valley (fig. 1). The western boundary is generally the eastern extent of transitional assemblages of rocks as defined by Stewart and Carlson (1978). These rocks separate the Paleozoic carbonate rocks to the east from fine-grained marine sedimentary and volcanic rocks that were deposited in a deep ocean basin to the west. The province covers an area of about 100,000 mi².

Population in the province is about 2.1 million as of 1984 (U.S. Department of Commerce, 1985). Most of these people live along the eastern border where perennial streams flow from the Wasatch Range into the adjacent valleys, or near other sources of surface water such as the Humboldt River and Lake Mead (fig. 1). More than one-half million people live in the Las Vegas metropolitan area, and more than a million people live in the vicinity of Salt Lake City. Population densities averaged over counties range from 2 to 900 people per square mile in Utah and from 3 people every 10 square miles to 68 people per square mile in Nevada.

Population in the province at the turn of the last century was less than 300,000 (fig. 3), and most of the people lived in the vicinity of Salt Lake City where surface-water supplies are plentiful. The number of people living in the province increased slowly until after World War II. Since World War II, the population has increased fivefold. The marked increase in the number of people living in Nevada (fig. 3) is largely in the Las Vegas area, where the population increased from about 16,000 people in 1940 to more than 550,000 in 1984. As the number of people in the province increases and surface-water supplies become less available, additional sources of water will be needed. One such source that has been proposed (Hess and Mifflin, 1978) is the water stored in the carbonate rocks beneath much of western Utah and eastern Nevada.

PURPOSE AND SCOPE

The purpose of this report is to describe a conceptual evaluation of ground-water flow in the carbonate-rock province, mainly in Nevada and Utah. In most other RASA studies, enough information existed to allow for comprehensive model simulations and evaluations of ground-water flow in regional aquifer systems. Although numerous wells have been drilled within the carbonate-rock province, most have been drilled into unconsolidated deposits in the valleys and usually to shallow depths, except at the Nevada Test

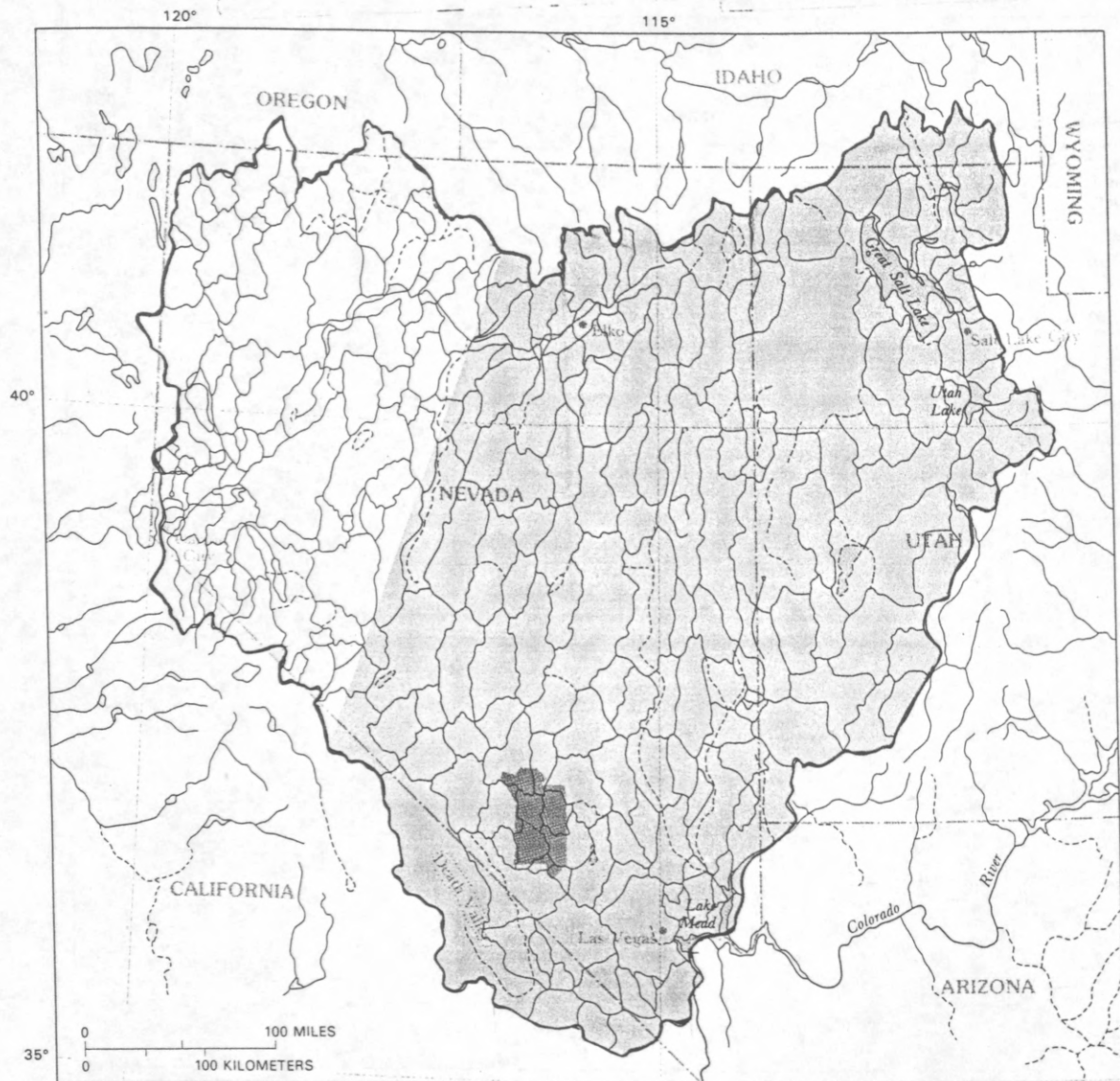


EXPLANATION

- Carbonate-rock province study area— Approximately shown
- Boundary of Great Basin Regional Aquifer-System Analysis (RASA) study area
- Approximate boundary of carbonate-rock province—80 percent of measured sections are composed of more than 50 percent carbonate rock (from Mifflin and Hess, 1979)
- Approximate boundary of Roberts overthrust belt— Queried where uncertain

Note: Lakes and rivers dashed where ephemeral

FIGURE 1.--Location of Great Basin Regional Aquifer-System Analysis (RASA) study area, and general extent and geographic features of carbonate-rock province study area.



Base modified from U.S. Geological Survey,
National Atlas, 1:2,000,000, 1970

EXPLANATION

- Carbonate-rock province study area—Approximately shown
- Nevada Test Site
- Boundary of Great Basin Regional Aquifer-System Analysis study area
- Boundary of hydrographic areas—Dashed where uncertain

Note: Lakes and rivers dashed where ephemeral

FIGURE 2.—Hydrographic areas and location of Nevada Test Site. Names of hydrographic areas in Harrill and others (1983, pl.1).

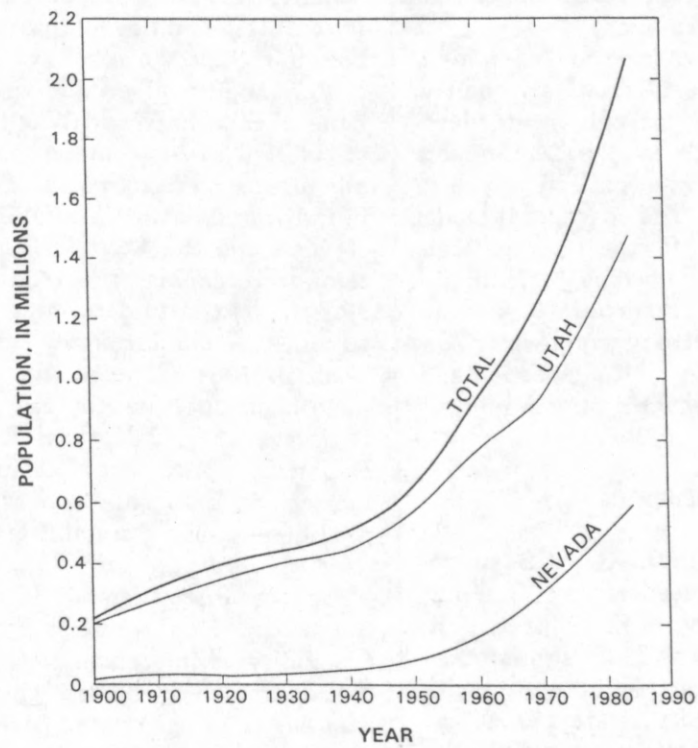


FIGURE 3.--Population growth in study area between 1900 and 1984. Data sources: 1900-83, U.S. Bureau of the Census (1913, 1922, 1952, 1983, 1985) and U.S. Bureau of the Census (written commun., 1985).

Site. Thus, little is known about the deeper and more regional ground-water flow in the carbonate rocks, but because of a greatly increased demand for water and a potential for disposal of nuclear wastes at the Nevada Test Site (fig. 2), an improved understanding of ground-water flow in the province is needed. Therefore, the main objective in this study was to develop a three-dimensional, conceptual model that incorporated the available information.

The simulation technique was used to determine if ground-water flow between the 17 relatively shallow flow systems delineated from topography, water-level measurements, discharge areas, and water budgets (Harrill and others, 1988) could be connected by deep flow through carbonate rocks. The conceptual model was also used to evaluate the effect of large geologic features—such as large intrusive bodies, regional lineaments and faults, and metamorphic core complexes—on water levels and inferred ground-water flow and to provide general estimates of the direction and magnitude of ground-water flow within the province.

PREVIOUS INVESTIGATIONS

Surveys of geologic features in the Great Basin began in the late 1860's under the leadership of Clarence King and J.W. Powell, and by G.K. Gilbert, A.R. Morvine, and E.E. Howell. Nolan (1943) summarized available geologic information pertaining to the entire Great Basin. Between 1938 and the late 1970's, numerous geologic investigations were completed in the Great Basin region. The results of all these studies and studies before 1938 are summarized on a map of Nevada by Stewart and Carlson (1978), a publication about Nevada by Stewart (1980), and a map of Utah by Hintze (1973). Since 1980, numerous articles have been published that pertain generally to metamorphic core complexes, geophysics, and geologic structure. The hydrogeologic framework of the Great Basin has been described by Russell W. Plume (U.S. Geological Survey, written commun., 1985) as another part of the Great Basin RASA project and is the primary source of geologic information used in this study.

Ground-water investigations within the carbonate-rock province began in the early 1900's. Mendenhall (1909, p. 13) suggested that many of the desert springs in southern Nevada were not dependent on rainfall in the area immediately surrounding the springs but had their source in ground water from distant mountains. Carpenter (1915, p. 18) noted that rocks exposed in the mountains in southeastern Nevada generally act to close the adjacent valleys by making the sides and bottoms of the valleys practically impervious. He did,

however, state that several topographically closed valleys higher in altitude than adjacent valleys lost water through fissures in the rocks because water levels in the higher valleys were far below land surface. Meinzer (1917, p. 150) reported that water from a valley near Tonopah, Nev. (fig. 1), leaked through a mountain range into an adjacent valley. These are some of the earliest reports that suggest the possibility of interbasin flow of ground water within the carbonate-rock province.

Few additional ground-water investigations were done until after World War II, when several studies of selected basins commenced. These studies generally focused on recharge and discharge of ground water in individual basins. In the early 1960's, the State of Nevada and the U.S. Geological Survey began systematic reconnaissance studies of all unstudied basins in Nevada to determine potential ground-water supplies. A similar series of investigations began in Utah in 1964. The results of these investigations have been published by the Nevada Department of Conservation and Natural Resources and the Utah Department of Natural Resources, and most are summarized in Eakin and others (1976). These reports provide the basic estimates of recharge and discharge used in this report.

Detailed discussion of interbasin flow also began in the 1960's. Hunt and Robinson (1960) discussed the possibility of interbasin flow into the Death Valley (fig. 1) area on the basis of chemical analysis of water samples from springs and wells. Loeltz (1960) discussed the source of water issuing from springs at Ash Meadows in the Amargosa Desert near Death Valley (fig. 1). Winograd (1962) discussed interbasin movement of ground water at the Nevada Test site. Winograd (1963) also summarized the ground-water hydrology of the area between Las Vegas Valley and the Amargosa Desert and discussed fault compartmentalization of the aquifers in the region. Eakin and Moore (1964) presented information about the uniformity of discharge at Muddy River springs in southeastern Nevada and related it to interbasin movement of ground water (fig. 1). Winograd and Eakin (1965) and Eakin and Winograd (1965) presented evidence and some economic implications of interbasin flow of ground water in south-central Nevada. Hood and Rush (1965) discussed the possibility of interbasin flow of water to and from Snake Valley (fig. 1) in western Utah. Eakin (1966) presented information that described interbasin flow in an area in southeastern Nevada that he named the White River area. Shortly afterward, Mifflin (1968) delineated ground-water basins for all Nevada, and concluded that interbasin flow of ground water

occurred wherever the consolidated rocks in the mountains and beneath the valleys were permeable or wherever the basins were connected by unconsolidated deposits. The area of interbasin flow through permeable consolidated rocks was primarily within the carbonate-rock province. Mifflin and Hess (1979) discussed regional carbonate flow systems in Nevada. Gates and Krueger (1981) discussed regional flow in west-central Utah, and Gates (1984) discussed regional flow in northwestern Utah and adjacent parts of Idaho and Nevada.

The U.S. Geological Survey began a study in 1981 to evaluate potential hydrogeologic environments for isolation of high-level radioactive waste in the Basin and Range physiographic province of the southwestern United States. The study includes a much larger area than is described in this report. Bedinger and others (1989, 1990) characterized the geology and hydrology of the Death Valley region and the Bonneville region; both areas are included in this study.

The most detailed information regarding ground-water flow in carbonate rocks is at the Nevada Test Site (fig. 2). Detailed studies began in 1957 and included the drilling of several deep test holes into carbonate rocks beneath the unconsolidated and volcanic deposits in the vicinity of the Test Site during 1962–64. Numerous reports have been written about the area. Most of the work from 1957–64 is summarized by Winograd and Thordarson (1975), which is the most detailed description of ground-water flow through carbonate rocks in the province. Some of the more recent reports that pertain to ground-water flow near the Test Site include Winograd and Pearson (1976), Waddell (1982), Claassen (1983), and Waddell and others (1984).

In addition to test wells drilled for nuclear testing, many wells were drilled in the province for other purposes, including several into carbonate rocks as part of the U.S. Air Force's MX missile-siting program in the Great Basin. Data from these wells and related studies by the contractor ERTEC, Inc. (or Earth Technology, Inc., formerly FUGRO) were very useful in this study. Selected hydrologic data collected for the Air Force were presented by Bunch and Harrill (1984). More recently, geochemical interpretations by Alan H. Welch and James M. Thomas (U.S. Geological Survey, written commun., 1986) of analyses of water samples collected from selected wells, regional springs, and high-altitude springs as part of the Great Basin RASA project provided additional evidence of interbasin flow in the White River area. Also, as part of the Great Basin RASA project, regional ground-water flow in the vicinity of Fish Springs (fig. 1) in western Utah was simulated by Carlton (1985).

DESCRIPTION OF THE CARBONATE-ROCK PROVINCE

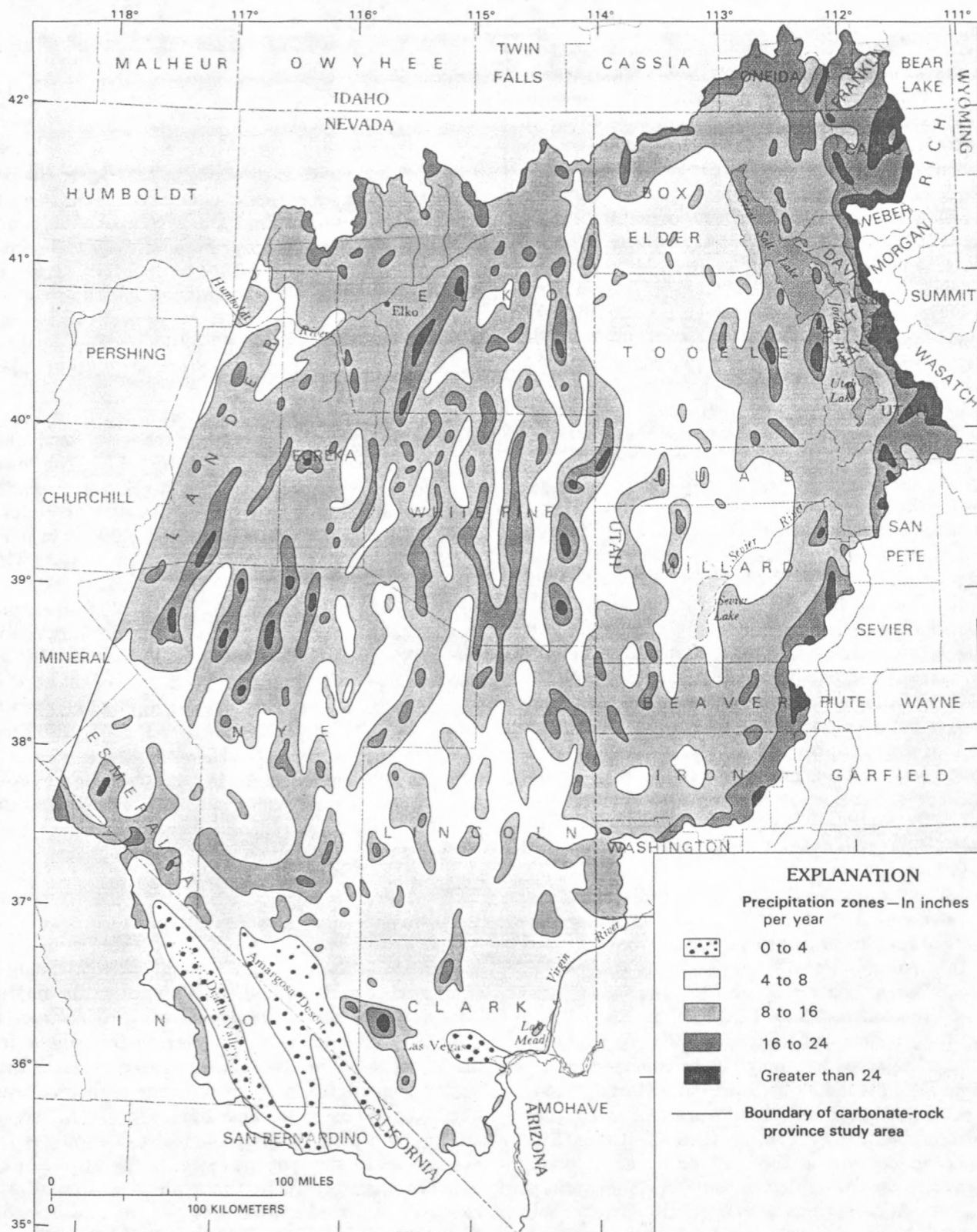
PHYSIOGRAPHY

The carbonate-rock province of the Great Basin is characterized by a series of generally north- to north-east-trending mountain ranges composed predominantly of carbonate rocks of Paleozoic age. The intervening valleys are partly filled with detritus from the mountains. Both the mountain ranges and the valleys are generally 5 to 15 mi wide and are typically elongate, commonly 40 to 80 mi long. The mountain ranges rise from 1,000 to more than 7,000 ft above the adjacent valleys.

Altitudes of valley floors in the southern part of the province range from below sea level to 3,000 ft above sea level. Death Valley (fig. 1) is the lowest point in the province, as well as the Nation, and at its lowest point is 282 ft below sea level. Altitudes of valley floors in the province exceed 6,000 ft in north-central Nevada, while valley floors in western Utah are between 4,000 and 5,000 ft. Several of the mountain ranges in the province exceed 10,000 ft in altitude. The highest mountains in the southern part are the Spring Mountains west of Las Vegas with altitudes exceeding 11,000 ft. The Ruby Mountains in northern Nevada exceed 12,000 ft, but the highest point in the province, at 13,063 ft, is Wheeler Peak in the Snake Range (fig. 1), which is in Nevada near the border of Utah. The Wasatch Range in Utah, which has several peaks that exceed 11,000 ft, forms the eastern boundary of the study area.

CLIMATE

Climate in the province is highly variable, ranging from arid to semiarid on most of the valley floors to humid alpine in the higher mountains. Average annual precipitation on the valley floors ranges from less than 3 in. in the Amargosa Desert and Death Valley to about 16 in. in some of the higher valleys in north-central Nevada and northern Utah. Average annual precipitation in the mountains ranges from about 8 in. in some of the lower southern mountains to more than 60 in. in the higher reaches of some ranges. Estimated annual precipitation in the province is shown in figure 4. Based on the map, about 54 million acre-ft of precipitation annually falls in the province. The regionally averaged annual precipitation for the province is less than 10 in., making it one of the drier regions in the United States.



Base modified from U.S. Geological Survey,
National Atlas, 1:2,000,000, 1970

FIGURE 4.--Distribution of average annual precipitation. Precipitation zones for Nevada from Hardman (1965); zones for Utah and Idaho from U.S. Weather Bureau (1963 and 1965, respectively); zones for California from Rantz (1972). Precipitation zones near Death Valley and Amargosa Desert modified from Winograd and Thordarson (1975, p. 8).

Houghton (1967) reported three sources of precipitation that falls in the province: (1) moisture from the Pacific Ocean, (2) moisture from the Gulf of Mexico, and (3) moisture evaporated within the Great Basin. Much of the precipitation occurs between October and May from storm fronts that begin in the subpolar North Pacific Ocean. Generally, these storm fronts are much less frequent in the southern part than in the northern part of the province (north of latitude 40°). However, unusually heavy amounts of precipitation from Pacific storms can occur in the southern part of the province (south of latitude 40°) when secondary lows develop south of the subpolar fronts and move inland.

Houghton (1967) also suggested that precipitation from moisture which moves inland from the Gulf of Mexico occurs only during the summer, when southeasterly winds carry moist tropical air into the southern and eastern parts of the province and produce scattered convective showers. More recent information (Brenner, 1974) suggests that these convective showers are from moisture which moves northward from the Gulf of California along the Colorado River and that no precipitation is derived from the Gulf of Mexico. In addition, the source of most of the precipitation in the southern part of the province is from tropical storms that originate in the Pacific Ocean near Central America. These storms generally move out to sea but occasionally move inland near northern Mexico and southern California and dissipate over Arizona, southern Nevada, and Utah (K.P. Smith, University of Arizona, Tucson, oral commun., 1986). The storms are most common from late August to November but do not necessarily occur every year.

Precipitation from water evaporated over the Great Basin is associated with surface cyclones (Houghton, 1967, p. 6) that usually develop in the spring and fall. The storms are most frequent from March until mid-June and gradually shift from south to north but generally provide little moisture.

Average annual temperature ranges from about 30 °F in some high northern valleys to about 60 °F in the extreme southern valleys (Eakin and others, 1976, p. 3). Temperatures are subject to large daily and seasonal fluctuations. Daily fluctuations in most valleys exceed 30 °F, and 40 °F changes are not uncommon. Large variations in temperature also occur within short distances due to the topography. Maximum summer temperatures can exceed 100 °F, particularly in the south, where the maximum summer temperatures can reach 120 °F. Minimum temperatures can drop below 0 °F in the northern part of the province.

Average annual humidity ranges from about 30 to 40 percent over most of the region and is about 20

percent in the extreme south. Low humidity, abundant sunshine, and light to moderate winds result in rapid evaporation. Average annual lake evaporation ranges from about 45 in. in the north to more than 90 in. in the extreme south (Kohler and others, 1959).

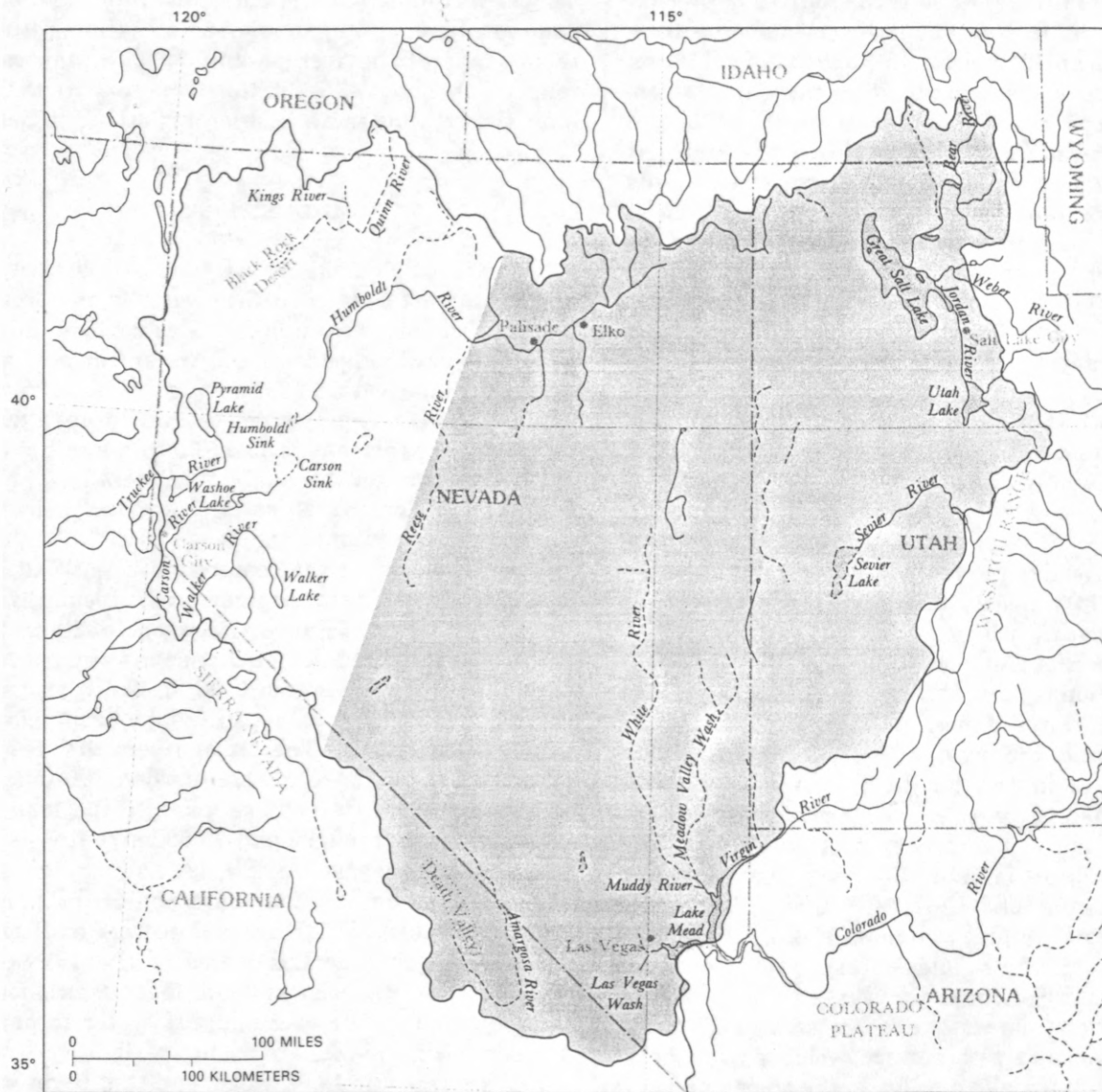
SURFACE WATER

The Great Salt Lake in northwestern Utah is areally the largest body of surface water in the province (fig. 5). The size of the lake varies considerably depending on the altitude of the water surface in the lake, which has varied 20 ft during the last 125 years (Arnow, 1984). The average size of the lake during the past 125 years has been 1,700 mi², and the average lake volume has been 16 million acre-ft. The lake is unique in North America in that it is considerably saltier than the oceans.

Most of the water that enters the Great Salt Lake is surface runoff that originates as precipitation in the nearby Wasatch Range. Between 1931 and 1976, the lake experienced no net change in volume. About 1.9 million acre-ft out of a total of about 2.9 million acre-ft of water that entered the lake each year was from surface runoff. The major rivers that feed the lake are the Bear, Weber, and Jordan. Another 0.9 million acre-ft of water is supplied to the lake from precipitation on the lake and 75,000 acre-ft/yr is from ground-water seepage (Arnow, 1984).

Lake Mead borders the south end of the province and was formed after Hoover Dam was built on the Colorado River near Las Vegas in the 1930's. The initial storage capacity of Lake Mead was about 31 million acre-ft. The lake supplies water to parts of Nevada, California, and Arizona. Tributary streams that discharge into Lake Mead, and that begin within or border the province, include (1) the Virgin River, which borders the southeastern edge of the province, (2) the Muddy River, which begins at the Muddy River springs about 50 mi northwest of Lake Mead, and (3) Las Vegas Wash, which discharges water from Las Vegas Valley.

In addition to the rivers and streams that drain into the Great Salt Lake and Lake Mead, a few other river systems either head within the province or enter it from bordering mountains and discharge into terminal sinks. The Sevier River drains several high-altitude basins along the western margin of the Colorado Plateau and discharges into ephemeral Sevier Lake (fig. 5). Its average annual discharge near where the river enters the province is about 180,000 acre-ft over the past 72 years (ReMillard and others, 1986, p. 378). The Humboldt River heads in northeastern



EXPLANATION

- Carbonate-rock province study area— Approximately shown
- Boundary of Great Basin Regional Aquifer-System Analysis (RASA) study area

Note: Lakes and rivers dashed where ephemeral

FIGURE 5.—Distribution of major rivers and lakes in the Great Basin Regional Aquifer-System Analysis study area.

Nevada, flows westward, and exits the province near Palisade (fig. 5) on its way to the Humboldt and Carson Sinks. The average annual flow near Palisades has been about 290,000 acre-ft for the past 78 years (Frisbie and others, 1985, p. 134). The Amargosa River is ephemeral over most of its course. The Amargosa River heads in southwestern Nevada (fig. 5) and flows south, east, and then north again on its way to Death Valley, which is the terminus for both surface- and ground-water flow in southwestern Nevada and southeastern California.

Streams are considerably less common within the interior of the province, however, than over the rest of the Great Basin (fig. 5), suggesting that the carbonate rocks exposed in the mountains allow for more recharge into and through the mountain blocks than do other types of rocks.

ACKNOWLEDGMENTS

We give special thanks to Russell W. Plume who provided his interpretations to the hydrogeology and who, along with Michael D. Dettinger and James R. Harrill, helped define the regional geologic features that may affect ground-water flow in the province. We also thank the numerous students who assisted in the initial compilation of the data.

GROUND WATER IN THE CARBONATE-ROCK PROVINCE

A detailed discussion of the hydrogeology in the Great Basin, which includes the study area, is presented in a companion report by Russell W. Plume (U.S. Geological Survey, written commun., 1985). A brief description of the rocks in the province and their water-transmitting properties is presented in the following section and provides a basis for understanding the occurrence and movement of ground water within the carbonate-rock province.

HYDROGEOLOGY

The geologic features of the province are very complex and involve rocks that range in age from Precambrian to Holocene. Its history includes major episodes of sedimentation, volcanic activity, and tectonic deformation by both compressional and extensional forces.

The oldest exposed rocks are Precambrian in age and consist mostly of gneiss, schist, and granitic rocks. The province is part of an area in which marine sedi-

ments accumulated in a shallow sea near the margin of western North America (referred to as the miogeosynclinal belt of the Cordilleran geosyncline) from late Precambrian time through the Paleozoic Era and into the early Mesozoic Era. During that period, more than 30,000 ft of marine sedimentary rocks accumulated in parts of the province. These rocks include sequences of clastic rocks that are mostly sandstone, quartzite, and shale, and carbonate rocks that are mostly limestone and dolomite. Rocks of late Precambrian to Middle Cambrian age are dominantly clastic, and those of Middle Cambrian to early Mesozoic age are dominantly carbonates. The thickness of carbonate rocks varies within the province. The general distribution of clastic and carbonate rocks from late Precambrian to early Mesozoic age are shown in two geologic sections through the middle of the province (fig. 6).

Beginning in Mesozoic time, the environment of deposition of the rocks changed from marine to continental. Rocks of this period include (1) shale, sandstone, and conglomerate and lesser amounts of freshwater limestone and evaporite that range in age from Middle Triassic to middle or late Tertiary; (2) volcanic rocks of middle Tertiary to Quaternary age that range in composition from basalt to rhyolite; (3) intrusive rocks of Jurassic to Tertiary age that are predominantly granodiorite and quartz monzonite; and (4) since about middle Miocene time, clastic deposits, referred to as basin fill, that consist of unsorted to well-sorted clay, silt, sand, gravel, and boulders.

Geologic structure in the province is complex. Thrust faulting during the Paleozoic and Mesozoic Eras superimposed older rocks on top of younger rocks. Extensional (normal) faulting since about middle Miocene time formed the north-south-trending mountains and basins that are characteristic of the entire Great Basin. Strike-slip faults found in parts of the Great Basin add to the structural complexity of the region and probably are directly associated with compressive and extensional events. Wernicke and others (1984) suggested that the strike-slip faults are mostly related to extension. Estimates of their age range from Early Jurassic to late Tertiary (Stewart, 1980, p. 86). Two major sets of strike-slip faults are present in the province: right-lateral faults in southwestern Nevada and southeastern California that form a zone referred to as the Walker belt (Stewart, p. 86), and left-lateral faults in southern and southeastern Nevada (Stewart and Carlson, 1978).

Isolated complexes of metamorphic rocks of possible Mesozoic age (termed metamorphic core complexes by Coney, 1980) have been identified at four locations in the province: the Ruby Mountains just south of Elko, the Snake Range east of Ely, the Deep

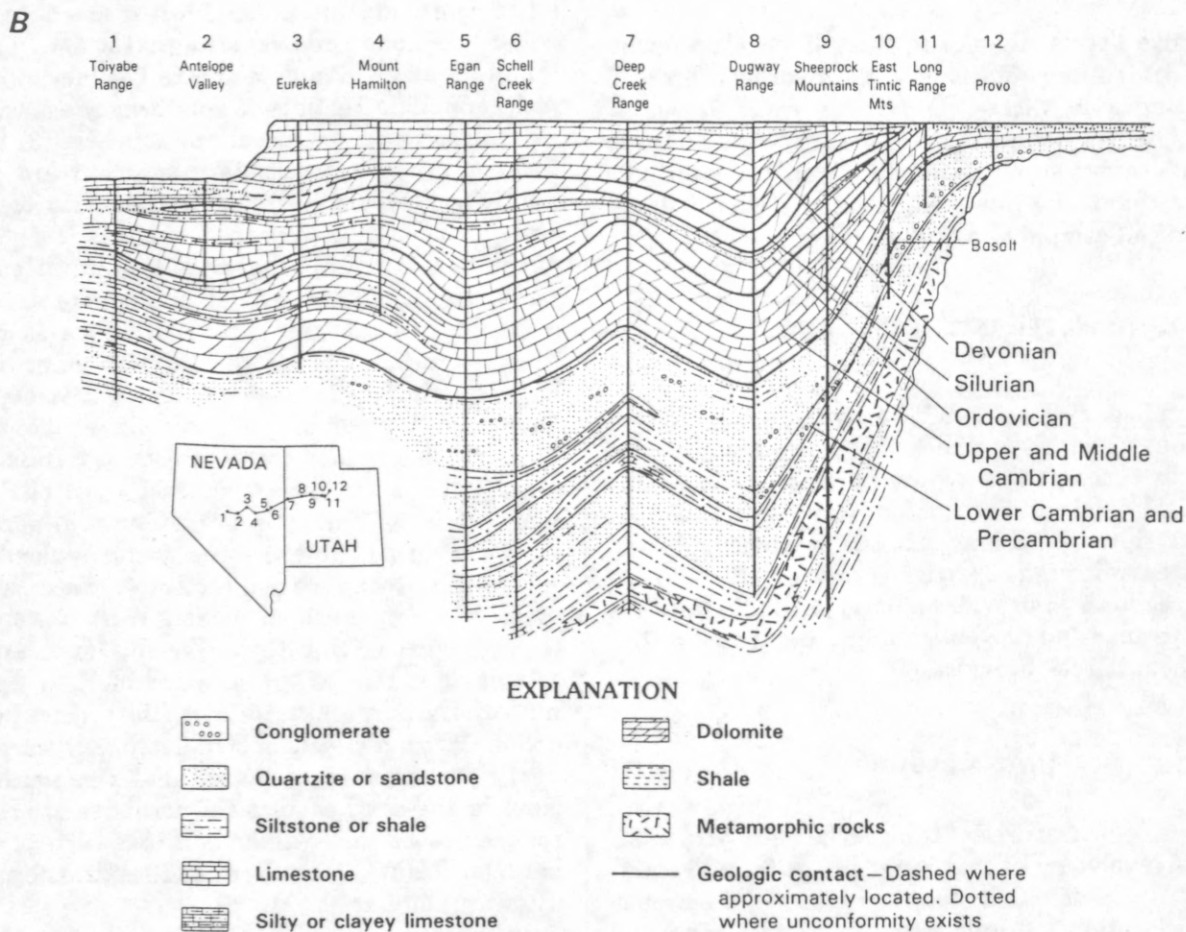
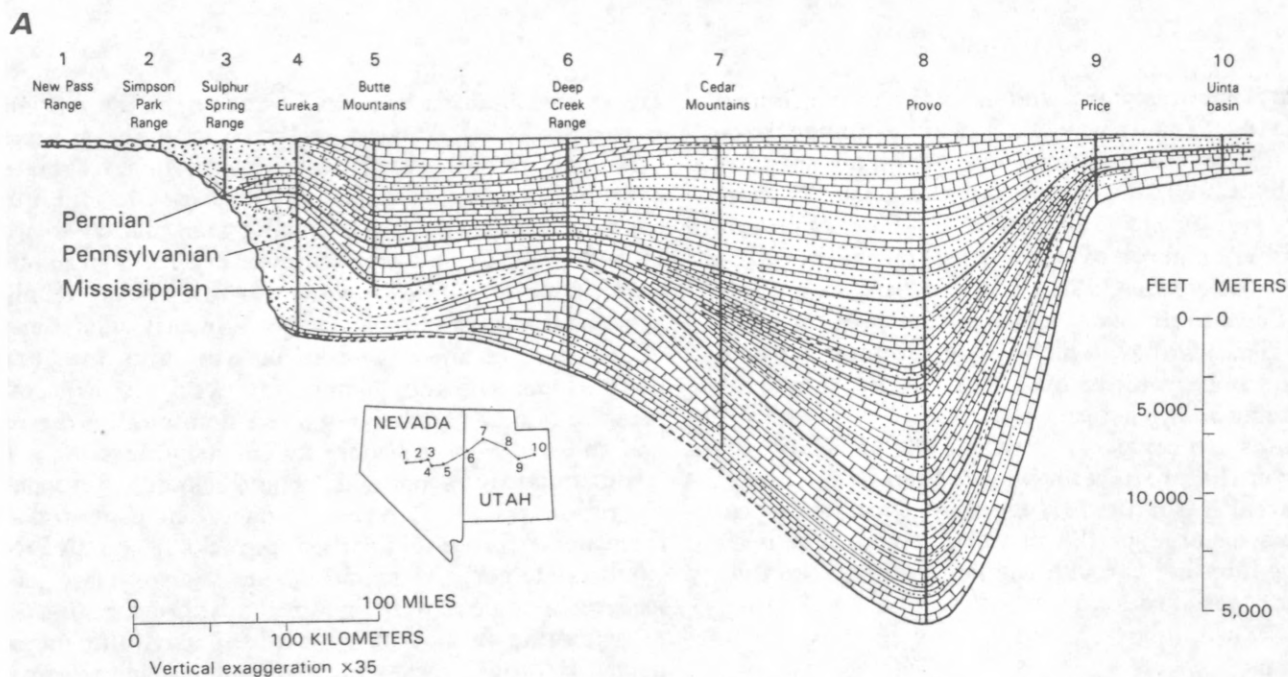


FIGURE 6.--Geologic sections of Precambrian and Paleozoic rocks in carbonate-rock (from Stewart, 1980, figs. 10 and 25). A, Northern section of Mississippian through Permian rocks. B, Southern section of Precambrian through Devonian rocks.

Creek Range north of the Snake Range, and the Grouse Creek Mountains in northwestern Utah at the northern boundary of the Great Basin with the Snake River drainage (fig. 1). The complexes generally consist of a mobile metamorphic-plutonic basement terrane, overlain by unmetamorphosed rocks that are deformed by low-angle extensional faults. The two zones are separated by a decollement which is a surface of dislocation (Coney, 1980, p. 15). Such complexes probably act as barriers to deep ground-water flow.

The depositional thickness and lithology of the Paleozoic sedimentary rocks are notable in their homogeneity over large areas in the province. Since deposition, however, compression, extension, intrusive and volcanic episodes, and erosion have greatly modified their distribution and thickness. The actual thickness and distribution of the various rock types at depth are not well known because the region is structurally complex and because granitic rocks are more extensive at depth than indicated by outcrops. Thus, geophysical techniques were used to delineate the possible extent of intrusive bodies at depth and to infer the relative thickness of Paleozoic and younger rocks within the province. Aeromagnetic data were analyzed to delineate the extent of intrusive bodies and near-surface basement rock which may act as barriers to regional ground-water flow. The techniques used to analyze the aeromagnetic data are presented by Plume (1984).

In addition to the analyses of aeromagnetic data by Plume, regional gravity maps by Hildenbrand and Kucks (1982) and Saltus (1984) that include the carbonate-rock province were used to infer areas where changes in gravity might reflect changes in the relative thickness of rocks younger than the Precambrian basement. For example, near the south end of the province a large gravity gradient exists, which might suggest that the depth to Precambrian basement is much less or the rocks are more dense than in surrounding areas. This gradient is referred to as the Transverse Crustal Boundary (Eaton, 1975; Eaton and others, 1978). The possible effects of major structures and changes in rock types on ground-water flow within the province are discussed in detail in the section "Correlation of Simulated Ground-Water Flow to Regional Geologic Features."

OCCURRENCE AND MOVEMENT OF GROUND WATER

Ground water occurs in all the types of rocks in the province. The basin-fill deposits are the primary ground-water reservoirs. Most of the water pumped from wells is from these deposits. Carbonate rocks that underlie much of the study area are also signifi-

cant ground-water reservoirs, particularly where the rocks are fractured or where openings have been enlarged by dissolution. Most of the larger springs in the area issue from carbonate rocks or from basin-fill deposits overlying or adjacent to carbonate rocks. The other types of consolidated rocks and the fine-grained basin-fill deposits generally transmit only small quantities of water and act as barriers to ground-water flow. However, there are some exceptions to this generalization. Some volcanic rocks, namely basalts and welded tuffs, can yield significant amounts of water to wells where the rocks are fractured over relatively large areas. Winograd (1971) discussed the welded tuffs as aquifers in the vicinity of the Nevada Test Site and in parts of Idaho. The welded tuffs are not as extensive as the basin-fill deposits or the carbonate rocks but where present could allow for the interbasin movement of ground water. The Precambrian and Lower Cambrian clastic, metamorphic, and granitic rocks beneath the carbonate rocks are relatively impermeable and probably provide a lower limit to ground-water circulation.

The source of ground water in the province is precipitation that falls directly onto the province or in adjacent areas whose surface waters drain into the province (for example, the Sevier River in Utah, fig. 5). Most of the precipitation is lost by evaporation or transpired by plants. Eakin and others (1976, p. 6) estimated that only about 5 percent of the total precipitation in the Great Basin is ground-water recharge. Much of the recharge is from winter and spring storms that produce heavy snows in the mountains; during spring melt, the water seeps into permeable bedrock or flows off to adjacent valleys where some of the water seeps into the basin fill. Areas estimated to recharge ground water are shown in figure 7.

Much of the ground water from the carbonate-rock province is discharged by evapotranspiration (a combination of direct evaporation and transpiration by plants) on the valley floors where the ground water is near land surface. Figure 7 shows areas where evapotranspiration of ground water occurs in the province. In addition to evapotranspiration, ground water is discharged to land surface by numerous springs. This water seeps back into the ground or discharges as evapotranspiration, or flows to a river that discharges to a terminal sink or leaves the study area. Many small springs occur in the mountains. The spring water is from nearby sources, and the locations of these springs are controlled by permeability variations in the rocks and water levels related to land-surface altitude which cause the water to discharge at the surface. These springs may commonly represent perched local systems that are not connected

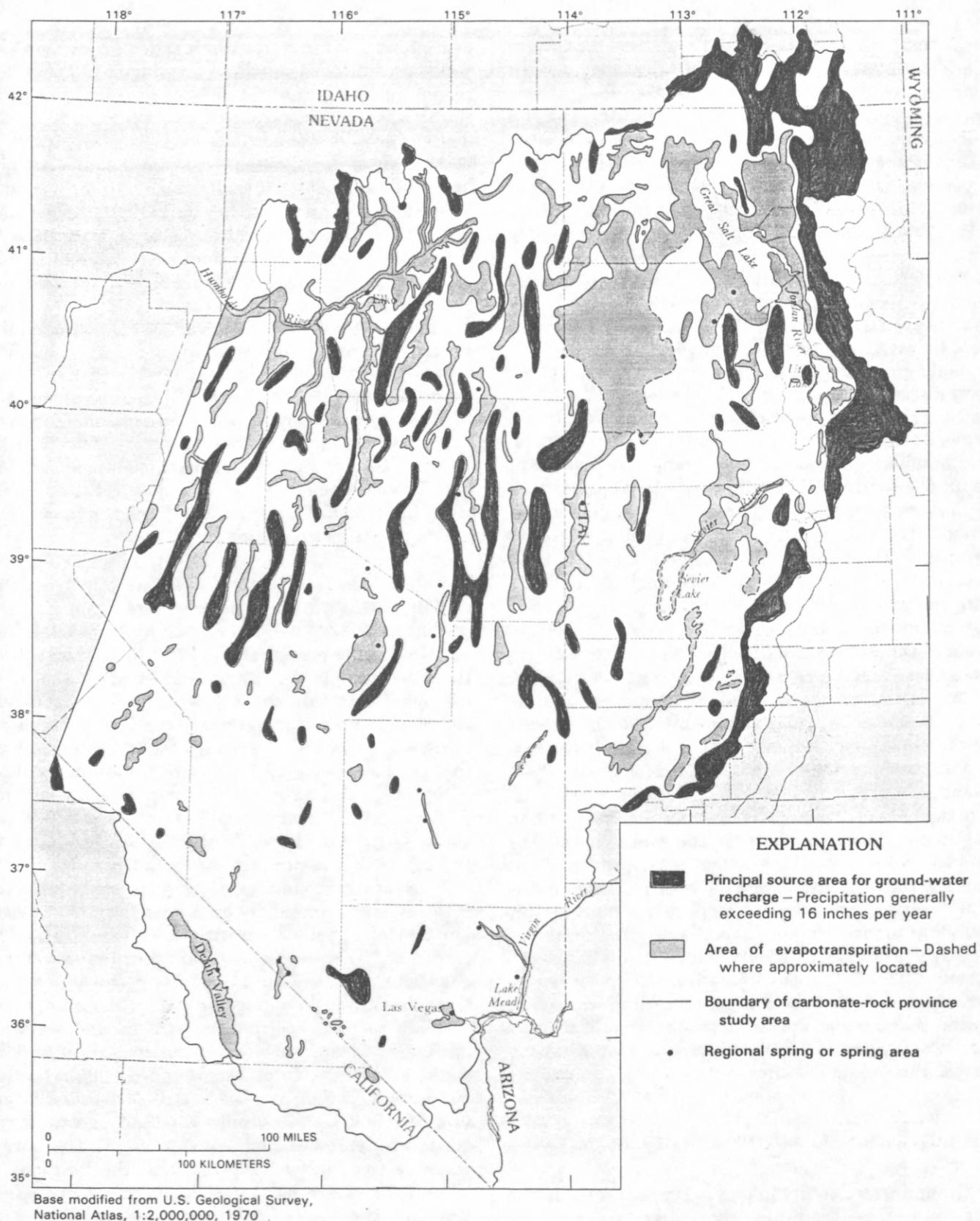


FIGURE 7.--Principal source areas for ground-water recharge, areas of evapotranspiration (from Harrill and others, 1988), and locations of regional springs. Base from figure 4.

to surrounding and underlying ground water. Some are discharge points for water that originates in the adjacent mountains, whereas at others the water originates in distant mountains and travels long distances beneath valleys and perhaps other mountain ranges.

Mifflin (1968) classified springs in Nevada as local, intermediate, and regional on the basis of water chemistry, water temperature, and fluctuation of flow from the springs. Similar criteria were used during this study to identify regional springs. These springs presumably represent the discharge of the deep flow through carbonate rocks. Locations of the regional springs are shown in figure 7. The largest concentration of regional springs is in a small area at Muddy River springs and totals about 36,000 acre-ft/yr (Eakin and Moore, 1964), a small fraction of the larger springs that discharge from carbonate rocks in Florida and Missouri. For example, the Spring Creek Springs in Florida discharge about 1.3 million acre-ft/yr (Rosenau and Faulkner, 1974).

Most ground-water withdrawals in the province are from wells drilled into the basin-fill deposits beneath the valley floors because (1) most of the people settled in the valleys where the climate is less severe than the mountains and where the land is more suitable for agriculture; (2) ground water in many of the valleys is generally within a few feet to several tens of feet below land surface in contrast to generally deeper water levels in mountain areas; and (3) the basin-fill deposits generally yield large quantities of water to wells. Eakin and others (1976, p. 15) reported yields as much as 8,600 gallons per minute from large-capacity wells in north-central Utah.

Prior to World War II, most of the ground-water withdrawals were from flowing wells drilled into basin-fill deposits. Areas of flowing wells were concentrated largely along the eastern side of the province in valleys adjacent to the Wasatch Range, although several other valleys, including Las Vegas Valley, had flowing wells. Ground-water withdrawals were generally small and constant until after World War II, when more efficient pumps and cheap energy greatly increased the amount of ground water withdrawn to irrigate crops and to supply a rapidly increasing population. The total amount of ground water withdrawn in the province during 1975 was approximately 1 million acre-ft. Major areas of ground-water withdrawals during 1975 are shown in figure 8.

CONCEPTUAL EVALUATION OF GROUND-WATER FLOW

Computer models are tools that can be used effectively to help understand the complex ground-water

flow system within a simulated area. However, rarely are computer models used to simulate ground-water flow over areas as large as 92,000 mi² as was done in this study. Endless arguments could be invoked as to the validity of the assumptions and hydrologic values used in simulating ground-water flow within such a large and complex area as the carbonate-rock province. For this reason, it must be stressed that the computer simulation discussed in this report is conceptual in nature. Only broad concepts and large-scale features can be inferred from the results of this study. Although a fairly detailed analysis of ground-water flow will be discussed, it does not intend to indicate that the study results presented here are adequate; in fact, the objective in presenting a detailed analysis of ground-water flow is to examine the possibility of the relatively shallow flow regions being interconnected by deep flow through carbonate rocks, and how regional geologic features might affect the direction of flow and water levels.

GENERAL ASSUMPTIONS

Many assumptions were made in the simulation of flow. In the province, ground water not only flows through porous basin-fill deposits but also flows through fractures and solution openings in the consolidated rocks. It was assumed that the fractures and solution openings through which water flows could be represented as a porous medium and that Darcy's Law was applicable at a regional scale. These assumptions may be reasonable because the model grid spacing is in miles; however, not enough information is available for the entire area to substantiate these assumptions.

The model simulations assumed steady-state conditions prior to development in which estimates of current recharge (1950-80) is assumed equal to estimates of current discharge (assuming no ground-water withdrawals). During the late Wisconsin glaciation (about 20,000 to 10,000 yr B.P.), climate in the province was significantly wetter than today and numerous lakes were present in closed basins (Hubbs and Miller, 1948), as were several major streams that flowed within the province. It is possible that both ground-water levels and spring discharge are not in equilibrium, because of the long distances between areas of recharge and discharge, and that both are still declining since the climate has become drier.

Winograd and Szabo (1986) discussed evidence of water-table declines near Ash Meadows, which is in the southern part of the province near Death Valley (fig. 1). They estimated a rate of water-table decline of

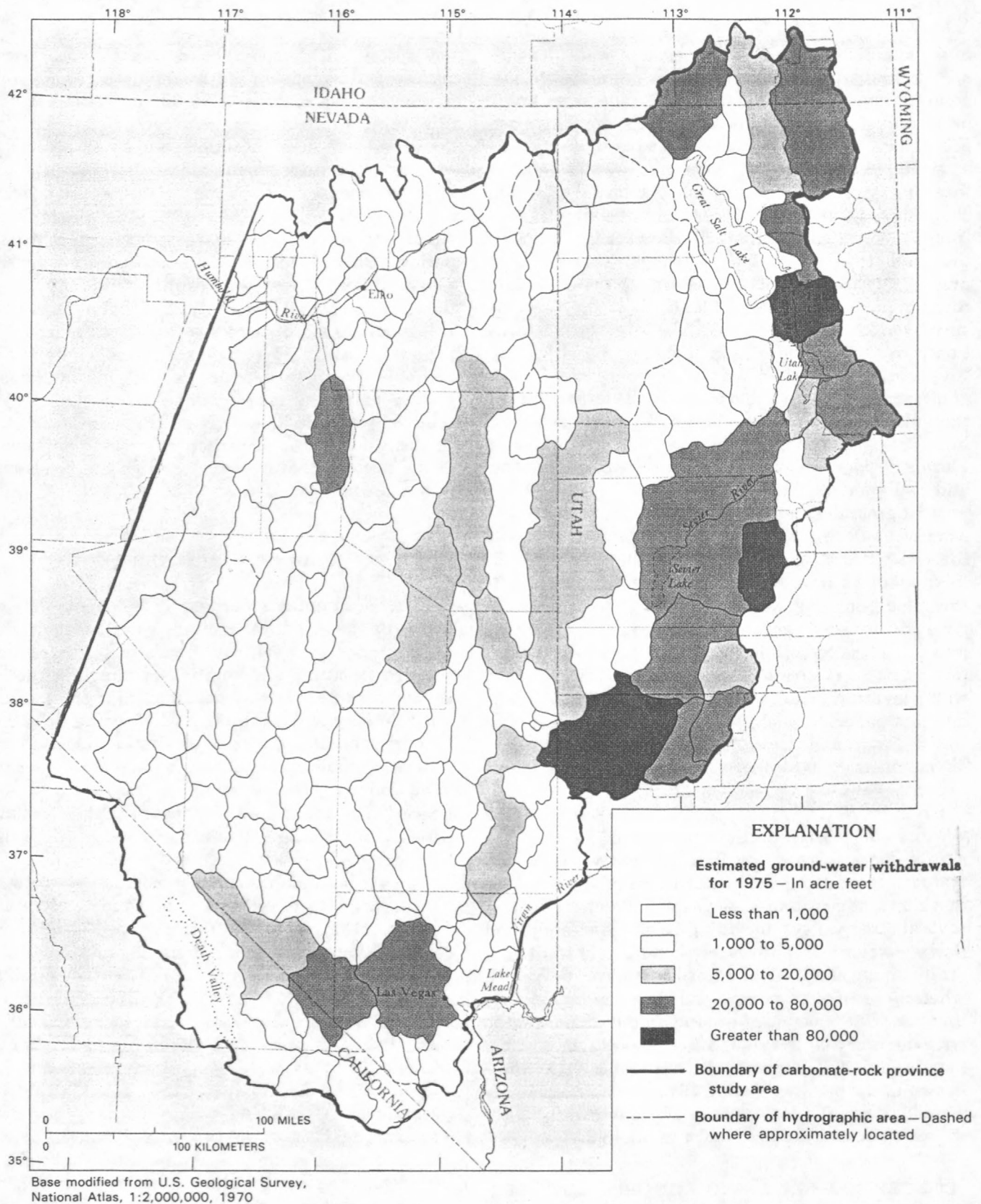


FIGURE 8.--Distribution of estimated ground-water withdrawals by hydrographic areas for 1975. Hydrographic areas from Harrill and others (1988). Estimates of ground-water withdrawals for Utah from Sumsion and others (1976). Estimates for Nevada from Bedinger and others (1984). Base from figure 4.

about 0.07 ft per 1,000 years, assuming a constant rate of decline for the past 510,000 to 750,000 years. The estimates were determined from uranium–disequilibrium dating of calcitic veins above and up gradient from the present water table at Ash Meadows. The calcitic veins are associated with other features indicative of paleo-ground-water discharge. Jones (1982) estimated that the water table on a fan north of Frenchman Flat at the Nevada Test Site was close to its present position for a long time and hypothesized it was within 150 ft of its present level through most of Quaternary time. Thus the evidence suggests that changes in water levels (at least in the southern part of the province) have changed slowly. In contrast, the water table in some of the northern valleys and, in particular, the Great Salt Lake Desert must have declined at least several hundred feet over the past 10,000 to 15,000 years as ancestral Lake Bonneville shrank to the present level of the Great Salt Lake.

Whether or not current ground-water discharge is in equilibrium with current recharge is unknown. The time that a change in recharge might be reflected in heads and in a change in discharge is also unknown because estimates of hydraulic properties, especially estimates of storage capacities, and the lengths of ground-water flow paths are largely unknown for the various rock types. However, the change in water-level decline is slow through geologic time, therefore the assumption of steady state might still be valid for the length of simulation time. If the steady-state assumption is not valid, then the results of the conceptual model described in this report could be affected.

Transmissivity in each model cell was assumed to be homogeneous and isotropic. The model can simulate heterogeneity caused by differences in hydraulic properties of the rocks by varying the transmissivity values of each model cell. It can also simulate heterogeneity between the vertical and horizontal direction, but the transmissivity in each model cell is assumed to be isotropic. The computer program by McDonald and Harbaugh (1984, p. 137) can simulate anisotropy in the horizontal direction except that the anisotropy is one uniform value that is used throughout a model layer. Different layers can have different values for anisotropy, but anisotropy cannot vary within a layer. Geologic structures that could result in preferred directions of ground-water flow are not uniform throughout the modeled area, thus each model cell was assumed isotropic. Some geologic structures, such as strike-slip faults, could produce a barrier to ground-water flow in one direction and a conduit to flow in another direction over parts of the province. Such features could not be adequately simulated in the model.

MODEL DEVELOPMENT

A three-dimensional finite-difference ground-water flow model developed by McDonald and Harbaugh (1984) was used for the computer simulations. The basic partial differential equation for an anisotropic, heterogeneous porous medium with a constant water density used in their computer program is defined as follows:

$$\frac{\partial}{\partial t} \left(K_{xx} \frac{\partial h}{\partial x} \right) + \frac{\partial}{\partial y} \left(K_{yy} \frac{\partial h}{\partial y} \right) + \frac{\partial}{\partial z} \left(K_{zz} \frac{\partial h}{\partial z} \right) - W = S_s \frac{\partial h}{\partial t} \quad (1)$$

where x, y, z = Cartesian coordinates corresponding to the major axes of the hydraulic conductivity tensors K_{xx} , K_{yy} , and K_{zz} (in length dimension);

h = hydraulic head (in length dimension);

W = volumetric flux per unit volume representing sources and (or) sinks (in 1/time dimension);

S_s = specific storage of the medium (in 1/length dimension); and

t = time.

For simulations that do not include changes in head with respect to time (steady state), the right side of the equation goes to zero and estimates of storage are not needed. This was the case for simulations used to conceptualize the ground-water flow in the province.

APPLICATION OF FINITE-DIFFERENCE EQUATIONS

The partial differential equation for ground-water flow can be closely approximated by finite-difference equations, which are sets of algebraic expressions that are solved simultaneously by using, in this model, the strongly implicit procedure. The solution of this algorithm involves setting up a three-dimensional grid system in which each model cell within the grid exhibits specific hydrologic properties that best approximate the true physical setting of that area. The reader is referred to McDonald and Harbaugh (1984, p. 370–431) for a detailed discussion of the solution technique used in the model.

MODEL GRID

The grid network contains 60 columns, 62 rows, and 2 layers (fig. 9). The width of each cell (in the row direction) was 5 mi and the length (in the column

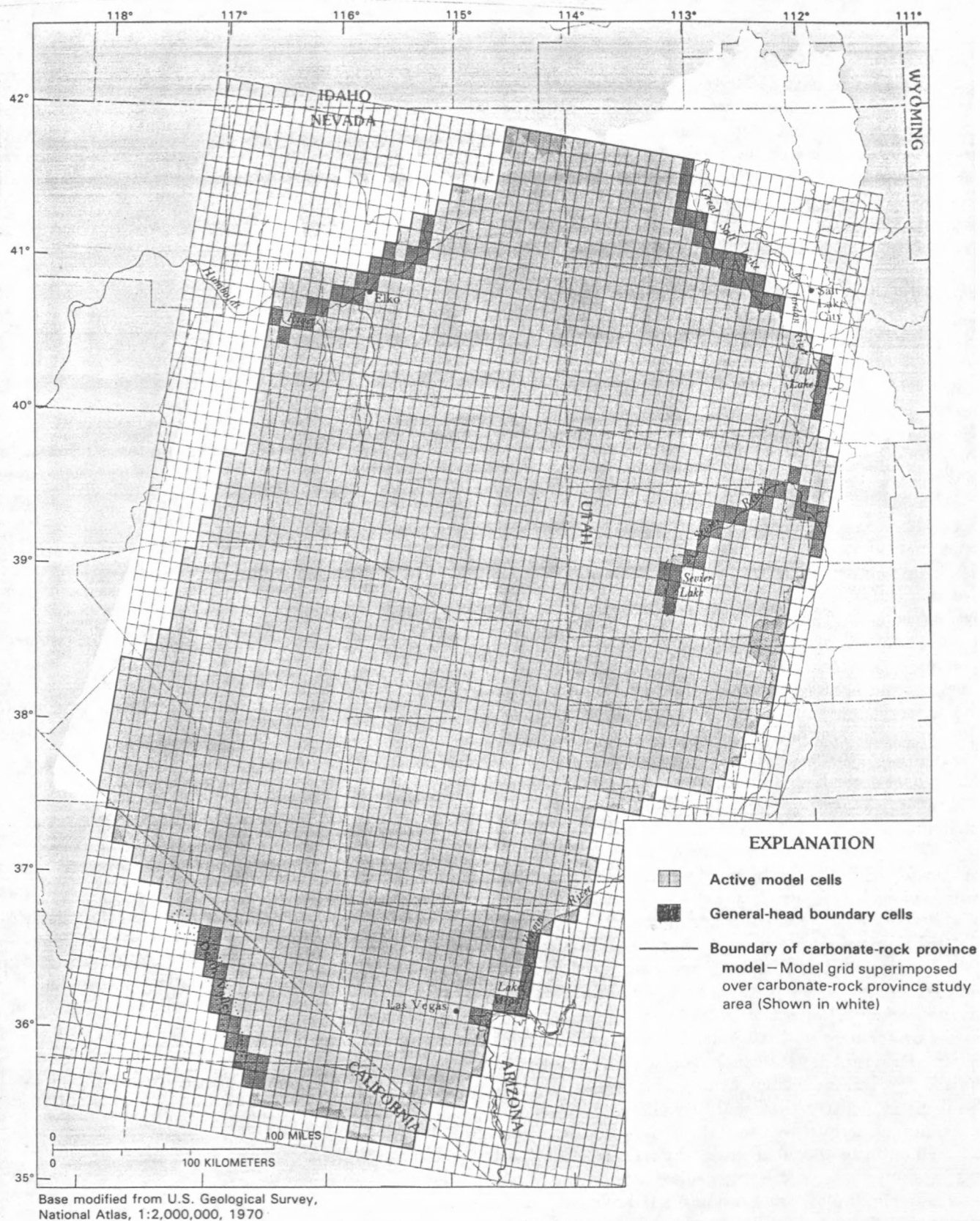


FIGURE 9.--Finite-difference grid network. Base from figure 4.

direction) was 7.5 mi. Four criteria were used in determining this particular size and orientation for the grid system.

1. The northeast-southwest orientation of the grid system parallels the prevailing direction of the fault-block mountains and adjacent valleys and, thus, the regional geologic structure.

2. The grid cell size was the largest that could be used while still maintaining the topographic and physiographic expression of the study area. Many mountain ranges and adjacent valleys tend to be approximately 10 mi wide. The length of the cells is longer to conform to the long linear pattern of many of the ridges and valleys in this physiographic province.

3. The width-to-length ratio selected avoids stability problems during solution of the finite-difference equations. When cell dimensions differ by more than a factor of 2, the model may become unstable, creating erroneous solutions or convergence problems (Remson and others, 1971, p. 71-77).

4. A smaller grid size could have been used (which would greatly increase computational time); however, due to sparse data over much of the study area a smaller grid size was considered ineffective and impractical.

REPRESENTATION AS A TWO-LAYER SYSTEM

Commonly, model layers are separated on the basis of permeability contrast. However, due to the complexity of the geologic structures in the province, the lack of data, and their thickness, the province was simply divided into two layers. The upper model layer was used to simulate relatively shallow flow primarily through basin-fill deposits and adjacent mountain ranges to depths of several thousand feet. The lower model layer was used to simulate deep flow beneath the basin fill and mountain ranges. The actual depth to the base of deep flow is unknown, but marine sedimentary rocks containing thick sequences of carbonate rocks may be more than 30,000 ft thick (Stewart, 1980), and fresh water has been identified in oil-well test holes to depths of about 9,400 ft (Winograd and Thordarson, 1975, p. 74).

BOUNDARY CONDITIONS

In general, the model boundaries of the carbonate-rock province were extended to mountain ranges consisting mostly of low-permeability consolidated rocks and were assumed to be no-flow boundaries. Carbonate rocks may extend northward beneath the basalts

of southern Idaho. The topographic divide between the Snake River drainage area in southern Idaho and the Great Basin was assumed to act as a divide not only for near-surface ground-water flow but also for deep flow. Ground-water flow to the north of the Great Salt Lake was not simulated in the model because the lake was used as a hydrologic boundary for ground-water flow in the model. The Great Salt Lake occupies a low area with no surface outflow, and it presumably is a sink area for the northern part of the province. Carbonate rocks may also extend westward from where the rocks are exposed in the mountains. The western modeled boundary of the province was extended westward to mountain ranges that consisted mostly of rocks from the transitional assemblage as defined by Stewart and Carlson (1978). Although some ground-water flow may occur across this transitional assemblage, the western boundary was simulated as a no-flow boundary.

Hydrologic boundaries were also used in three other places along the edge of the modeled area: Utah Lake and the Jordan River, the Virgin River and Lake Mead, and Death Valley (fig. 9). The hydrologic boundaries were simulated as head-dependent flow boundaries to the upper model layer. The simulation of flow across the head-dependent boundaries was computed by multiplying the head difference across the boundary with a conductance term. The head difference was determined by comparing a specified boundary head to that in the adjacent model cell. The conductance term is the hydraulic conductivity times the cross-sectional area of the boundary through which flow is simulated divided by the length of the flow path.

The head-dependent flow boundary allows flow to occur either to or from the model cell depending on whether the head in the model cell adjacent to the boundary is less than or greater than the specified boundary head. An explanation of the equation used is presented by McDonald and Harbaugh (1984, p. 343-369). The boundary was applied above the upper model layer, thus the conductance term used for each model cell was in the vertical direction. An initial estimate of vertical conductance was determined for each cell by multiplying an approximate vertical hydraulic conductivity with the planimetric area of the model cell and then dividing by an estimate of the vertical flow-path length. The length of the flow path was assumed to be half the estimated thickness of the basin-fill deposits, which probably represents the average value of the flow length. The conductance terms were adjusted during model calibration.

The same type of boundary was used to simulate the interaction of ground-water flow with the Sevier

and Humboldt Rivers where the rivers flowed through the modeled area (fig. 9). The conductance term for each model cell was limited to the area of the river.

Recharge to the model was simulated as a constant flux to the upper model layer in cells that corresponded to mountain ranges. Recharge was not simulated in model cells that corresponded to valleys, because much of that recharge does not infiltrate into the deep part of the aquifer system and discharges as evapotranspiration or issues as small springs.

Discharge from evapotranspiration was simulated as a head-dependent flow boundary. Evapotranspiration was simulated only in the upper model cells that corresponded to valleys and was the principal discharge of water from the upper model layer. The equation used for simulation of evapotranspiration is different from the one used for the head-dependent boundaries along the edge of the modeled area and for the rivers. The simulation of evapotranspiration is based on a discontinuous function that is related to land surface. The equation requires that land surface, maximum evapotranspiration rate occurring at land surface, and extinction depth (the depth below land surface at which evapotranspiration ceases) be specified in each model cell where evapotranspiration is to be simulated. Figure 10A shows how evapotranspiration is computed in the simulations. A detailed explanation of the equation is presented by McDonald and Harbaugh (1984, p. 316-342).

The equation used to simulate evapotranspiration for this study was modified, because during initial simulations, numerical oscillations developed whenever the simulated head in the model cell exceeded the specified land surface (fig. 10A). To alleviate this problem, the equation was changed whereby evapotranspiration rates continued to increase even when the computed head in the cell was above land surface (fig. 10B). However, the simulation of discharge from evapotranspiration could be unrealistic, thus after each simulation, discharge from evapotranspiration was closely checked to make sure that it did not exceed the maximum lake evaporation rate less average precipitation for a particular area.

Spring discharge was not specifically simulated in the upper model layer but was incorporated into estimates of evapotranspiration because the discharge could represent flow from both model layers. Spring-flow was simulated as head-dependent flow in the lower model layer. Figure 11 shows the location and names of springs that were simulated as discharge from the lower model layer (Texas, Nevaras, and Travertine springs were simulated as part of the general-head boundary of Death Valley) and their relation to the model grid. The equation used to simulate

spring discharge is similar to the equation used to simulate head-dependent flow around the edge of the model except that it simulates only discharge from model cells. The equation requires an estimate of the land surface and an assumed conductance value. The conductance values of the springs were adjusted during calibration such that the head in the model cell was nearly equal to the land surface near the spring. Thus, flow to the springs was controlled by the transmissivities of model cells adjacent to the cell with the spring.

MODELING APPROACH

Simulation of ground-water flow in the carbonate-rock province required a different approach from that used for most modeled areas, because all the variables in the ground-water flow equation (equation 1) either are unknown over large parts of the area or are only rough estimates. The distributions of recharge and discharge are generally known, although the amounts of recharge and discharge by evapotranspiration are only approximately known. Water levels in the upper part of the basin fill are generally known (Thomas and others, 1986), but water levels in the consolidated rocks beneath the basin fill are known only at a few locations. Also, the known water levels in consolidated rocks represent only heads in the uppermost part of the consolidated rocks as wells penetrate only a small part of the total thickness. Water levels are generally unknown in the mountains because there are few wells. Hydraulic properties of shallow basin-fill deposits are generally known because most of the ground water used in the province is from wells drilled into basin-fill deposits. Estimates of hydraulic properties of the various consolidated rocks are largely unknown, except at a few locations such as the Nevada Test Site. In addition, the subsurface geology is largely unknown, as is the depth of ground-water flow.

Several approximations and assumptions about the data were used to model ground-water flow in the province. Recharge was assumed to occur in the mountains except where general-head boundaries were used to simulate rivers and lakes. During a simulation, recharge was held constant and the transmissivity values were adjusted until (1) simulated water levels in both model layers approximated general water-level trends that were interpolated and extrapolated from known points, (2) simulated areas of evapotranspiration approximated areas of known evapotranspiration, and (3) simulated discharge from regional springs approximated the known discharges.

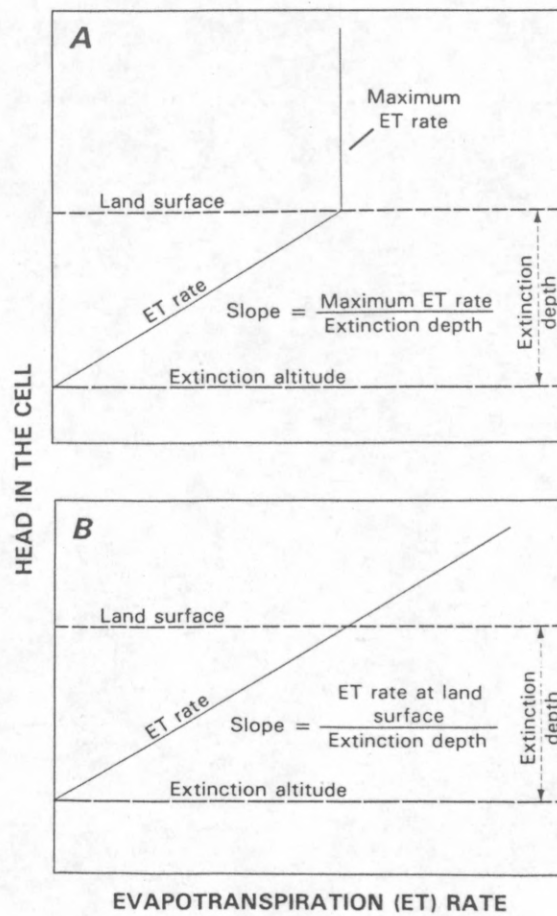


FIGURE 10.--Evapotranspiration (A) and modified evapotranspiration functions (B) incorporated into computer program.

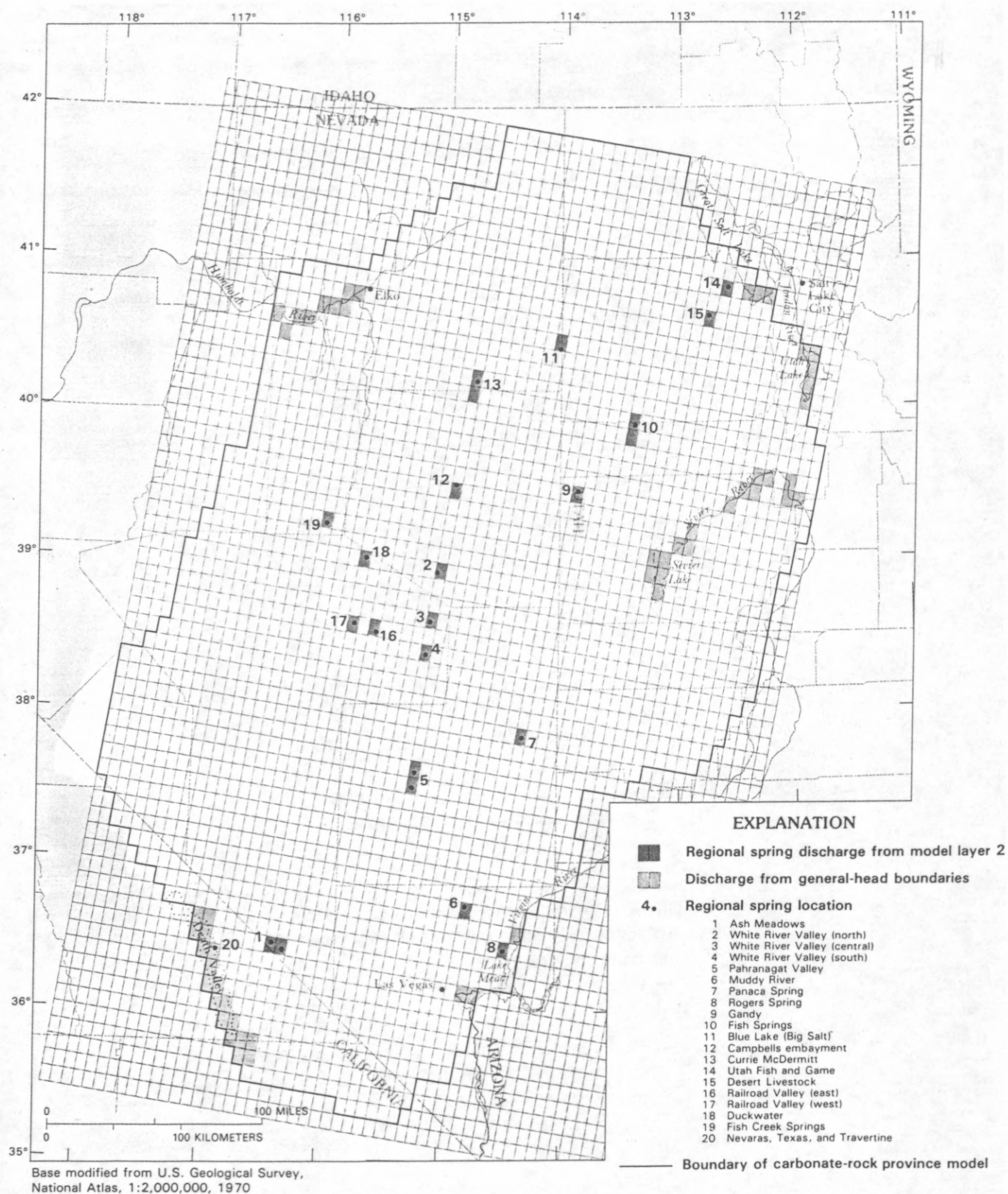


FIGURE 11.--Regional spring discharge locations and discharge locations at general-head boundaries in relation to model grid. Discharges from Nevaras, Texas, and Travertine springs in Death Valley were included in discharge from general-head boundaries. Base and grid from figure 9.

Although initial estimates of transmissivities and vertical leakance values used in the model were based on geology, the transmissivities were allowed to change regardless of geology. The calibrated transmissivities were therefore dependent on water levels, distribution and amount of recharge, the distribution of evapotranspiration, and the amount and distribution of spring discharge but were independent of the geology.

Water levels were a major control on the distribution of simulated transmissivities. Simulated water levels in the upper model layer were compared to known water levels in basin-fill deposits and water levels from shallow wells in mountainous areas. The data were compiled by Thomas and others (1986), and the locations of data points are shown in figure 12. In basins with little information, water levels were interpolated and extrapolated from known points. In model cells that corresponded to mountains where water levels were unknown, the simulated water levels were not allowed to exceed the average land-surface altitude of the cell. Water levels in some basins shown by Thomas and others, in particular Las Vegas Valley, have been affected by ground-water withdrawals. In these basins water levels prior to withdrawals were used in the simulations.

Water levels in the lower model layer were based on limited data from wells, test holes, or mine shafts that penetrated consolidated rocks beneath the basin fill, from deep mine shafts and holes in the mountain areas, and from the land-surface altitude of regional springs. The data were compiled by Thomas and others (1986), and the locations of the data are shown in figure 13. Estimated water levels were extended from the known points by interpolation and extrapolation.

The magnitudes of the computed transmissivity and leakance values were dependent on the amount of recharge used in the simulations, because steady-state conditions were assumed in the simulations. Increasing recharge results in a corresponding increase in discharge and a proportional increase in transmissivity and leakance values. The estimates of recharge are only approximations, thus during model calibration, recharge was increased by a factor of 2 and decreased by a factor of 2 to evaluate the effect of recharge on computed transmissivity and leakance values.

Admittedly, different methods could be used to synthesize the sparse data, and different approaches could be used in the simulation of ground-water flow in the carbonate-rock province that may produce different results. However, the overall trends in the simulation of ground-water flow in the province would be similar, at least in a conceptual sense.

ESTIMATES OF RECHARGE

The method used to estimate recharge in Nevada and Utah was reported by Maxey and Eakin (1949, p. 40-41) and Eakin and others (1951, p. 26-27). The method is empirical and estimates the recharge derived from a given area as a percentage of the estimated annual precipitation. The percentage increases from 0 percent for the annual precipitation zone below 8 in. to a maximum of 40 percent for annual precipitation zones of more than 40 in. (along the Wasatch Range in Utah), but excludes precipitation that falls on the valley floors. Initially, the percentages were obtained by trial-and-error calculations such that estimates of recharge were balanced against estimates of ground-water discharge from natural losses in 13 hydrographic areas in the province. Although recharge was estimated by this empirical method in Utah, the percentage of recharge applied to each precipitation zone varies considerably between hydrographic areas. The reason for the variation is that the estimates of recharge were adjusted to match estimates of discharge. The percentages of recharge applied to each precipitation zone were also adjusted arbitrarily when the technique was applied to other hydrographic areas in Nevada. Thus, the percentage of precipitation estimated to become recharge for a particular precipitation zone may vary by several percent among different hydrographic areas in both Nevada and Utah. Watson and others (1976) quantitatively evaluated the method for estimating recharge and concluded that the method could not reliably predict recharge other than provide an approximation.

Estimates of recharge for a given mountain range were obtained by determining the areas within each precipitation zone from maps of average annual precipitation for Nevada and Utah (Hardman, 1936; U.S. Weather Bureau, no date) because estimates of recharge in the reconnaissance reports (the reports are included in the list of references) were by hydrographic areas and not by mountain ranges. The estimate of recharge for each mountain range was then compared for consistency to the estimated recharge for individual or selected groups of hydrographic areas. The distribution of recharge used in the model simulations is shown in figure 14. The total estimated annual recharge from precipitation within the modeled area of the province is about 1.6 million acre-ft.

The amount of precipitation that is estimated to recharge the aquifers in the province is about 3 percent of the estimated total annual precipitation. This approximation is at the low end of the range (3-7 percent) reported by Eakin and others (1976, p. 10). However, their study included hydrographic areas that

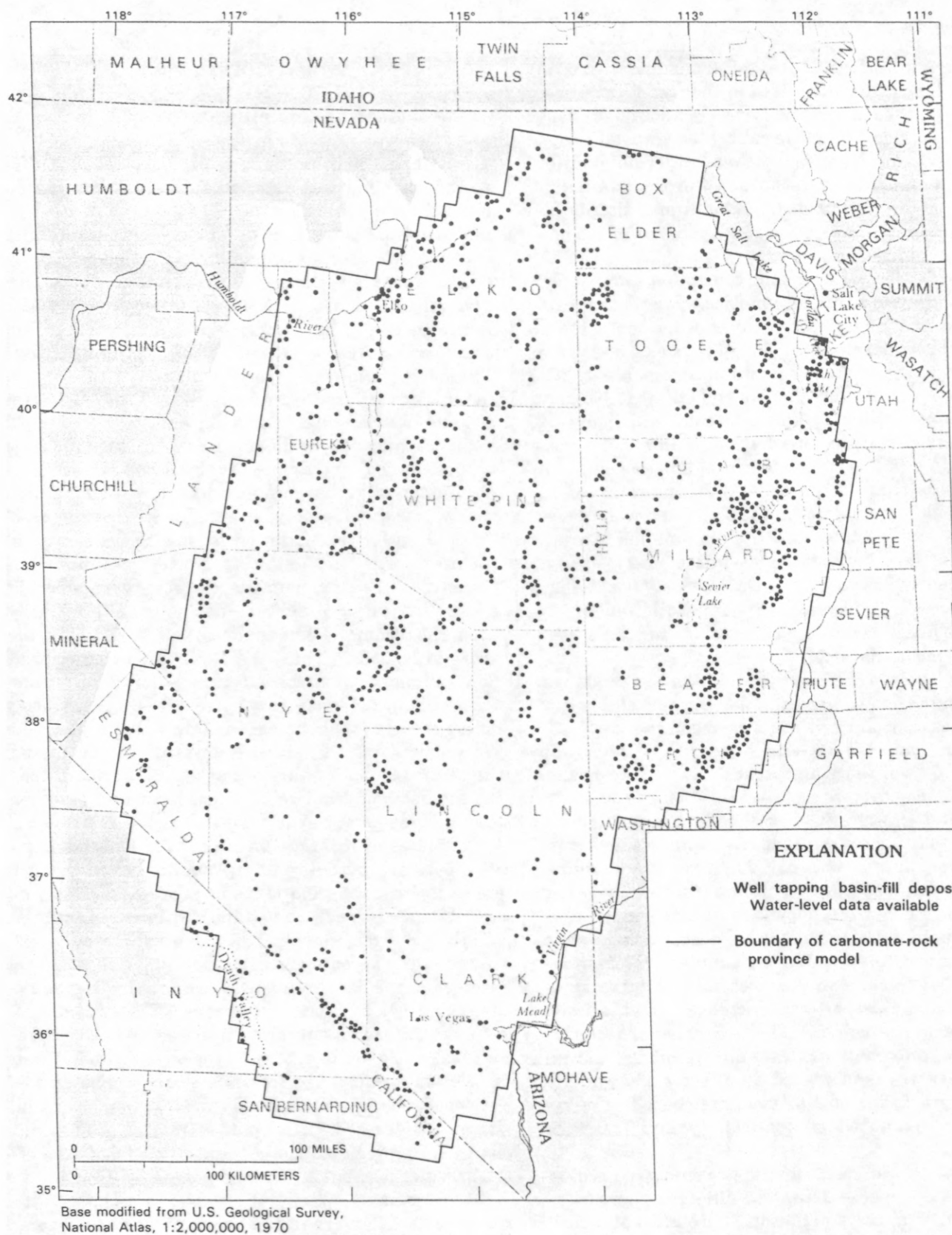


FIGURE 12.--Locations where water-level measurements are available from wells tapping basin-fill deposits (modified from Thomas and others, 1986). Carbonate-rock province study area shown in white.

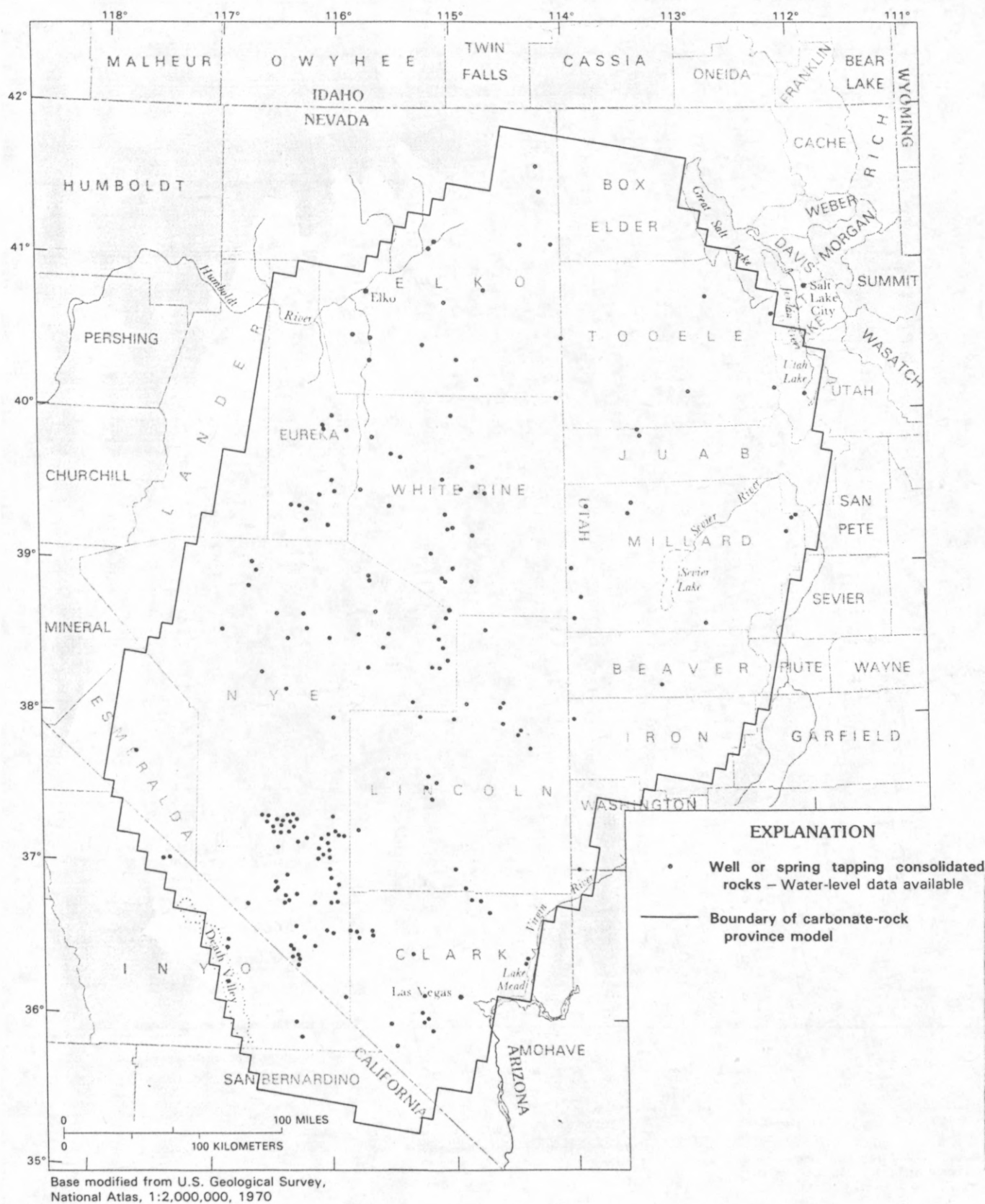


FIGURE 13.--Locations where water-level measurements are available from wells tapping consolidated rocks (modified from Thomas and others, 1986). Base from figure 12.

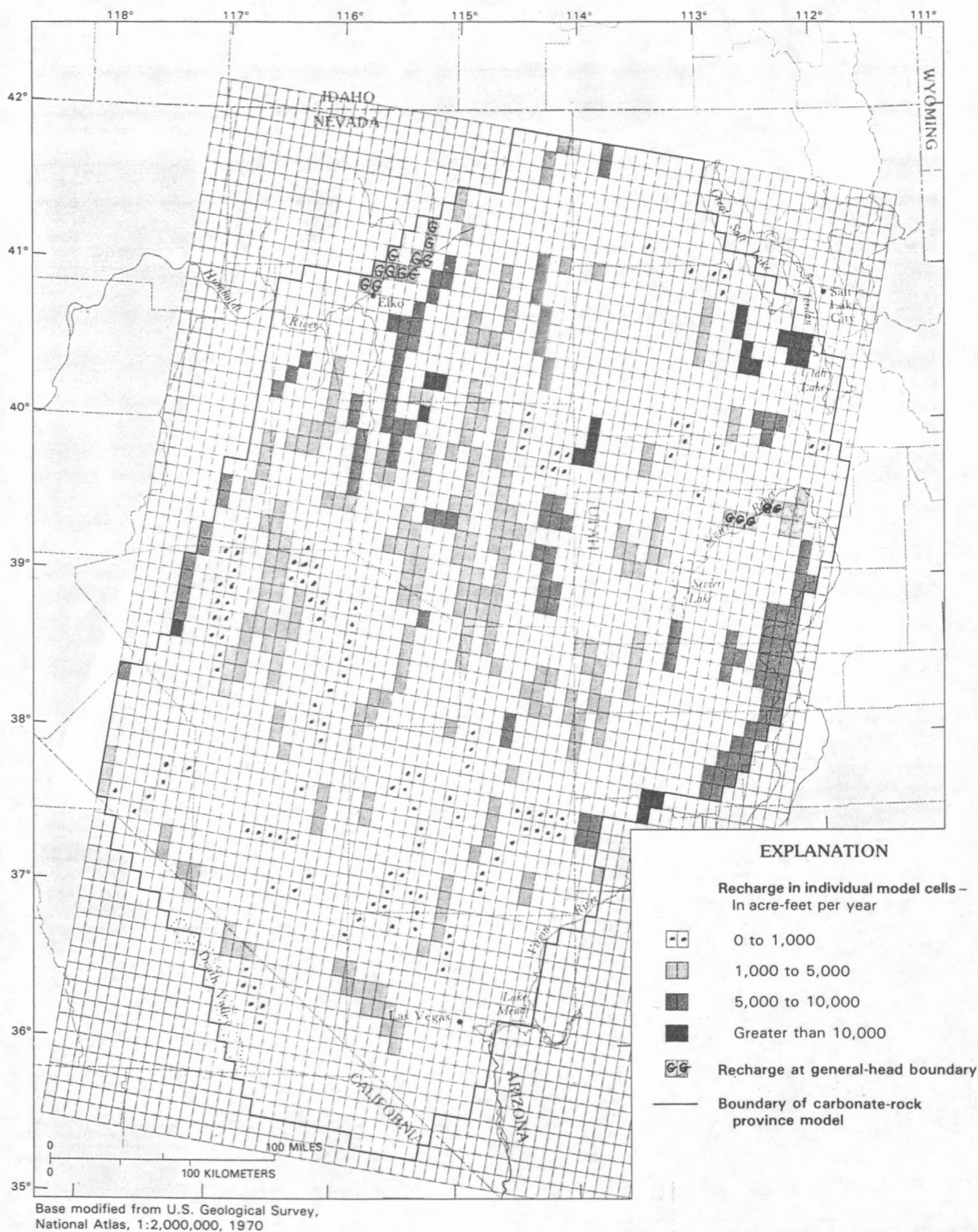


FIGURE 14.--Distribution of recharge in individual model cells and areas of recharge from general-head boundaries. Base and grid from figure 9.

received water from the much wetter Sierra Nevada, the mountains in extreme northern Nevada, and areas along the north and east sides of the Great Salt Lake that receive some water from the Wasatch Range. Their study area also excluded several hydrographic areas in the much drier southeastern Nevada. Thus, the 3 percent estimate is probably reasonable or may be toward its high end. Also, the estimates of recharge presented herein and in most of the numerous reconnaissance reports do not include water that locally recharges ground water only to be discharged nearby.

INITIAL ESTIMATES OF TRANSMISSIVITY AND LEAKANCE

Initial estimates of transmissivity for the model layers were based on geology. The estimates were made to provide a starting point in the calibration process as transmissivity values were changed during model calibration. The geologic units within the modeled area were grouped into three principal types (Harrill and others, 1988; Plume and Carlton, 1988) and are (1) basin-fill deposits, which include Tertiary tuffs, and terrigenous sediments along with all Quaternary stream, alluvial fan, and lacustrine deposits; (2) thick sequences of carbonate rocks of Paleozoic and early Mesozoic age; and (3) other consolidated rocks, which include most volcanic, metamorphic, and crystalline rocks, Precambrian basement rocks, and locally thick units of Tertiary clay and silt. Figure 15 shows how the principal rock types were distributed in the upper model layer. The basin-and-range physiography can be easily distinguished with the resolution provided by the 5-by-7.5-mi grid.

Carbonate rocks were assumed to have the highest transmissivity due primarily to secondary openings. The initial transmissivity assigned to the carbonate rocks was 0.25 ft²/s, within the range of values reported by Winograd and Thordarson (1975, table 3 and p. 73), Bunch and Harrill (1984, p. 119), and Plume (1984). Reported values range from about 0.002 ft²/s (200 ft²/d) to about 9 ft²/s (800,000 ft²/d). An initial transmissivity value assigned to the other consolidated rocks was 0.001 ft²/s; the initial value used for the basin-fill deposits was 0.02 ft²/s, within the range of values presented by Winograd and Thordarson (1975, table 3) and Bunch and Harrill (1984, p. 115).

Transmissivities of each rock type actually vary widely, due to either changes in thickness or differing hydrologic properties of the rocks. The transmissivity values for each model cell were changed during model calibration.

The vertical resistance to ground-water flow was simulated in the model with a leakance term. Leakance is defined as the vertical hydraulic conductivity divided by length of flow path (Lohman, 1972, p. 30). A leakance value of 1×10^{-11} per second was initially assumed for the model. No attempt was made to initially distinguish leakance values according to hydrogeologic conditions because of the uncertainty of the geologic units at depth and because of uncertainties in estimating the vertical hydraulic conductivity and the length of the flow path. The leakance values were changed during model simulations.

MODEL CALIBRATION

Calibration of the model began by adjusting transmissivities of each model cell in both layers and vertical leakance between the layers after comparing simulated heads to estimated heads. At the end of each model simulation, transmissivity and leakance values were adjusted based on the ratio of simulated heads to estimated heads. The process was repeated until the simulated heads approximated those that were interpolated and extrapolated from known values. The final part of model calibration involved making local changes (1) in transmissivities and leakance values in model cells near simulated spring discharge areas, (2) in the conductance values at head-dependent boundaries that simulated the interaction of ground water with surface water, and (3) by changing initial estimates of land-surface areas in the valleys to approach more closely estimated evapotranspiration values. These modifications resulted in local changes in simulated heads but did not significantly affect the regional water levels.

ALGORITHMS USED TO CALIBRATE MODEL

Transmissivities were reestimated at the end of every other simulation using an algorithm called TRANS, in which transmissivity in model cells where estimated heads were available were reestimated to force the simulated heads to approximate the estimated heads. The TRANS algorithm assumes that flow through a model cell remains constant, therefore the transmissivity in a model cell is directly proportional to the ratio of the simulated head in a model cell to the estimated head. The TRANS algorithm can be expressed as

$$T_{NEW}(I,J) = T_{OLD}(I,J) * [SSH(I,J)/KH(I,J)] \quad (2)$$

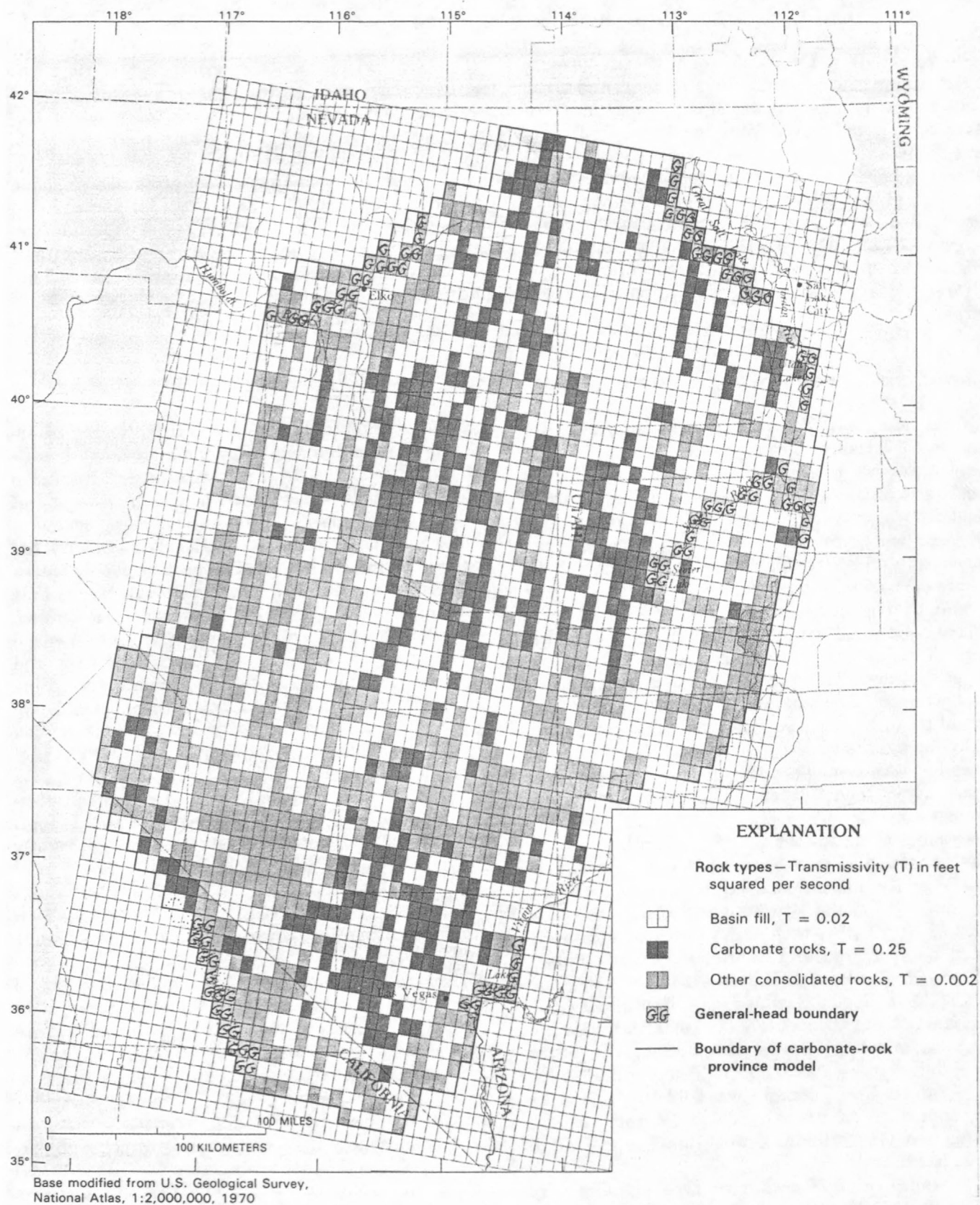


FIGURE 15.--Principal rock types in upper model layer and initially assigned transmissivity values. Base and grid from figure 9.

where TNEW(I,J) = reestimated transmissivity in cell (I,J),
 TOLD(I,J) = transmissivity in cell (I,J) for the current simulation,
 SSH = simulated head value for the current simulation, and
 KH = estimated head value.

The algorithm will not correctly adjust the transmissivity on the first computation because flow to and from a model cell will change after adjusting the transmissivity in adjacent cells. Changing the leakance value between model cells will also affect flow to and from a cell. Thus, the process involved numerous model simulations that reestimated not only the transmissivity values but also vertical leakance until the simulated heads approximated the estimated heads.

A second algorithm called LEAKANCE was alternated with TRANS. The LEAKANCE algorithm recalculated vertical leakance between cells in the upper and lower model layer on the basis of the ratio of the simulated vertical head difference between the model cells to an estimated vertical head difference. The algorithm can be expressed in the following manner:

Let
 $DIFF = [SSHT(I,J) - SSHB(I,J)] / [HT(I,J) - HB(I,J)]$
 then set
 $LNEW(I,J) = LOLD(I,J) * FAC * DIFF$
 where LNEW(I,J) = reestimated leakance value for cell (I,J),
 LOLD(I,J) = leakance value for the current simulation,
 SSHT = simulated head in the upper layer,
 SSHB = simulated head in the lower layer,
 HT = estimated head in the upper layer,
 HB = estimated head in the lower layer,
 FAC = a multiplication factor, and
 DIFF = an intermediate term, as defined by the equation.

Williamson and others (1989) found for a model of the Central Valley aquifer system of California that best results from the algorithm were obtained with

FAC = 0.9 when DIFF > 1.0
 FAC = 1.1 when DIFF < 1.0
 FAC = 1.0 when DIFF = 1.0

After every 10 computer simulations, or after TRANS and LEAKANCE were each used 5 times, an algorithm TREND was used to change transmissivity and leakance values in model cells that did not have an estimated head. TREND was used over a specified group of 25 or more model cells, and the transmissivity or leakance value was either increased by 20 percent or decreased by 20 percent based on whether the simulated heads in model cells were generally too low or too high compared to the estimated heads. In cases where a 20 percent change in transmissivity over-extrapolated the simulated heads in model cells with respect to the estimated heads, the next sequence of model simulations compensated for the over-extrapolation.

Once the simulated heads approximated the estimated heads, model calibration was focused toward simulating the observed discharge from selected springs and the estimated amount of ground-water evapotranspiration. Simulated spring discharge from the lower model layer was calibrated by first adjusting the conductance value of the head-dependent function used to simulate springs in the model and then by adjusting the transmissivity and leakance values in the vicinity of the simulated springs. In a few instances, the altitudes of the spring pools were adjusted, particularly in areas of large relief where estimates of land-surface altitude as well as the estimated head values were averaged for the cell.

Changing the conductance values of the springs had little effect on simulated discharge rates but tended to increase or decrease the simulated head in the model cell. The conductance values of simulated springs were then set high enough such that the heads in the model cells were only slightly greater than the altitude of the spring pools. The discharge to the springs was then calibrated by adjusting the transmissivity and leakance values in the vicinity of the spring. Table 1 shows the observed and calibrated discharge rates for each spring or spring area, and figure 11 shows the model cells in which springs were simulated in the model.

The fit of simulated distributions of evapotranspiration to observed distributions depended almost entirely on the accuracy of the land-surface altitude values for each cell. Initially, average altitudes of land surface for each cell were specified. Where the terrain is rugged, using average land-surface altitude values usually did not produce good results in the model in that calculated evapotranspiration was either too high when compared to the estimated amount, or evapotranspiration was not simulated where it is known to exist. In these areas, the specified land-surface altitude had to be increased or decreased to

TABLE 1.--Observed versus simulated spring discharge rates following calibration

Spring	Discharge (acre-feet per year)		Map number (fig. 12)
	Observed	Simulated after calibration	
Ash Meadows	17,000	20,000	1
White River Valley (N)	18,000	13,000	2
White River Valley (C)	5,500	6,000	3
White River Valley (S)	16,000	23,000	4
Pahranagat Valley	26,000	22,000	5
Muddy River	36,000	35,000	6
Panaca Spring	8,000	5,500	7
Rogers Spring	700	1,000	8
Gandy	10,000	10,000	9
Fish Springs	26,000	24,000	10
Blue Lake	16,000	14,000	11
Currie-McDermitt	6,500	5,000	12
Campbells embayment	8,000	6,500	13
Utah Fish and Game	4,500	2,500	14
Desert Livestock	3,000	2,000	15
Railroad Valley (E)	3,500	3,000	16
Railroad Valley (W)	2,500	2,000	17
Duckwater	11,000	12,000	18
Fish Creek Springs	3,500	2,000	19

the altitude where phreatophytes are known to exist. For example, if a cell represented alluvial fans and terraces at the margins of the valley where evapotranspiration is known not to occur as well as low-lying areas where evapotranspiration is known to occur, using the average altitude led to no simulated evapotranspiration for that cell. After manually changing the land-surface altitude values in these cells based on the altitude of phreatophyte areas as determined from 1:250,000-scale topographic sheets, existing evapotranspiration was reproduced reasonably well. Figure 16 shows the distribution of simulated evapotranspiration after calibration while figure 17 shows areas of observed evapotranspiration as compiled by Harrill and others (1988).

In gently sloping areas, there was little problem in obtaining close approximations to estimated evapotranspiration rates. Because a linear function was used to simulate evapotranspiration, caution had to be exercised in areas where ground water is near land surface so that erroneously high rates would not be simulated. In areas where too much evapotranspiration was simulated, land-surface altitude values were increased slightly; if that did not work, transmissivity and leakance values were changed.

Some minor changes were necessary at the head-dependent flow boundaries that simulate the interaction of ground water with surface water. These changes involved increasing or decreasing the conductance values to adjust simulated head gradients near these boundaries so as to approximate the estimated head gradients. The final steady-state heads for both model layers are shown in figure 18.

LIMITS OF CALIBRATION

Obviously, the results from the model simulation are only approximate because of uncertainties in the distribution and amount of recharge and because heads in the consolidated rocks are unknown over much of the area. Although discussed in detail, the model results should be considered conceptual because none of the variables in the ground-water equation are known. Model results are also dependent on the general assumptions discussed previously.

Transmissivity values computed for both model layers are in part dependent on the amount and distribution of recharge used in the model, particularly for model cells that correspond to mountains. Recharge was simulated in the mountains except where head-dependent boundaries were used to simulate the interaction of ground water with surface water. Simulating all recharge in mountains that consist of

carbonate rocks is probably reasonable because little surface water flows to the nearby valleys. But in mountains that consist of low-permeability rocks, much of the water flows into nearby valleys where recharge occurs mostly on the adjacent alluvial fans. Thus, the transmissivities computed for model cells that represent these mountains are probably high and should be considered to also include the adjacent alluvial fans.

Computed transmissivities in the upper model layer are highly sensitive to changes in both the amount and location of recharge, which should be taken into account when interpreting regional trends in transmissivity in the upper model layer. Transmissivities for the lower model layer are not as sensitive to changes in recharge, because recharge is not added directly to model cells in this layer. Recharge to the lower model layer is dependent on the leakage between the upper and lower model layers, which is controlled by the vertical leakance term.

The errors in the estimates of recharge are unknown but could be well in excess of 100 percent. If recharge is increased in the model by 100 percent, a similar distribution of head could be simulated by proportionately increasing transmissivity and leakance values. Because the model assumes steady-state conditions, the simulated discharge would also increase by 100 percent. A different distribution of transmissivity near regional springs would be simulated if the additional ground water moving through the province were forced to equal the estimate of discharge from the springs instead of allowing discharge to increase everywhere.

Estimates of heads used to calibrate transmissivity in the lower model layer were based on limited data. The transmissivities of the lower layer could be changed by at least an order of magnitude and the model results might still be reasonable with respect to areas of known heads and estimates of transmissivities. In addition, the estimates of heads were smoothed by interpolation and extrapolation from known points and resulted in a more gradual change in simulated transmissivities than what could be expected. Winograd and Thordarson (1975, p. 64-68) documented head changes of as much as 2,000 ft in 3 mi. If such abrupt changes occurred in areas of no control, which is likely, the computed transmissivities in model cells that correspond to those areas would vary more than in simulations with gradually changing heads.

Estimates of heads in the intermediate- and deep-flow regions were based on data from wells, test holes, mine shafts, and springs. The wells, test holes, and mine shafts do not generally penetrate the rocks in the province to any great thickness. It is possible,

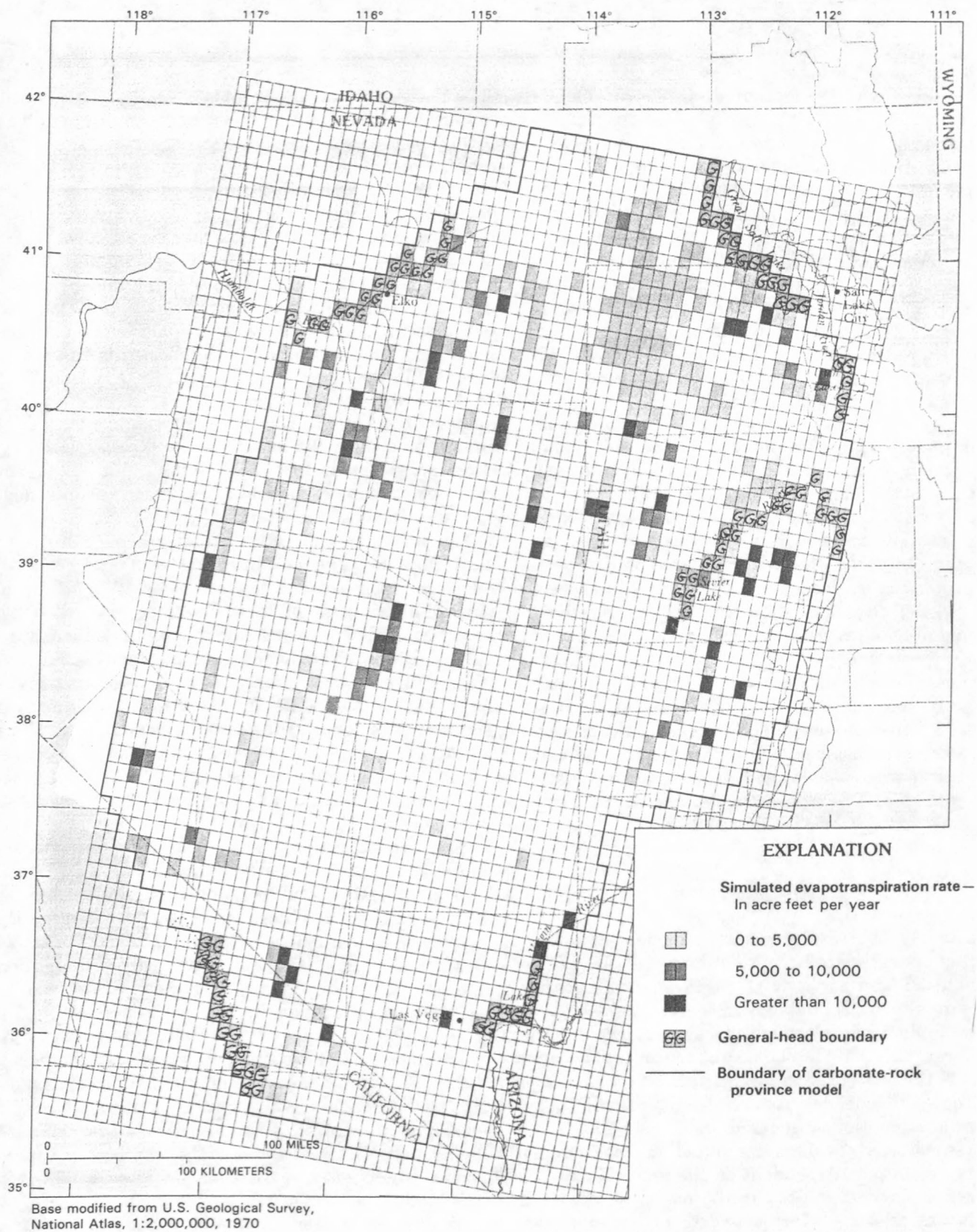


FIGURE 16.--Simulated evapotranspiration rates. Base and grid from figure 9.

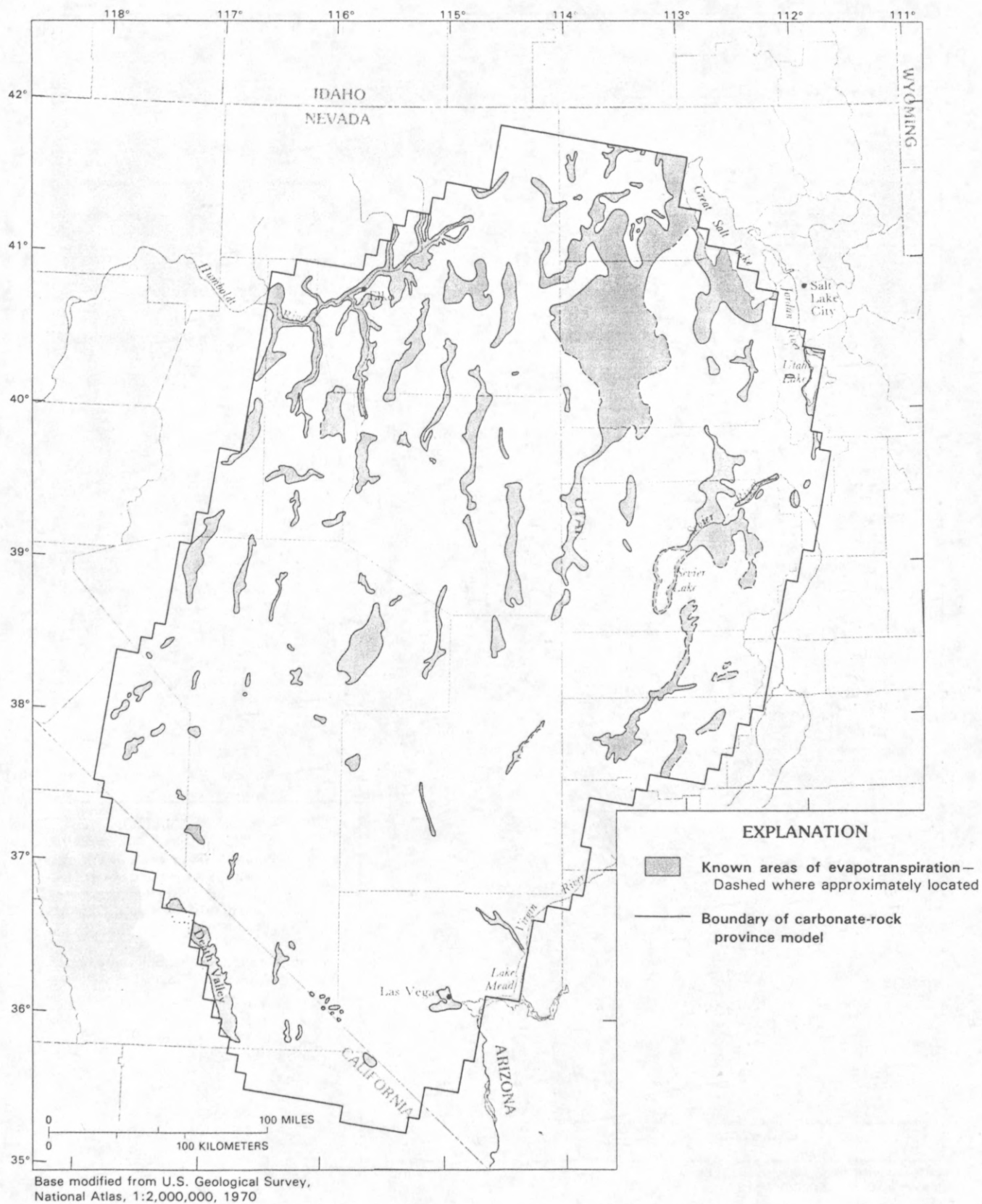


FIGURE 17.--Observed evapotranspiration areas (from Harrill and others, 1988).
Base from figure 12.

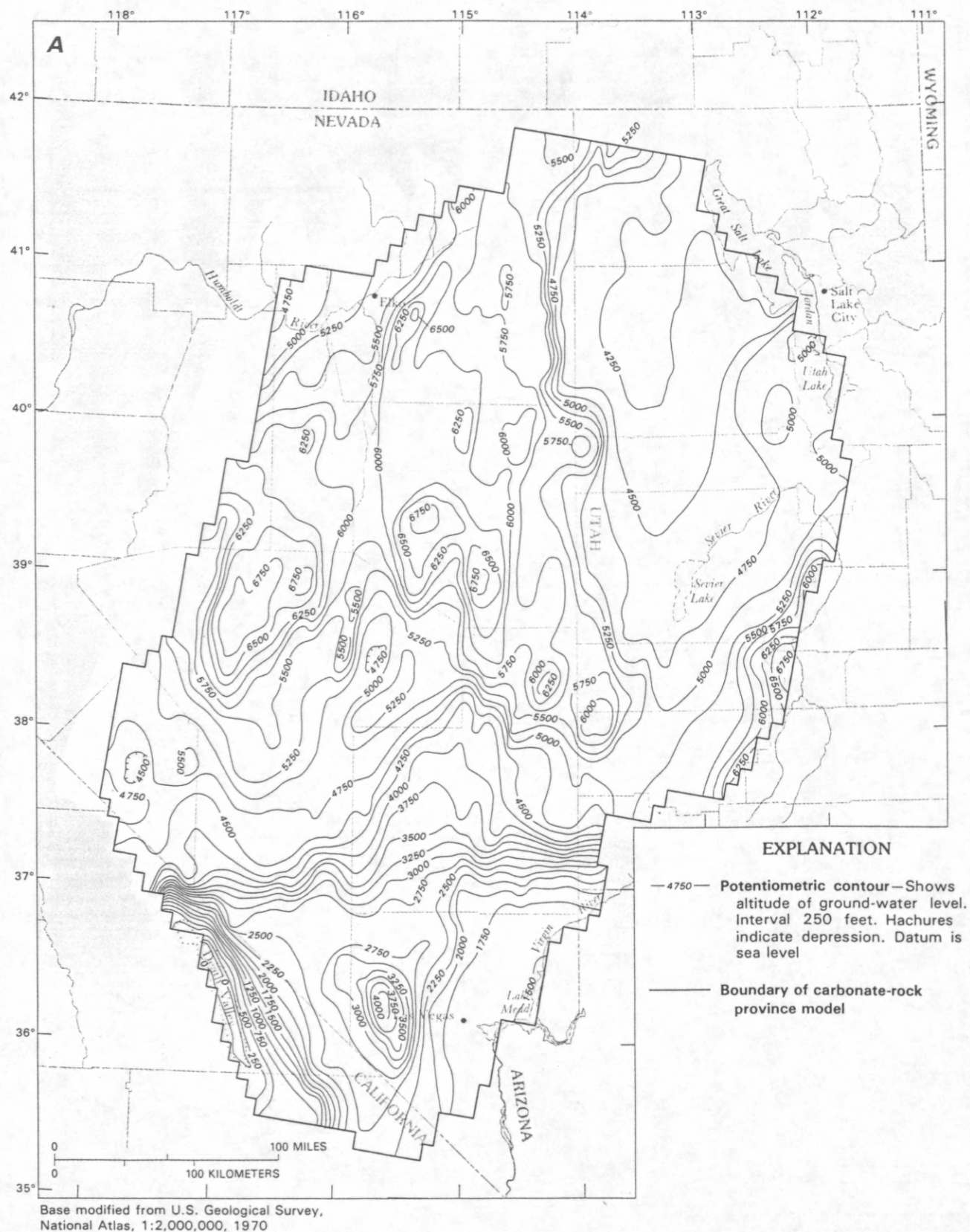


FIGURE 18.--Simulated steady-state water levels. A, Upper model layer. B, Lower Model layer.
Base from figure 12.

perhaps, that a still deeper flow region exists which was not simulated by the model.

The model was designed to simulate ground-water flow at a regional scale. The model grid and cell size was selected with range-front faults generally coinciding with the sides of the model cells and were thus parallel and perpendicular to the two directions of horizontal transmissivity. No other geologic structures were specifically included in the model. However, range-front faults are not the only faults present in the province, but the mountains are extensively faulted as presumably are the rocks beneath the basin fill. Orientation of the model grid to coincide with the range-front faults therefore may be unnecessary. Also, the transmissivity value in one of the two principal directions could be changed with respect to the other direction over the entire modeled area, but no compelling reason was discovered to simulate such a condition. Anisotropy probably exists on a more localized scale, but available computer programs do not allow anisotropy to be specified by individual model cells. However, localized anisotropic conditions could be simulated if cell sizes were reduced. The simulation of ground-water flow with smaller cell sizes is not beyond the scope of this study, but insufficient data over large areas preclude such a detailed simulation.

SIMULATION RESULTS

Discussion of the simulation results have been divided into three sections: (1) computed transmissivity, (2) correlation of ground-water flow with regional geologic features, and (3) distribution of flow in the model layers.

COMPUTED TRANSMISSIVITIES

Although initial transmissivity values were assigned to the upper model layer on the basis of surficial geology, transmissivity values in both model layers were adjusted until model-simulated head values approximated the limited head data and the distribution of discharge approximated the observed distribution. The transmissivity values are also dependent on the amount and distribution of recharge assigned to cells corresponding to mountain ranges. Computed transmissivity values for the upper and lower model layers are shown in figure 19. Values shown in the figure are only approximate; the absolute values are dependent on the estimated amount of recharge assigned to specified model cells. If recharge is increased or decreased proportionately throughout the model, then

the computed transmissivities will increase or decrease in the same proportion.

Errors in transmissivities are unknown but could be off by a factor of 5 and perhaps even more. Other uncertainties used in the model also result in unknown errors, especially the assumption of isotropy in each 37.5-mi² model cell in an area of complex geology. Consequently, it is far more logical to discuss transmissivity trends in qualitative terms. The lowest values on the transmissivity maps (less than 0.0006 ft²/s) will be described as low transmissivity. Occasionally, the term "extremely low" is used to indicate transmissivities at the low end of the spectrum of low values. At the other end of the scale, high transmissivities will be used to denote values greater than 0.18 ft²/s. All other divisions on the maps will be described as intermediate values.

The upper model layer displays a much greater range in values than does the lower model layer. This probably reflects the amount and distribution of recharge and (or) a greater diversity of rock types in the upper model layer or a large variation in the thickness.

Computed transmissivity values for the upper model layer were divided into three generalized groups of rocks on the basis of surficial geology: basin fill, carbonate rocks, and consolidated rocks of low permeability (fig. 20). In some areas, the surficial rocks may be unsaturated, and the computed transmissivity may actually represent flow through some other type of rock. However, the distribution of transmissivity values in figure 20 shows a general pattern when divided into the three rock groups.

Transmissivity values associated with consolidated rocks of low permeability (mostly volcanic and basement rocks) in the upper model layer are generally the lowest. A few model cells corresponding to consolidated rocks of low permeability have high computed transmissivity values, but this may be related to fractured welded tuffs, which Winograd (1971) identified as possible aquifers, or basalts which are known to be aquifers locally in a few areas within the province. The high computed transmissivity values could also be a function of the amount of recharge applied to the model cell. The transmissivity in the cells with large amounts of recharge was increased so that head values did not exceed the average land surface of the cell. Much of the recharge to the aquifers may actually occur on the alluvial fans. Thus, the higher transmissivity values in cells corresponding to consolidated rocks of low permeability may include the transmissivity of the adjacent alluvial fans.

Initially, the carbonate rocks were assumed to be more transmissive than the basin fill. However, the

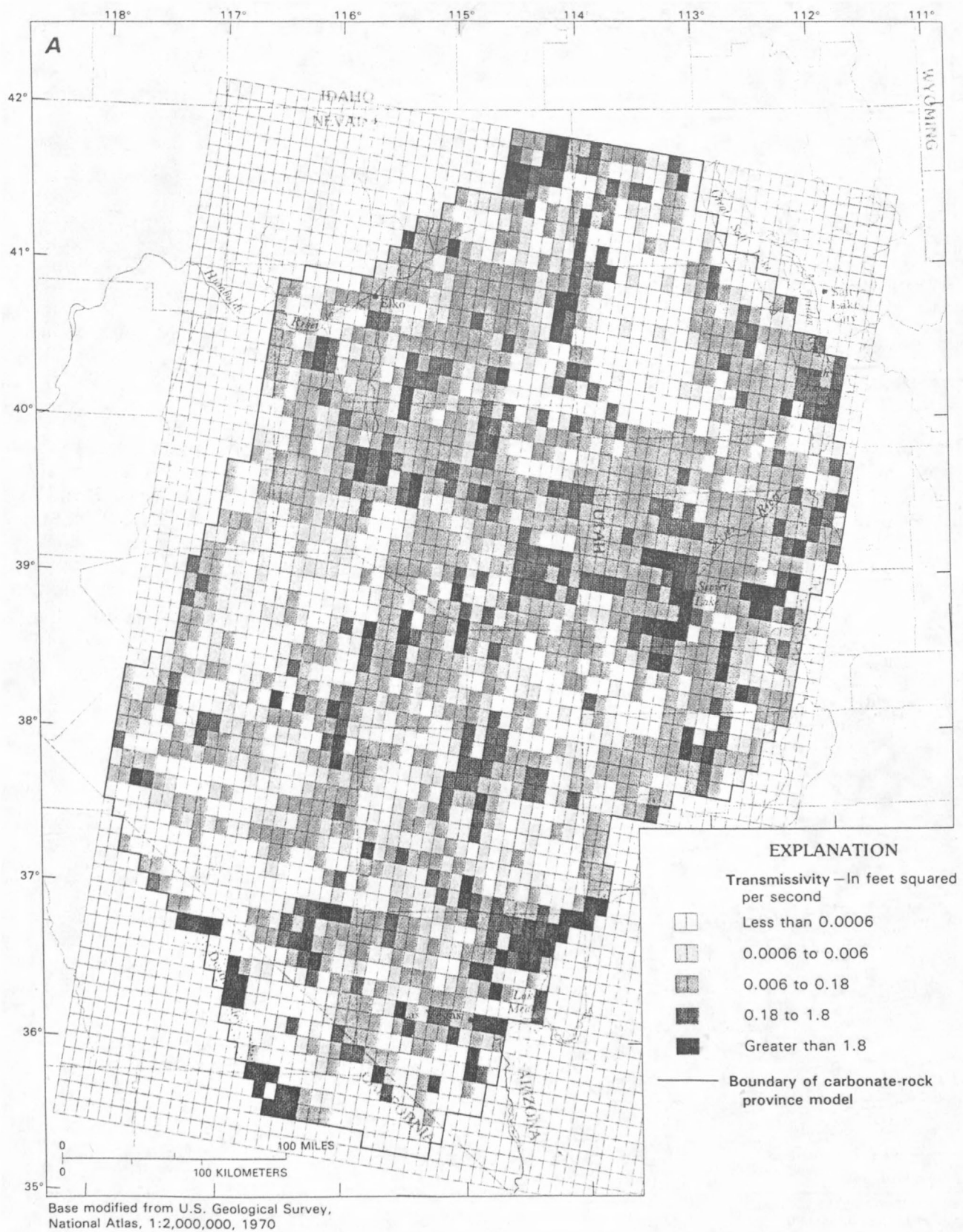
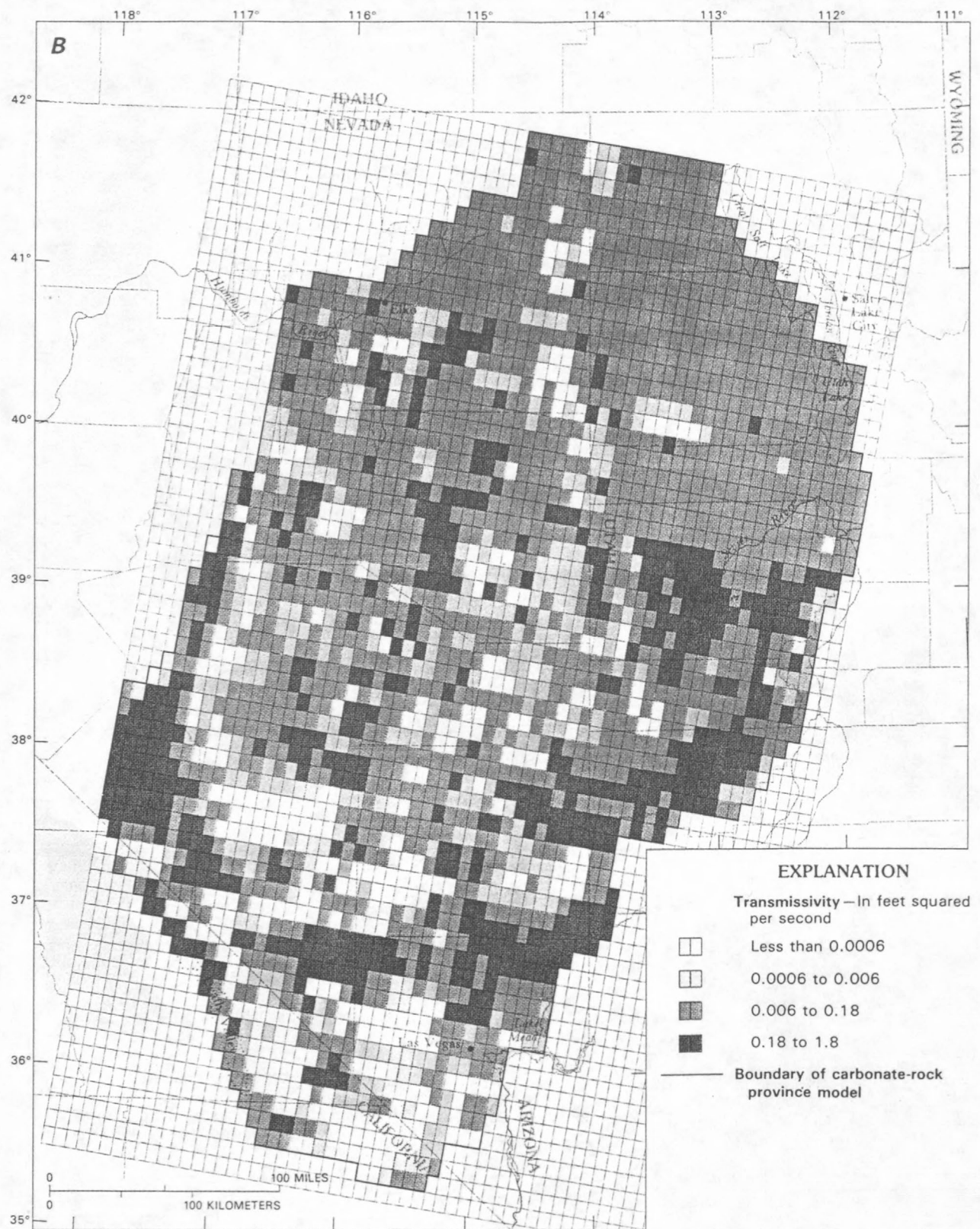


FIGURE 19.—Computed transmissivities. A, Upper model layer. B, Lower model layer. Base and grid from figure 9.



Base modified from U.S. Geological Survey,
National Atlas, 1:2,000,000, 1970

FIGURE 19.--Continued.

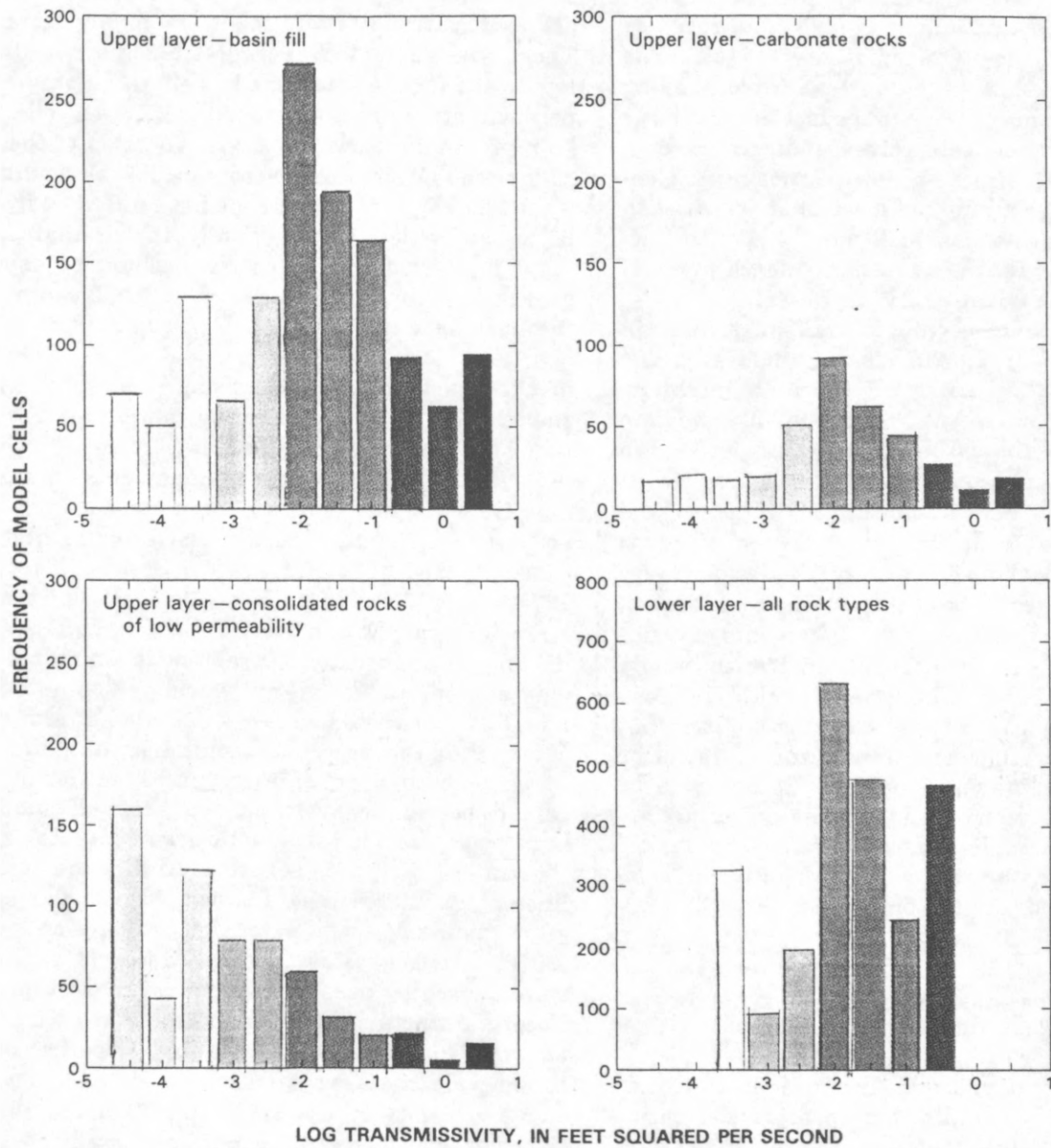


FIGURE 20.--Computed transmissivities in upper model layer in relation to basin fill, carbonate rocks, and consolidated rocks of low permeability and in lower model layer in relation to all rock types. Shades correspond to transmissivity ranges on figure 19.

computed transmissivities of model cells in the upper layer corresponding to basin fill and carbonate rocks have nearly the same distribution (fig. 20), except that model cells corresponding to carbonate rocks do not have as many low transmissivity values. The smaller number of low values in cells corresponding to carbonate rocks may be due to the fact that recharge was generally in model cells corresponding to carbonate and consolidated rocks of low permeability. Conversely, the greater number of low transmissivities in cells corresponding to basin fill may be due to fine-grained sediments that are present beneath many of the playas and the Great Salt Lake Desert.

The distribution of computed transmissivities in the lower model layer (fig. 20) has three distinct peaks. The low transmissivities may correspond to intrusive, metamorphic, or basement rocks; the intermediate values to most of the carbonate rocks or perhaps to fractured welded tuffs; and the high values to fractured carbonate rocks or noncarbonate rocks that are well fractured, such as basalt.

The upper model layer transmissivities are very sensitive to changes in both the volume and location of recharge, and this should be taken into account when interpreting regional trends in transmissivity within the upper layer. The lower model layer, however, is not as sensitive to the location of recharge but changes in proportion to the amount of recharge simulated in the province. Finally, it needs to be restated that these computed transmissivities are approximations. Actual transmissivities may change drastically even within a model cell due to the complexity of the geology in the province.

CORRELATION OF SIMULATED GROUND-WATER FLOW TO REGIONAL GEOLOGIC FEATURES

The most striking geologic structures in the study area are the normal faults that separate the basins and mountains. These faults are the result of extension that has been occurring over the past 17 million years. The model indirectly incorporated the normal faults because the model cells were oriented to correspond to the general strike of the mountain ranges and adjacent basins. Therefore, the edges between model cells that represent basin-fill deposits and consolidated rocks in the mountains also generally coincide with the normal faults.

Faults may provide conduits for flow or act as barriers by abutting rocks of different permeabilities. Discontinuities in rock types along a fault would cause a marked change in the hydraulic gradient across the fault (referred to as fault compartmentalization by

Winograd and Thordarson, 1975, p. 119). In addition, broken rock adjacent to faults could act as a conduit, if the rubble is porous and not cemented, but could act as a barrier if the rock were highly cemented. The model simulated average transmissivity values and heads for the whole model cell, therefore head or permeability changes due to faults within a cell cannot be represented. However, a step function of the head change can be simulated across model cell boundaries whenever adjacent model cells have different hydraulic conductivities. Unfortunately, the simulated head maps for each model layer were contoured using an averaging technique that drew smoothed contours on the basis of a linear interpolation and extrapolation of heads between adjacent model cells. Therefore, marked change in heads among the cells was also smoothed. The smoothed contours were used to show regional trends in simulated flow.

Several east-west-trending lineaments that generally are at right angles to the north-south-trending normal faults have been discussed in the literature (Roberts, 1964, 1966; Eaton, 1975; Stewart and others, 1975, 1977; Ekren and others, 1976; Rowley and others, 1978; and Rowan and Wetlaufer, 1981). These lineaments are usually several tens to a hundred miles long and one to several miles wide. The lineaments tend to be associated with disruption and termination of mountain ranges, stratigraphic discontinuities, east-to east-northeast-trending faults, mineral belts, caldera boundaries, volcanic deposits, and changes in both gravity and aeromagnetic gradients. Rowan and Wetlaufer (1981, p. 1414) proposed that the east-west lineaments are conjugate shears formed during and after middle Miocene extension. Ekren and others (1976, p. 1) suggested that the east-west lineaments were caused by deep-seated crustal control but were uncertain whether the lineaments are partly the result of conjugate shears or were caused by perhaps a continent-wide fracture system.

Stewart and others (1977, p. 67) noted that the Cenozoic igneous rocks crop out in generally east-west-trending belts and that the rocks become successively younger southwestward. The oldest igneous rocks are about 34 to 43 million years old near latitude 40°, and the youngest rocks are about 6 to 17 million years old along an east-west belt near latitude 37°. They postulated that the volcanic front was related to igneous activity localized along a southward propagating transverse break or structural warp in a subducting plate. A similar conclusion was reached by Ekren and others (1976, p. 15), but they also noted that the faulting along the lineaments became younger toward the west and southwest ends, which agrees

with a southwestward decrease in the age of silicic volcanism.

The east-west lineaments could act as barriers to ground-water flow because the features usually extend across many tens to a hundred miles, are several to many miles wide, and may disrupt the continuity of Paleozoic carbonate rocks by the repositioning of less permeable intrusive and (or) extrusive rocks, or by movement along left-lateral strike-slip faults. The lineaments are superimposed on the model simulated heads in figure 21 for upper and lower layers. One lineament, the Oregon-Nevada lineament described by Stewart and others (1975), trends in a northwesterly direction essentially parallel to the Walker belt, a zone of right-lateral shears. The Oregon-Nevada lineament (also referred to as the Cortez rift) is characterized by north-northwest trending belt of closely spaced faults, centers of volcanic activity during the late Miocene, and a conspicuous aeromagnetic anomaly. Also shown in figure 21 are the known volcanic source areas in Nevada, known metamorphic core complexes, and east-west-trending mineral belts.

Of the lineaments shown in figure 21, only the transverse crustal boundary of Eaton (1975) clearly corresponds to a marked change in the simulated heads in both model layers, as the gradient simulated in the model increases across this lineament. Wells drilled into basin-fill deposits across the lineament also have much steeper gradients than elsewhere (Thomas and others, 1986). The lineament is also marked by a considerable decrease in altitude; valley floors north of the lineament are generally 4,000 ft above sea level, whereas south of the lineament, valley floors are 2,000 ft or less above sea level.

The lineament marks the southern limit of Cenozoic igneous activity as Cenozoic volcanic rocks are virtually absent south of it. Known volcanic source areas along the lineament are concentrated at the east and west ends. The low computed transmissivity values at these locations (fig. 19) cause most of the simulated flow to be channeled across the middle of the lineament.

Aligned along the transverse crustal boundary are left-lateral shear zones. These zones may also act to restrict flow across the lineament, as suggested by the discharge of ground water from springs just up-gradient of the Pahrnagat shear zone (fig. 21A). Ekren and others (1976) discussed the presence of other left-lateral faults along the lineament near the Utah-Nevada border and in the southern part of the Nevada Test Site.

The other lineaments shown in figure 21 do not correspond to changes in simulated head as noticeable as the transverse crustal boundary, although many of

the regional springs (discharge points in the lower model layer shown in fig. 21B) may be controlled at least in part by structures related to the lineaments. Computed transmissivity values (fig. 19) are generally lower in model cells that correspond to lineaments, although no consistent pattern exists. The Oregon-Nevada lineament corresponds to a discontinuous zone of low transmissivity values in the lower model layer (compare figs. 19B and 21B). This lineament also corresponds to the presence of anomalous springs at several places along its extent.

The Warm Springs lineament in Nevada (feature 1 in fig. 21) and the Blue Ribbon lineament (feature 5 in fig. 21) generally cut across the study area at latitude 38°. The Blue Ribbon lineament in Utah is associated with the Pioche mineral belt, which has abundant volcanic deposits that are elongated in an east-west direction (Ekren and others, 1977; Rowley and others, 1978, p. 180), and generally corresponds with the simulated divide between northward flow toward the Great Salt Lake Desert and southward flow toward the Virgin River and Lake Mead.

The lack of pronounced changes in simulated heads, simulated transmissivity values, and water levels in wells along the lineaments north of the transverse crustal boundary could be due to normal faulting disrupting the lineaments, which are considerably older in age than the normal faults. Based on known heads, the older lineaments act as leaky barriers to ground-water flow. In contrast, igneous activity along the transverse crustal boundary began at about the same time as the normal faulting. Perhaps the structures and implaced intrusions along this lineament have not been disrupted, so that the lineament still acts as a barrier to flow.

Water levels in wells immediately north of the transverse crustal boundary are more than 1,000 ft higher than water levels in wells 15 mi to the south (Thomas and others, 1986), creating a much steeper hydraulic gradient than generally exists elsewhere in the study area. For example, the hydraulic gradient in central Utah is about 1,000 ft in 100 mi.

Some structures that might affect ground-water flow could not be correlated with the simulated heads and computed transmissivity values. In general, major thrust faults could not be correlated with simulated and observed heads or with computed transmissivity values at the regional scale of the model. Perhaps this is due to masking by other features or due to the size of the model cells used in the simulations, or perhaps the effects of these features on regional ground-water flow are minimal. Thrust faults might act as barriers to flow, particularly to vertical flow, where less permeable rocks have been thrust over more permeable rocks

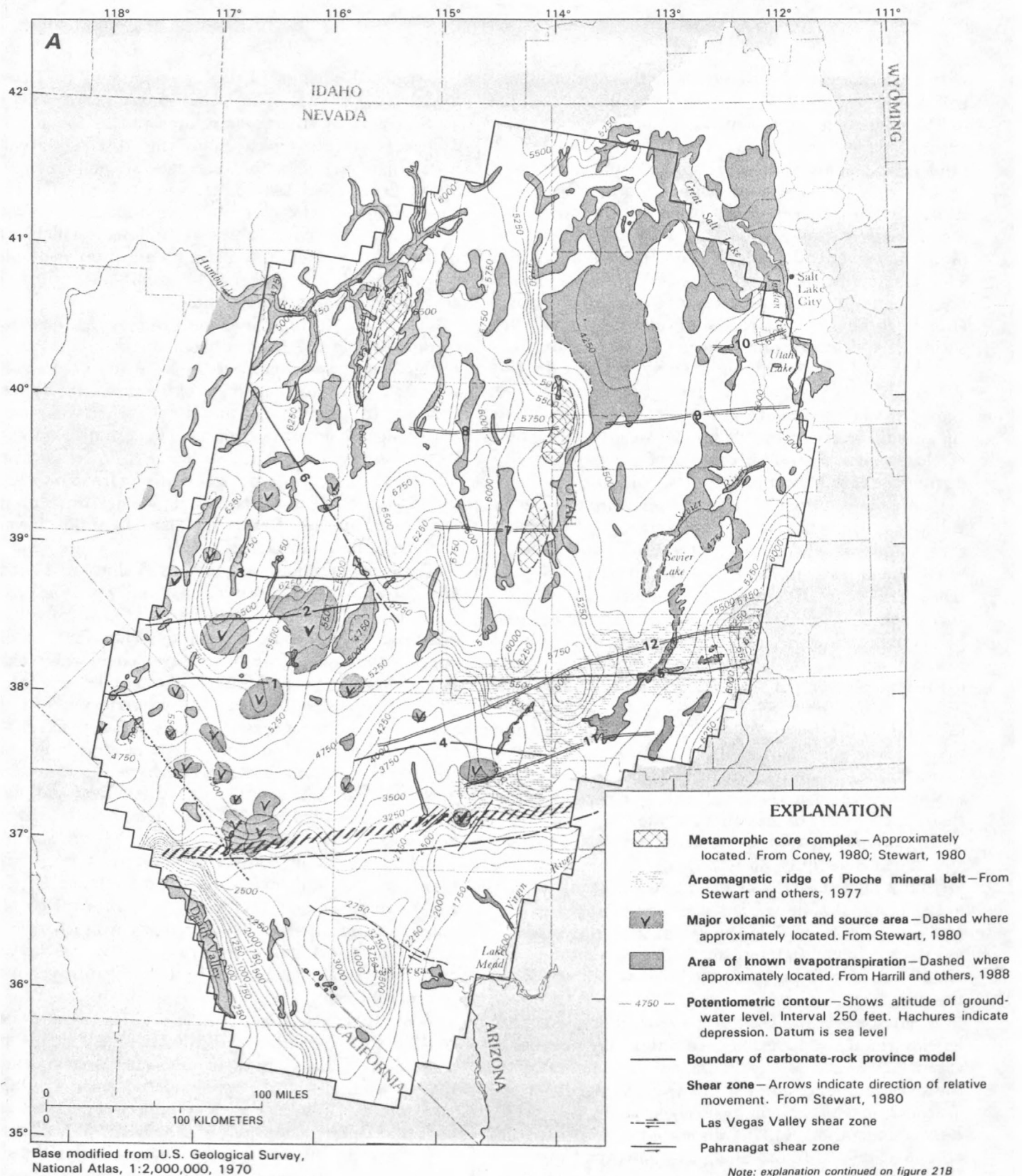


FIGURE 21.--Selected geologic features and simulated water levels. A, Upper model layer including areas of evapotranspiration. B, Lower model layer including regional springs. Base from figure 12.

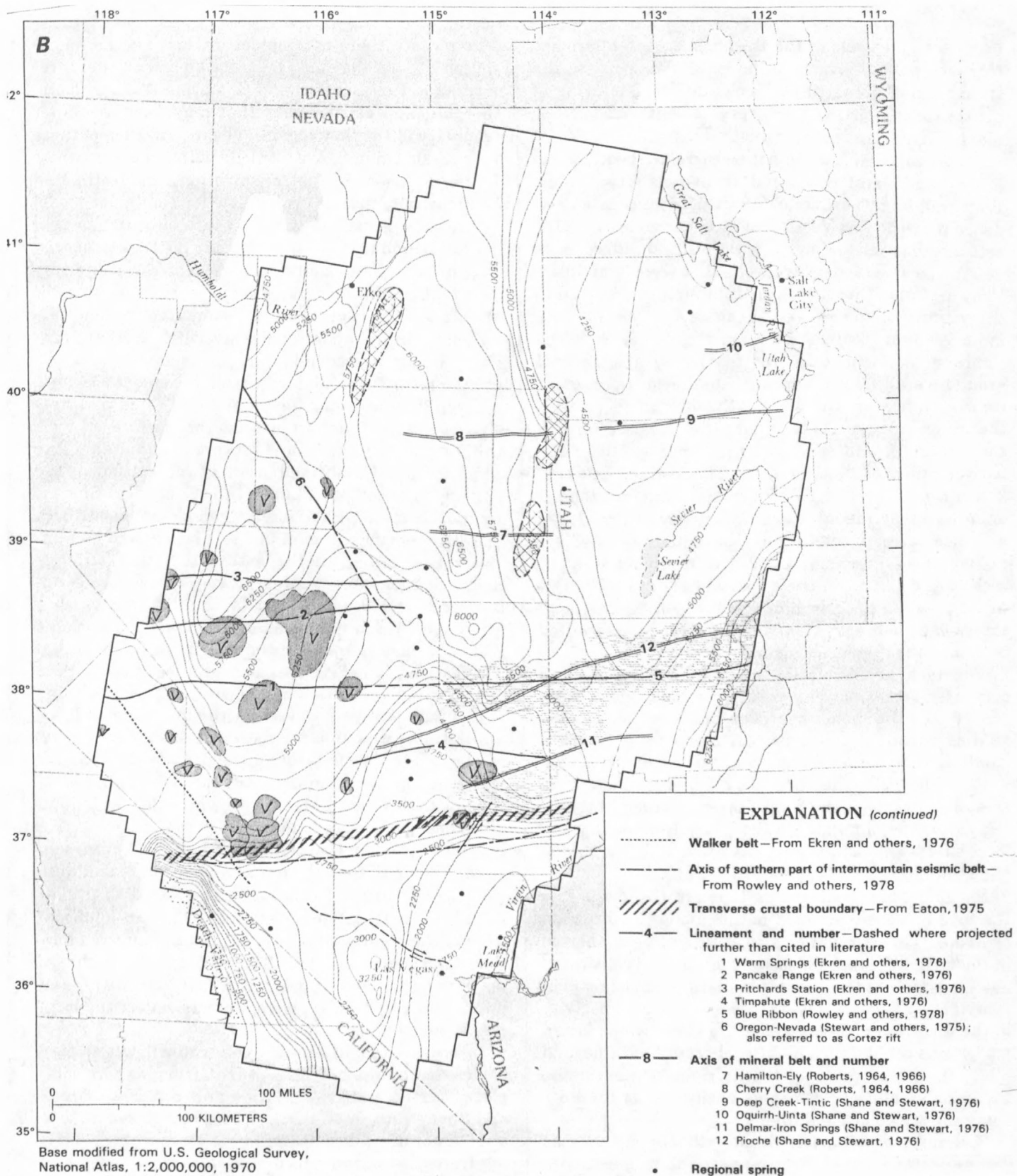


FIGURE 21.--Continued.

or where gouge along the thrust has been altered to clay. However, thrust faults could also increase the transmissive properties of rocks due to fracturing of brittle rocks, particularly near the center of folds or along the margins of the thrust plates.

Shear zones also could not be correlated with simulated heads and computed transmissivity values. Winograd and Thordarson (1975, p. 67) discussed evidence that the Las Vegas Valley shear zone (fig. 21A) acts as a barrier to flow, as a water-level difference of 600 ft was observed in two wells that were 3 mi apart. They assumed that most of this difference occurred in the vicinity of the shear zone instead of assuming a more gradual gradient between the two wells. The Pahranaagat shear zone (fig. 21A) may also restrict ground-water flow as springs discharge upgradient from it; however, the shear zone is coincident with the transverse crustal boundary (fig. 21) described by Eaton (1975), and springs may be the result of the barrier effect of that feature. The Walker belt (fig. 21A) also may restrict flow across it, but the zone is an area of abundant volcanic activity (Carr, 1984) and also corresponds to the approximate area where exposures of Precambrian and Cambrian basement rocks are common in the mountain ranges. Thus, it is not possible to determine if strike-slip faults along the Walker belt act as barriers or if flow is restricted by some other geologic feature.

The lack of correlation of simulated heads and computed transmissivity with strike-slip faults could reflect how the model averages heads and transmissivities within a cell area. A steep drop across a small distance of a mile or so could not be simulated with model cells that are 5 by 7.5 mi. Instead, a smoother gradient and a less severe change in transmissivity was simulated, thus possibly masking any local effects that could be related to a series of strike-slip faults.

Shear zones might act as barriers to flow across the zone but could act as conduits along the direction of strike. This possibility also could not be simulated in the model because anisotropy of selected cells could not be simulated without simulating anisotropy in every cell of a model layer. Increasing transmissivity in the direction of strike along the shear zones for all model cells could not be justified, because most normal faults in the study area are at right angles to the shear zones and could just as easily act as conduits along the strike of the faults.

Perhaps more important than the lineaments as ground-water barriers are the associated igneous intrusive rocks. Russell W. Plume (U.S. Geological Survey, written commun., 1985) delineated the outcrops of rocks that he considered to be of low permeability.

The rocks include outcrops of intrusive rocks, metamorphic rocks that may be associated with the intrusives, and Precambrian and Cambrian igneous, metamorphic, and clastic rocks that may form the lower boundary of the flow region. The distribution of these rocks is shown in figure 22 along with simulated water levels, areas of evapotranspiration, and estimated boundaries of ground-water flow for the upper model layer. Low-permeability rocks south of the transverse crustal boundary (south of latitude 36°) are generally Precambrian and Cambrian basement rocks and suggest that carbonate rocks are either not very thick or absent over parts of the area. Computed transmissivity values in the upper model layer (fig. 19A) are generally low in model cells that correspond to outcrops of the Precambrian and Cambrian basement rocks.

Deep ground-water flow may be affected by intrusive bodies that do not extend the surface or by a thinning of the carbonate rocks such that the Precambrian and Cambrian basement rocks are near the surface. Russell W. Plume (U.S. Geological Survey, written commun., 1985) interpreted aeromagnetic data to derive a distribution of possible barriers to ground-water flow based on the assumption that strongly magnetic rocks were representative of low-permeability intrusive rocks and Precambrian basement rocks. The technique first filtered out the surficial volcanic rocks that act as "noise" from the aeromagnetic data. The distribution of rocks that might act as barriers to deep ground-water flow is shown in figure 23, along with simulated water levels for the lower model layer and estimated boundaries between deep-flow regions in the lower model layer. Low-permeability clastic rocks may be considerably more extensive in the subsurface than in the outcrops shown in figures 22 and 23. These clastic rocks may also prove to be effective barriers to deep flow (Winograd and Thordarson, 1975). Some of the regional springs used to simulate discharge from deep flow could be related to the inferred low-permeability rocks (fig. 23). In addition, most of the simulated flow is around the inferred barriers, which suggests that the distribution of discharge may in part reflect buried regional structures and implies that hydraulic gradients may reflect the location of such barriers.

Intermediate and deep ground-water flow also may be affected by the presence of metamorphic core complexes in the Ruby Mountains and the Deep Creek and Snake Ranges (fig. 23). These complexes include a metamorphic-plutonic basement terrane, an overlying transition zone of abrupt change in lithology and structure characterized by intense strain, and an unmetamorphosed suprastructure characterized by low-angle detachment faults (Stewart, 1980; Coney, 1980).

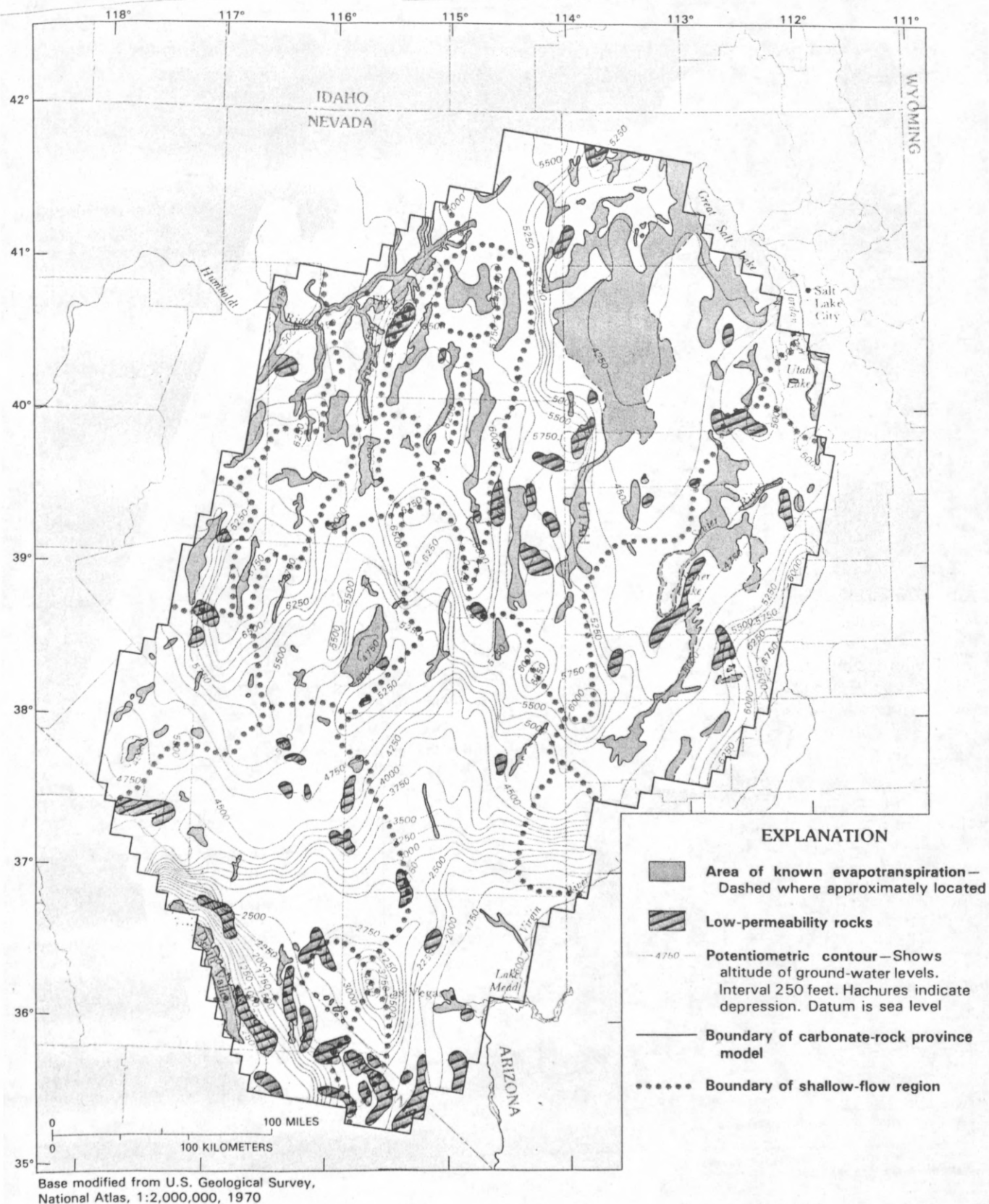


FIGURE 22.--Outcrop areas of rocks that are potential barriers to ground-water flow (Russell W. Plume, U.S. Geological Survey, written commun., 1985), distribution of evapotranspiration, simulated water levels, and estimated flow regions in upper model layer. Base from figure 12.

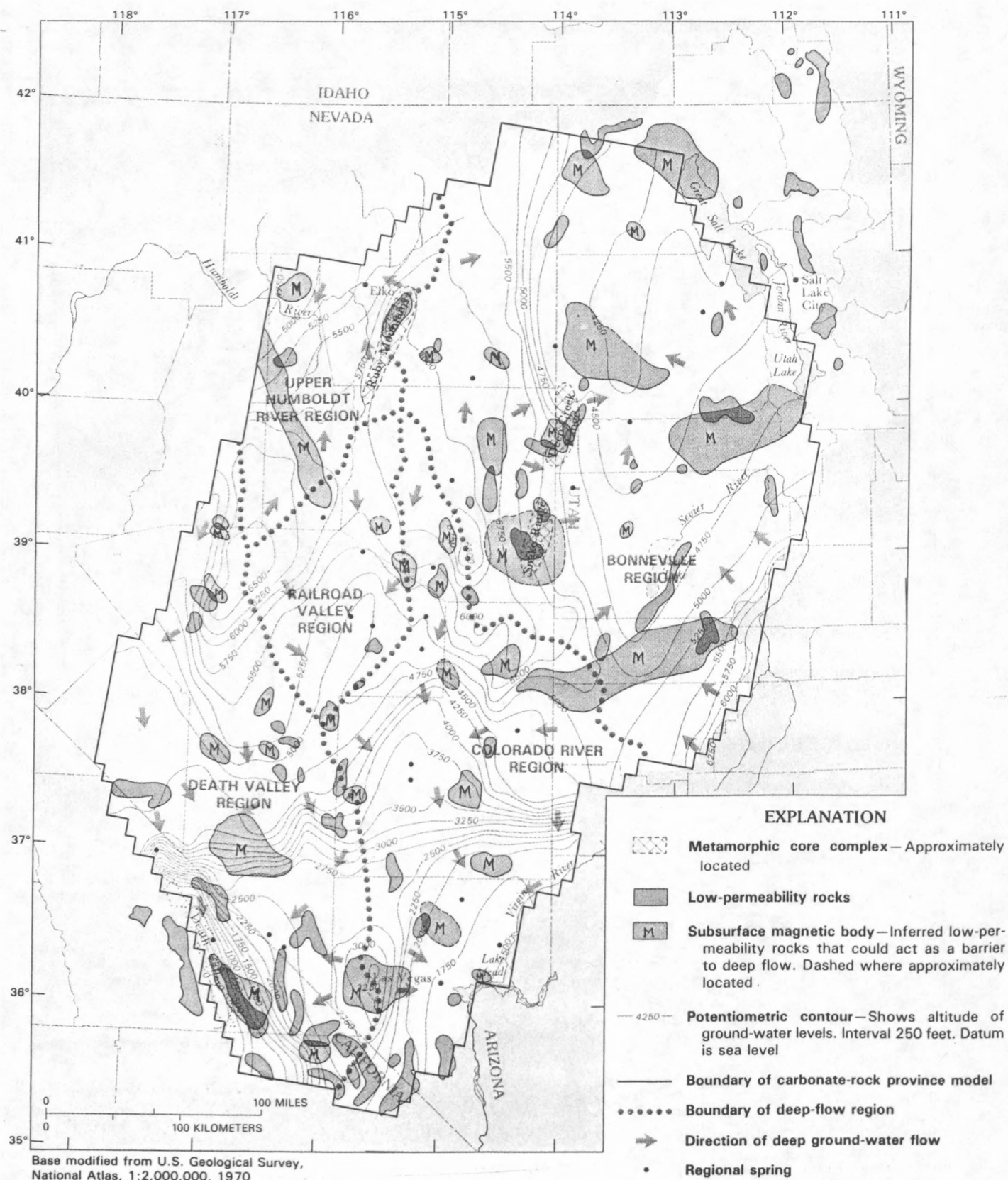


FIGURE 23.--Metamorphic core complexes (Coney, 1980; Stewart, 1980), subsurface magnetic source bodies, outcrop areas of rocks that are potential barriers to ground-water flow (Russell W. Plume, U.S. Geological Survey, written commun., 1985), distribution of regional springs, simulated water levels, and estimated flow regions in lower model layer. Base from figure 12.

Metamorphic core complexes, which in general do not coincide with strong magnetic anomalies (Russell W. Plume, U.S. Geological Survey, written commun., 1985), may act as barriers to ground-water flow. Computed transmissivities of the lower model layer generally are low in the vicinity of the metamorphic core complexes (fig. 19B), causing mounding effects at these locations. Simulated ground-water flow in areas of the core complexes was radially outward. Estimated recharge in mountains associated with the core complexes was higher than in adjacent mountains because the mountains are higher in altitude, thus contributing to the radial flow pattern.

DISTRIBUTION OF FLOW INTO REGIONS

Ground-water flow simulated in the lower model layer was divided into five regions (fig. 23). Flow regions are used to describe the five areas instead of flow systems because the boundaries that separate the areas were determined from calculations of horizontal flux for each model cell instead of some known geologic boundary. The five deep-flow regions in the lower model layer—the Death Valley region, the Colorado River region, the Bonneville region, the Railroad Valley region, and the Upper Humboldt River region—are named for the terminal discharge area within each region. The Bonneville region encompasses both the Great Salt Lake and the Great Salt Lake Desert, which together act as the terminal sink for much of western Utah.

Superimposed on the deep-flow regions in the lower model layer are 17 shallow-flow regions (fig. 22) as identified from calculations of horizontal net flux for each model cell in the upper model layer. The shallow-flow regions approximately coincide with 17 flow systems delineated by Harrill and others (1988) according to topography, water levels, discharge areas, and water budgets.

Boundaries of the deep-flow regions do not always correspond to the boundaries of the shallow-flow regions. For example, the boundary of the Colorado River region in the lower model layer includes parts of shallow-flow regions simulated in the upper model layer that are generally included in the Bonneville and Death Valley flow regions. Furthermore, the Railroad Valley region includes parts of shallow-flow regions simulated in the upper model layer that are generally included in the Death Valley and Upper Humboldt River flow regions. Overall, the Death Valley region includes all or part of eight shallow-flow regions while the Bonneville region includes all or part of six shallow-flow regions. The other three

deep-flow regions include only a few shallow-flow regions.

The interconnection between model layers is illustrated by a vertical flow component map (fig. 24). The map shows where flow is predominantly upward, downward, or horizontal and depicts the general concept of flow between the two model layers. Downward flow generally occurs in areas of recharge, particularly in model cells corresponding to carbonate rocks. Upward flow generally occurs in model cells corresponding to areas of discharge. In model cells that simulated little vertical flow (areas of horizontal flow in fig. 24), the vertical leakance values could not be determined with any reliability because changing the values had no effect on the heads in adjacent cells in the two model layers.

The horizontal direction of ground-water flow in the upper model layer may be opposite to flow in the lower model layer. Dinwiddie and Schroder (1971) discussed such a difference in ground-water flow between shallow and deeper flow in the Railroad Valley region on the basis of water-level trends. Such variations in flow may be caused by differing controls, the shallower flow being controlled by more localized features such as topography while deeper flow may be controlled by geologic features such as low-permeability rocks or thinning of the carbonate rocks.

The next sections discuss the results of model simulations, in particular the direction and magnitude of ground-water flow in each of the five deep-flow regions delineated from flux calculations in the lower model layer. The discussions include simulation results of ground-water flow directions and magnitude of flow through the upper model layer where somewhat different regions are superimposed over each of the five deep-flow regions. In several instances, the flow regions are compared to flow systems defined by other investigators.

FLOW REGIONS

DEATH VALLEY REGION

The Death Valley region includes some of the most intensively studied areas within the Great Basin. Before and since the inception of nuclear testing on the Nevada Test Site in December 1954, numerous studies have been undertaken in an effort to delineate ground-water flow in the vicinity of the Test Site to assess the possibility of radionuclide migration to areas off-site. Numerous authors have published reports on the hydrogeologic framework of south-central Nevada

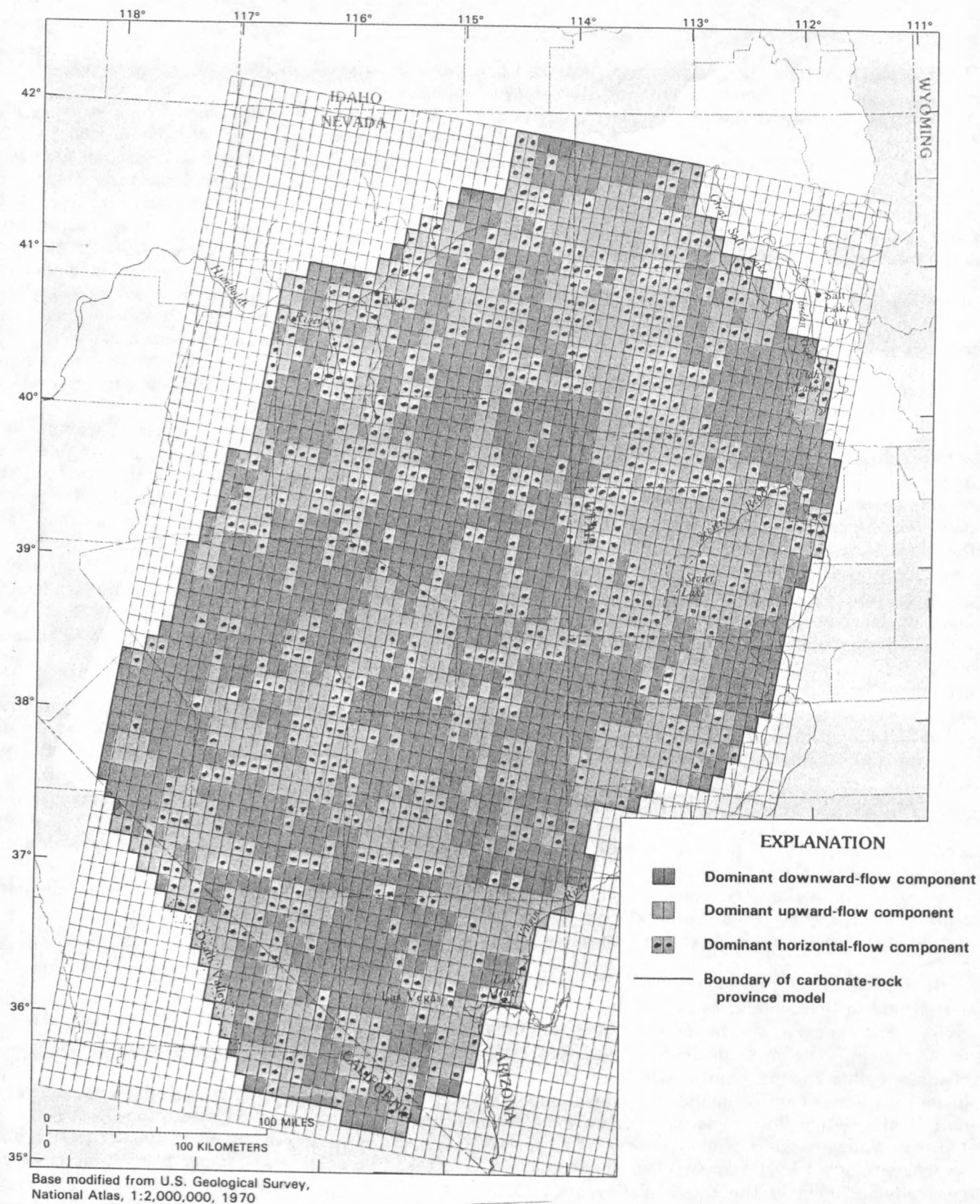


FIGURE 24.--Distribution of simulated flow in areas having components of predominantly upward, downward, and horizontal flow. Base and grid from figure 9.

and adjoining California (Winograd and Eakin, 1965; Winograd and Thordarson, 1968, 1975; Rush, 1970; Winograd and Friedman, 1972; Blankennagel and Weir, 1973; Winograd and Pearson, 1976; Waddell, 1982; and Waddell and others, 1984).

The Death Valley flow region is in the southwestern part of the study area (fig. 23). Its total area is slightly less than 20,000 mi² and includes the north end of Big Smoky Valley to the north, Death Valley to the south and west, and the Pintwater and Groom Ranges to the east (fig. 25). This flow region includes all or part of eight shallow-flow regions simulated in the upper model layer (fig. 22).

RECHARGE

Recharge areas for the Death Valley region (fig. 25) include the eastern slope of the Toiyabe Range, Toquima Range, southern Monitor and Hot Creek Ranges in the north and Spring Mountains in the south. Many other smaller mountain ranges were also simulated as recharge areas, but the amounts of water were small. Total estimated recharge to the region is about 165,000 acre-ft/yr. Great care had to be taken in estimating total recharge in areas where flow from the upper model layer crosses over the flow boundary for the lower model layer because recharge was simulated only to the upper layer. No water was simulated as entering the Death Valley region from Pahrnagat Valley or the Sheep Range to the east, which are part of the Colorado River region, as postulated by Winograd and Thordarson (1975) and Waddell and others (1984). Reasons for this difference in flow will be discussed below.

DISCHARGE

Simulated discharge from the Death Valley region was by evapotranspiration (ET) and regional springs (fig. 25). Springs that discharge water from the upper model layer alone were included as ET in the simulation. Major areas of ET occur in the northern parts of Big Smoky and Clayton Valleys. Pahrump and Death Valleys, Sarcobatus Flat, and small areas in the Amargosa Desert (which includes Ash Meadows) also discharge minor amounts of water by ET. Spring discharge occurs in numerous localities, although only Ash Meadows was simulated since that area, along with perhaps the springs at Furnace Creek and the Mesquite Flat area in northern Death Valley, were considered regional springs. Springs at Furnace

Creek, which include Nevares, Texas, and Travertine springs, were included in the general-head boundary at Death Valley. In the simulation, discharge out of this area was determined by calculating flow out of the cells assigned as general-head boundaries.

FLOW SYSTEMS

Simulation results suggest that the Death Valley flow region contains individual or compartmentalized flow paths that ultimately have Death Valley as the terminal sink, yet behave somewhat independently of each other. Blankennagel and Weir (1973) and Winograd and Thordarson (1975) further divided the Death Valley region into two flow systems (areas west and north of Cactus Flat were not discussed in either of the above mentioned reports; however, this large area is included in the Death Valley region in this study). Figure 26 outlines these systems; the Pahute Mesa-Oasis Valley flow system borders the Ash Meadows flow system along the Belted Range, which trends north-northeast to south-southwest just east of Kawich Valley and Pahute Mesa. Neither a northern nor a southern boundary was fixed in either report, although both reports indicated that underflow into the flow system from the north and southward flow to Death Valley is possible. Blankennagel and Weir (1973) suggested that recharge to this system flows southwest through Pahute Mesa from Kawich Valley and Gold Flat. Roughly 5,500 acre-ft/yr of ground water originates from areas to the north and northwest, according to Eakin and others (1963). An additional 2,500 acre-ft/yr was added at Pahute Mesa; thus, a total of 8,000 acre-ft/yr was estimated to flow from Pahute Mesa to Oasis Valley, parts of southwestern Nevada Test Site, and possibly to Death Valley, where ground water is discharged by ET or springs.

Simulation results (fig. 26) suggest that a ground-water divide runs through the eastern part of Pahute Mesa that trends northeast into Kawich Valley and is nearly coincident with the divide discussed by Blankennagel and Weir (1973) and Winograd and Thordarson (1975). Flow through the lower model layer from the Toquima, Monitor, and Kawich Ranges beneath northern Sarcobatus Flat, Cactus Flat, and Kawich Valley was about 7,500 acre-ft/yr. Along with the estimated 2,500 acre-ft/yr of recharge atop Pahute Mesa, a total of 10,000 acre-ft/yr was simulated to flow from these northern areas to discharge areas in Oasis Valley, the Amargosa Desert, Death Valley, and Ash Meadows springs where about 2,000 acre-ft/yr of

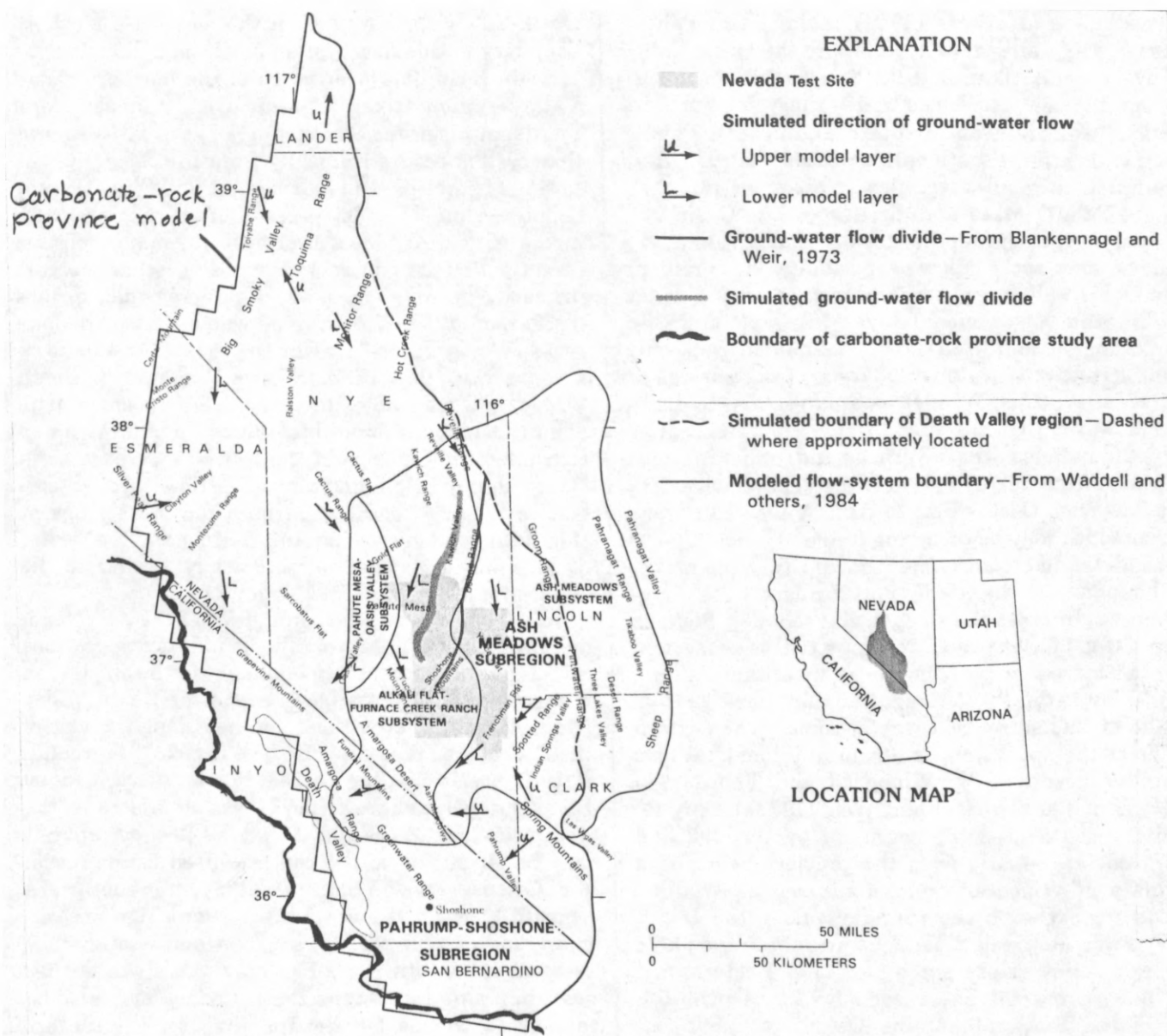


FIGURE 26.--Simulated flow-system boundaries, ground-water divides, and flow paths compared with those described in previous hydrologic studies for Death Valley region.

the total was simulated as crossing the Ash Meadow flow system boundary near Yucca Mountain (fig. 26).

Waddell and others (1984) divided the Pahute Mesa–Oasis Valley flow system into the Oasis Valley subsystem and Alkali Flat–Furnace Creek Ranch subsystem (fig. 26). The Oasis Valley subsystem includes parts of Gold Flat and western and central Pahute Mesa and extends southward to Oasis Valley. In this simulation, ground-water flow crosses western and central Pahute Mesa and discharges into Oasis Valley. Discharge of ground water into Oasis Valley may occur because rocks of low permeability downgradient from Oasis Valley result in a barrier to ground-water flow in the lower model layer (figs. 23 and 26). Blankennagel and Weir (1973) estimated that only 2,000 acre-ft/yr of water discharges at the springs at Oasis Valley; thus, Waddell and others had to disregard flow from Cactus Flat in order for their water budget to balance. On the other hand, underflow was simulated from Cactus Flat to Oasis Valley, suggesting that flow from Cactus Flat to Oasis Valley and areas farther south may be occurring (table 2).

Waddell and others (1984) thought that the northern boundary of the Alkali Flat–Furnace Creek subsystem might cross the Cactus, Kawich, and Reveille Ranges (fig. 26). Principal recharge to this subsystem was considered to be from these mountain ranges. Waddell and others also recognized that recharge from outside of this subsystem was possible. The eastern border of the subsystem is essentially identical to a boundary described by Winograd and Thordarson (1975) and Blankennagel and Weir (1973). Only toward the south does the boundary by Waddell and others deviate greatly from the previously proposed boundary of Winograd and Thordarson as Waddell and others extended the boundary along the Death Valley–Furnace Creek shear zone just above the playa in Death Valley. Hunt and others (1966) determined that flow across the shear zone (which is near the base of the Black Mountains west of the Funeral Mountains and along the margin of the valley) must occur since phreatophytes thrive high up on the fans on the east side of Death Valley. On the basis of interpretations by Winograd and Thordarson, Waddell and others, and this study, discharge at the Furnace Creek area is probably a mixture of water from the Oasis Valley and Alkali Flat–Furnace Creek subsystems (Pahute Mesa–Oasis Valley flow system) along with the Ash Meadows flow system.

According to studies by Winograd and Friedman (1972), Winograd and Thordarson (1975), and Waddell and others (1984), the Ash Meadows flow system extends from Pahrangat Valley southward through the Sheep Range to the Spring Mountains and westward

to Ash Meadows in the southern Amargosa Desert (fig. 26). This flow system borders the Pahute Mesa–Oasis Valley flow system on the west. No northern boundary to this flow system has been delineated due to scant head data over much of the northern Death Valley region (figs. 12 and 13). Winograd and Friedman suggested that recharge to the Ash Meadows flow system occurs primarily from the Sheep Range, Spring Mountains, and Pahrangat Valley (which may supply as much as 35 percent of the spring water discharging at Ash Meadows) with only minor amounts from the Belled and Groom Ranges. Discharge occurs primarily at Ash Meadows, where regional springs discharge 17,000 acre-ft/yr of water from carbonate rocks (Winograd and Friedman, 1972). An unknown amount may flow beneath Ash Meadows to Death Valley; however, no estimates have been made as to what this amount might be. Winograd and Friedman concluded that springs in the Furnace Creek area in Death Valley originate from deep flow through carbonate rocks. Geochemical data for the springs at this locality suggest that the 5,000 acre-ft of water discharging each year is isotopically similar to the water discharging at Ash Meadows.

In the simulation, the boundaries of the Ash Meadows flow system differ from the boundaries of previous investigators. The eastern boundary in the simulation is the ground-water divide between the Death Valley and Colorado River regions and lies along the axis of the Groom and Pintwater Ranges (fig. 26). A ground-water barrier similar to the barrier described by Blankennagel and Weir (1973) was simulated as the west boundary of the Ash Meadows flow system but may be offset due to the cell size used in the model simulations. Flow in both model layers is southward beneath Yucca Flat and southwestward from Frenchman Flat to Ash Meadows. The north-south flow component beneath Yucca Flat may actually be farther east than simulated, thus the boundary may also be farther to the east—perhaps through the Desert Range.

Water discharging at Ash Meadows was simulated as originating primarily from mountain ranges near the eastern part of the Nevada Test Site southward to the Spring Mountains. However, as much as 3,000 acre-ft/yr was simulated as entering the Ash Meadows flow system as deep flow through the lower model layer originating in the southern Hot Creek and Monitor Ranges. Deuterium values in Reveille Valley north of the Test Site indicate fairly light water (-110 permil)¹, similar to the water that would be “expected” as recharge in the mountain ranges in the northern

¹The Deuterium-to-hydrogen ratio is determined for a sampled water and then related to the comparable ratio for the reference standard Vienna Standard Mean Ocean Water (V-SMOW). Units are in parts per thousand (permil). A negative value indicates that the sampled water is isotopically lighter (has a smaller proportion of deuterium) than the standard.

TABLE 2.--Simulated ground-water flow budgets, Death Valley region,
in acre-feet per year

	Pahute Mesa- Oasis Valley system ^a	Ash Meadows system ^b	Pahrump- Shoshone subregion	Death Valley region
Recharge				
Mountain blocks	117,000	26,000	22,000	165,000
Subsurface inflow from adjacent flow	3,000	2,000	0	(c)
Head-dependent boundaries	0	0	0	0
	-----	-----	-----	-----
Total recharge	120,000	28,000	22,000	165,000
Discharge				
Evapotranspiration	95,000	5,000	22,000	122,000
Regional springs	0	20,000	^d 0	20,000
Subsurface outflow	^e 2,000	^f 3,000	0	(c)
Death Valley playa	^g 23,000	0	0	23,000
	-----	-----	-----	-----
Total discharge	120,000	28,000	22,000	165,000

^a Simulation results are on the basis of system boundaries derived by Waddell and others (1984); includes Death Valley area and vicinity.

^b Simulation results are on the basis of system boundaries derived from Winograd and Thordarson (1975) with the exception of the eastern boundary, which was confined to the Death Valley region boundary.

^c Subsurface inflow and outflow is between flow systems and subregions within the Death Valley region.

^d Discharge from springs in the upper model layer are included as evapotranspiration.

^e To Ash Meadows flow system.

^f To Death Valley playa.

^g Includes 3,000 acre-feet per year from the lower model layer from areas east of the Amargosa Range.

part of the Death Valley region. Although much of the simulated water from the north comes from volcanic rocks and is high in dissolved silica (about 75 mg/L for the 70-100 °F water), about 40 percent of the discharge, or 8,000 acre-ft/yr, at Ash Meadows was simulated from the Spring Mountains and is low in dissolved silica (about 8.4 mg/L). Water discharging at Ash Meadows contains about 22 mg/L dissolved silica, indicating that an excess of 1,000 acre-ft/yr was simulated as recharge from the northern Death Valley region, or that an additional 4,000 acre-ft/yr of recharge is needed from the Spring Mountains to balance the silica.

Additional recharge to the Ash Meadows flow system in the simulation includes 4,500 acre-ft/yr from the Belled Range, approximately 3,000 acre-ft/yr from the Reveille Range, 1,000 acre-ft/yr each from the Shoshone Mountains and Groom and Spotted Ranges, and 2,000 acre-ft/yr of underflow from the Pahute Mesa-Oasis Valley flow system. Total regional spring discharge at Ash Meadows was simulated as 20,000 acre-ft/yr, all from the lower model layer. About 3,000 acre-ft/yr was simulated as underflow to Death Valley (table 2), which when added to the nearly 3,000 acre-ft/yr of flow simulated from the Pahute Mesa-Oasis Valley flow system accounts for the 6,000 acre-ft/yr of discharge simulated at Furnace Creek, which is close to the estimate of 5,100 acre-ft/yr reported by Hunt and others (1966). The simulation supports the conclusions of Winograd and Thordarson (1975) that the source of the springs at Furnace Creek is deep flow originating from distant areas.

Hunt and others (1966, p. B38, table 25) estimated that about 13,000 acre-ft/yr of water discharges from the saltpan in Death Valley by ET and springs. Hunt and others did not include Mesquite Flat at the far north end of Death Valley in their estimates. Miller (1977) estimated that at least another 5,000 acre-ft/yr discharges in this area. The 18,000 acre-ft/yr total is significantly lower than the simulated discharge of 23,000 acre-ft/yr. Part of the simulated discharge is from recharge assigned to the nearby ranges (fig. 25), which suggests that the estimated recharge from these nearby mountain ranges may be somewhat high. At the north end of Death Valley, discharge in Mesquite Flat was simulated as originating from mountain ranges far to the north such as the Monte Cristo and Montezuma Ranges and the Grapevine Mountains. Deuterium values for springs located in Mesquite Flat are all about -110 permil (Alan H. Welch, U.S. Geological Survey, written commun., 1985). These values are typical for water originating from the more northern mountain ranges and thus support the results of the model simulation.

The southernmost part of the Death Valley region includes part of the Spring Mountains, Pahrump Valley, and the Shoshone area along the Amargosa River, and because it has not been previously defined as a flow system it is referred to as the Pahrump-Shoshone subregion (fig. 26, table 2). Recharge from the Spring Mountains is discharged by ET in Pahrump Valley and Shoshone. Harrill (1986) estimated that about 10,000 acre-ft/yr discharges as ET in Pahrump Valley while another 18,000 acre-ft/yr flows beneath Pahrump Valley and discharges in the Shoshone area. A total of 22,000 acre-ft/yr was simulated as discharge as ET in the upper model layer at these localities. The discrepancy in total discharge between the simulation and that reported by Harrill (1986) may be due to the underestimate of recharge in the Spring Mountains. Winograd and Thordarson (1975) concluded on the basis of the geochemistry that water does not enter the Ash Meadows flow system from Pahrump. Flow in the upper model layer (fig. 22) coincides with the boundary of Waddell and others (1984; and fig. 26). Virtually no flow was simulated in the lower model layer in this subregion.

SIMULATION OF ALTERNATIVE FLOW PATHS

Unlike reports by Winograd and Friedman (1972), Winograd and Thordarson (1975), Waddell (1982), and Waddell and others (1984) that report significant recharge to the Ash Meadows subsystem from both Pahranaagat Valley and the Sheep Range, the simulations suggest that the axis of the Pintwater Range may be the location of a ground-water divide in the carbonate-rock province. The simulated location of this divide, however, could reflect the steep gradient along the transverse crustal boundary (fig. 21B), which inhibits flow around the Pintwater and Groom Ranges to the north. In the south, the simulated recharge mound beneath the Spring Mountains inhibits southward flow. The result is a bottleneck that splits the Colorado River and Death Valley regions at the Pintwater and Groom Ranges. Although the ground-water divide in the lower model layer is approximately through the Pintwater Range, sparse head data may have contributed to its apparent location as estimates of heads were extrapolated from surrounding areas. The Desert Range to the east of the Pintwater Range represents a denuded Precambrian terrane (Wernicke and others, 1984) and might be a more logical location

for the deep-flow divide as low-permeability rocks are exposed at this location and extend to great depths (fig. 22). Water-level data in Three Lakes Valley, 3 mi east of the Pintwater Range (Winograd and Thordarson, 1975), also suggest that the ground-water divide could be located to the east of the Pintwater Range. The ground-water divide in the upper model layer is through the Desert Range to the east.

A series of simulations was made to see what it would take to bring the model into better agreement with previous studies by forcing water from both Pahranaagat Valley and the Sheep Range westward to Ash Meadows. The first approach was to build up heads in the Sheep Range to create a westward gradient from this recharge area. Geologically, it would seem logical that ground water from the Sheep Range would flow westward because low-permeability rocks inferred from aeromagnetic data to the east of this range may inhibit eastward movement of ground water (figs. 22, 23, and 26). The exposed basement rocks have been thrust eastward over Paleozoic carbonate rocks, creating a west-dipping surface, so that recharge entering the Sheep Range would flow toward Ash Meadows. Transmissivities were lowered to near zero in the lower model layer beneath the Sheep Range in an effort to duplicate the effect low-permeability rocks may have on the hydrology along the eastern margin of the Sheep Range, which may induce westward flow. This effort failed to move the divide eastward to the Sheep Range, but the divide did move to the east side of the Desert Range. Because data east of the Sheep Range show water levels to be about 1,800 ft in altitude, variations in the transmissivities in this area were somewhat restricted on the basis of these known water levels. However, even near-zero transmissivities in the lower model layer beneath the Sheep Range did not create a westward component of flow from this locality. A 3,000-ft head drop in less than 5 mi developed to the east side of the Sheep Range, which contradicts known heads in that area. To initiate a westward component of flow, transmissivities were increased to the west of the Sheep Range in both model layers, having the effect of raising heads to the west of the Desert Range such that water levels rose to the surface in Yucca Flat and Frenchman Flat and evapotranspiration was initiated. If compartmentalization plays a key role in stacking up heads behind faulted and fractured rocks in the Sheep Range and Spring Mountains, then extremely steep gradients may exist west of the Sheep Range and north of the Spring Mountains. This would allow for more realistic water levels in Yucca Flat and Frenchman Flat while still inducing a westward gradient but little flow.

Another simulation involved the introduction of near-zero transmissivities along the axis of the Las Vegas Valley shear zone (fig. 21B and 19B) in an effort to push the ground-water mound beneath the Spring Mountains in the model southward, causing the ridge of the water mound along the Pintwater Range to disappear so that westward flow could be initiated. One drawback to this approach was that the width of the shear zone must be represented by the cell length of 7.5 mi. Since the region was modeled as hydraulically isotropic within a cell, flow parallel to the shear zone was restricted as well. This approach kept the elevated heads of the Spring Mountain mound farther south, but the flow pattern did not change significantly until transmissivities north of the shear zone from Yucca Flat to Pahranaagat Valley were drastically increased (to 3.0 ft²/d). This allowed up to 8,500 acre-ft/yr of water from Pahranaagat Valley to flow to Ash Meadows via Tikaboo Valley (fig. 26). However, in this simulation, the ground-water divide was still west of the Sheep Range while the discharge at Ash Meadows increased and flow to Las Vegas Valley decreased (fig. 26), but this may be due to the distribution of recharge in the Spring Mountains. Overall, the discharge deviated more greatly during sensitivity simulations than during the final calibration presented earlier.

Only the most likely approaches to forcing flow to the west from Pahranaagat Valley and the Sheep Range were tested; many others might be possible. Testing was limited by the following constraints and limitations in the model.

1. Only sparse water-level measurements are available within an area north of Spring Mountains extending from Yucca Flat on the west to the Sheep Range and Pahranaagat Valley on the east. This area is restricted to the public. Water levels in this area were extrapolated from a few available locations; thus, calibrated model results may not accurately portray the actual hydrologic conditions in this area.

2. The behavior of the Las Vegas Valley shear zone at depth is still not clearly understood. Owing to the large cell size and the assumption of isotropy within a cell, it is difficult to get an accurate representation of how the shear zone really behaves, especially if it acts as a good conduit for ground-water flow along the fault itself and a tight barrier to flow across it. Water-level information in the carbonate rocks at depth on both sides of the fault in Indian Springs Valley (fig. 26) would be extremely beneficial in order to determine the effectiveness of the shear zone as a tight barrier and to obtain an accurate ground-water head north of the shear zone. Winograd and Thordarson (1975, p. 68) indicated that the shear

zone may behave as a tight barrier at shallow depths in Indian Springs Valley.

3. If the Pahrnagat shear zone extends westward to the north of the Desert and Pintwater Ranges, there is a possibility that ground water may be stacked up behind the fault to the north, allowing for water from Pahrnagat Valley to move westward. This flow path may be further enhanced if recharge in the Spring Mountains is compartmentalized, minimizing the mounding effect to the north and effectively opening up a broader region for water from the east to flow to Ash Meadows.

4. It is unclear what role Precambrian rocks play either in the Desert Range or along the eastern side of the Sheep Range. The potentiometric surface in the deep-flow region beneath the Sheep Range may be much higher than the model could simulate, depending on how continuous the thrust plate is beneath this mountain range. The model did not help to clarify what effect these Precambrian terranes may have on the overall hydrogeology. Additional head data may provide more clues.

5. Recharge from the Pintwater and Desert Ranges may slightly enhance the ridge of the water levels formed between the transverse crustal boundary (fig. 21) and Spring Mountains in the lower model layer. If no recharge actually occurs here, the westward component of flow could be enhanced. However, simulations of no recharge in these mountain ranges did not result in flow from either Pahrnagat Valley or the Sheep Range entering the Ash Meadows flow system.

Much additional work is needed to further the understanding of the Death Valley region. However, this model simulation offers alternatives to suggestions in current reports concerning the flow patterns within the region. Although only conceptual in nature, simulated results of discharge and flow often correlate well with reported estimates. Because many of the flow boundaries are not known and many constraints are imposed by the model, the simulation results undoubtedly contain uncertainties. Nevertheless, the Death Valley region was projected as a large flow region composed of several smaller subregions (or systems) with Death Valley being the ultimate discharge point. The simulation also provides a clue to the possible northern extent of the region, which has not been previously discussed by any investigators.

COLORADO RIVER REGION

The Colorado River region, as delineated from the simulation of flow in the lower model layer, is similar to the Colorado system defined by Harrill and others

(1988). The Colorado River region occupies the southeast quarter of the carbonate-rock province and totals about 18,500 mi² (fig. 23). Only two shallow-flow regions were delineated from the simulation of flow in the upper model layer. One shallow-flow region includes a relatively small area near the Virgin River in extreme southwestern Utah and eastern Nevada, while the other includes the rest of the deep-flow region (fig. 22). Eakin (1964) defined the White River flow system, which is within the larger of the two shallow-flow regions. The White River flow system has been further discussed and modified by Eakin (1966), Winograd and Friedman (1972), and Alan H. Welch and James M. Thomas (U.S. Geological Survey, written commun., 1986). Thus, for the purposes of comparing the results of simulations to the White River flow system originally defined by Eakin and modified by Welch and Thomas, the Colorado River region was divided into three subregions (fig. 27). The Virgin River subregion generally corresponds to the area of the shallow-flow region delineated in the upper model layer. The Las Vegas subregion was separated from the White River subregion on the basis of the location of discharge. Discharge in the Las Vegas subregion was primarily simulated in Las Vegas Valley while the discharge in the White River subregion was primarily simulated along the White River and at Muddy River springs. Some flow was simulated between the White River and Las Vegas subregions, mostly near the western part of the boundary between the subregions.

RECHARGE

An estimated 249,000 acre-ft of water recharges the Colorado River region each year (table 3). This estimate is based on boundaries and flows determined through model simulations. Recharge areas, shown in figure 32, extend from the Butte Mountains in the north to the Spring Mountains in the south. Roughly 20 mountain ranges are the source areas for recharge. The greatest estimates of recharge, excluding the Virgin River subregion, are from the Egan Range, White Pine Range, and Spring Mountains in Nevada where altitudes above 10,000 ft are common. The Pine Valley and Bull Valley Mountains of Utah recharge about 31,000 and 27,000 acre-ft/yr to the Virgin River subregion. Most of the estimated recharge in the Nevada part of the Colorado River region are from mountain ranges in the White River subregion (figs. 27 and 28).

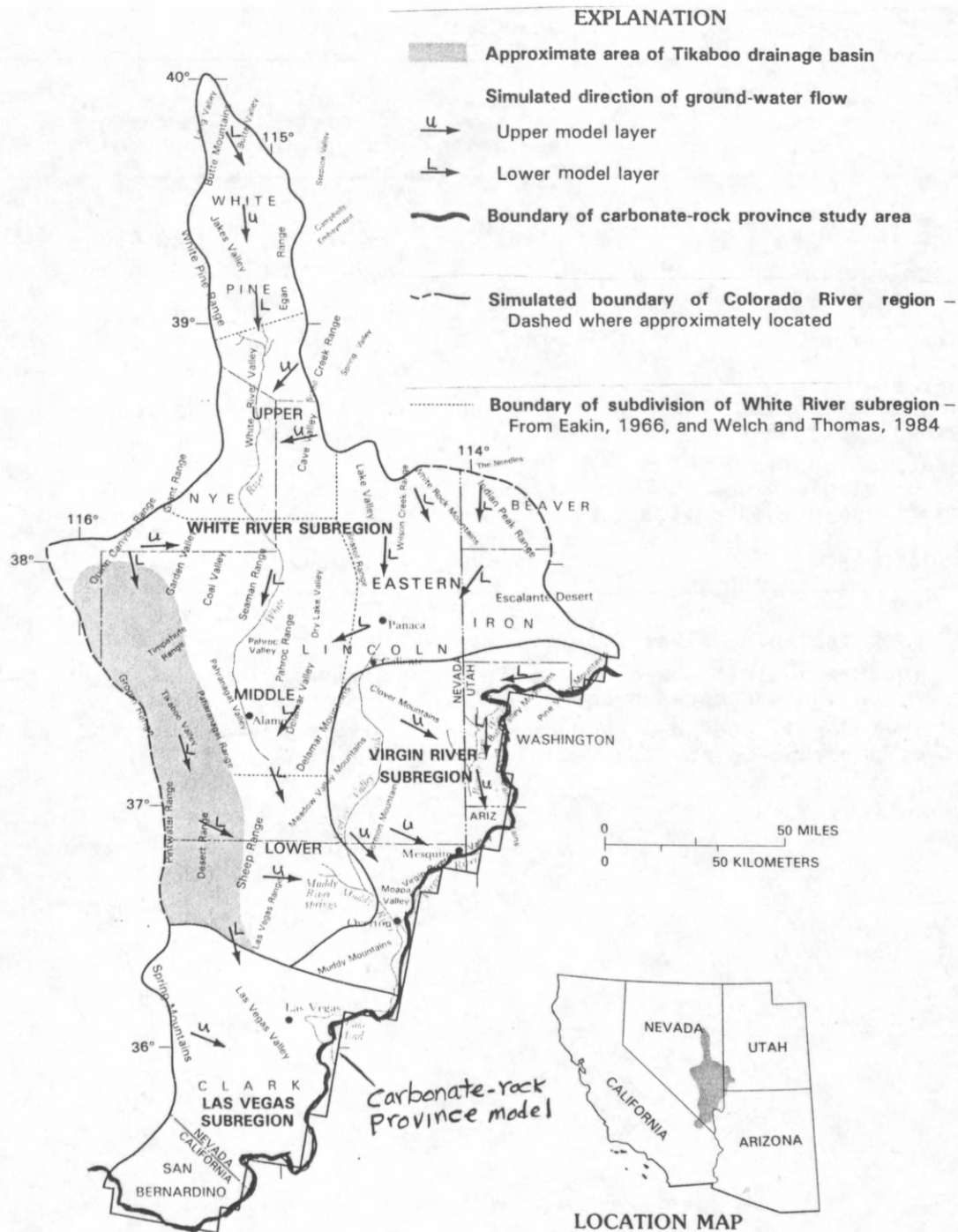


FIGURE 27.--Simulated ground-water flow paths in Colorado River region.

TABLE 3.--Simulated ground-water flow budgets, Colorado River region,
in acre-feet per year

	White River subregion	Virgin River subregion	Las Vegas subregion	Colorado River region
Recharge				
Mountain blocks	156,000	73,000	20,000	249,000
Subsurface inflow	0	24,000	^a 8,000	(b)
Head-dependent boundaries	0	0	0	0
	-----	-----	-----	-----
Total recharge	156,000	97,000	28,000	249,000
Discharge				
Evapotranspiration	19,000	16,000	23,000	58,000
Regional springs	105,000	1,000	0	106,000
Subsurface outflow	^c 32,000	0	0	(b)
Flow to Virgin River	0	48,000	0	48,000
Head-dependent boundaries	0	32,000	5,000	37,000
	-----	-----	-----	-----
Total discharge	156,000	97,000	28,000	249,000

^a From the White River flow system.

^b Subsurface inflow and outflow is between subregions within the Colorado River region and not between the five regions.

^c Includes 24,000 acre-feet per year to Virgin River subregion and 8,000 acre-feet per year to the Las Vegas subregion.

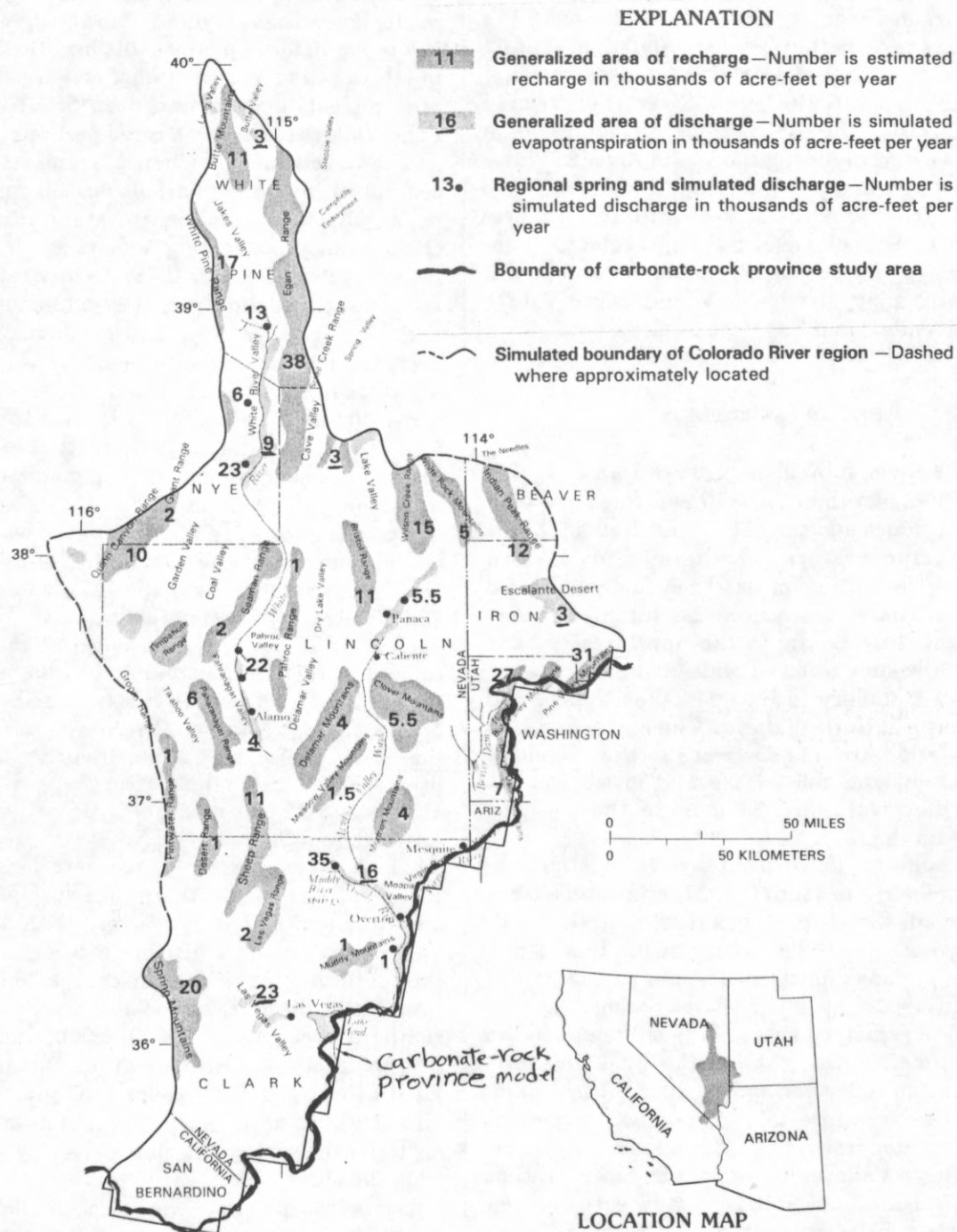


FIGURE 28.--Areas of estimated recharge, simulated regional spring discharge, and simulated evapotranspiration in Colorado River region.

DISCHARGE

The Colorado River region is unusual among the five deep-flow regions that were simulated, in that 62 percent of the discharge was simulated as regional springs or seepage into the Virgin River as opposed to evapotranspiration (fig. 28). Major spring-discharge points occur primarily along the White River in White River Valley, Pahrangat Valley, and the Muddy River springs area; the terminus of the White River subregion (fig. 27). Evapotranspiration not related to regional spring discharge was simulated as occurring in White River Valley, the lower Virgin River Valley, Pahrangat Valley, and Las Vegas Valley.

WHITE RIVER SUBREGION

The White River subregion as defined here (fig. 27) is somewhat broader than the system defined by Eakin (1966) and includes additional recharge and discharge areas along the eastern, northern, and western boundaries. The subregion has been further divided into four sections whose boundaries differ from sections delineated by Eakin; in the upper section, the boundary in the simulation extends further northward than Eakin's boundary to include Jakes Valley, and parts of Long and Butte Valleys. The eastern section in the simulation extends eastward to the Escalante Desert in Utah, and the middle and lower sections extend further westward to include the Tikaboo drainage basin (fig. 27).

In the simulation, flow within the White River subregion is from north to south (fig. 27) and is consistent with observed water-level gradients in the area (Thomas and others, 1986). Much of the flow is discharge from regional springs along the axis of part of the White River and at Muddy River springs (fig. 28). Because of the expanded areas of the subregion in the simulations, more recharge from the Egan Range is simulated in the subregion than estimated by Eakin. Additional recharge into the White River subregion was also simulated from mountains adjacent to Jakes, Long, and Butte Valleys. It is possible, however, that some of this additional recharge may actually discharge at Campbells embayment in Steptoe Valley (fig. 28). Eakin and others (1967, p. 21) suggested that some water might move from Long and Butte Valleys to the springs at Campbells embayment, but they argued against this idea on the basis of a very low hydraulic gradient toward Campbells embayment from Butte Valley and the "likelihood" of a hydrologic barrier in the Egan Range due to high recharge rates and associated ground-water mounding. Recharge in

the Egan Range was simulated as creating a recharge mound in the upper model layer; however, in the lower model layer, the computed hydraulic gradient was too low to argue for or against this hypothesis. By changing the location and amount of recharge in the vicinity of Campbells embayment, deep flow from Butte and Long Valleys to this area could perhaps be simulated.

The geochemical evidence seems to support the concept of long and short flowpaths as well. Campbells embayment discharges water containing about 6 tritium units, suggesting a short residence time, and recent recharge (post 1952) from nearby mountain ranges such as the Egan Range (James M. Thomas, U.S. Geological Survey, oral commun., 1986). However, the modern carbon content of the spring water indicates moderately old water (10,000–14,000 years), a reasonable time for water to flow from Butte Valley. Thus, the simulation and the geochemistry of the springs suggest that mixing of older and younger waters may be occurring.

Approximately 26,000 acre-ft/yr of water was simulated as entering the northern White River Valley from areas to the north (fig. 27), as opposed to the 20,000 acre-ft/yr estimated by Alan H. Welch and James M. Thomas (U.S. Geological Survey, written commun., 1986). The simulated value is almost identical to the 25,000 acre-ft/yr estimated by Eakin (1966, p. 265, fig. 6). Additional recharge to the upper section of the subregion (White River Valley) originates in the Egan and White Pine Ranges and is about 19,000 and 12,000 acre-ft/yr, respectively, according to Welch and Thomas.

Three regional spring areas are located in White River Valley. The northernmost springs discharge at an annual rate of slightly more than 18,000 acre-ft. The central springs discharge 5,500 acre-ft/yr, and the southernmost springs discharge 16,000 acre-ft/yr. Simulated discharges for the north, central, and southern springs are 13,000, 6,000, and 23,000 acre-ft/yr, respectively. Although the estimated and simulated discharges differ considerably for the northern and southern springs, the total simulated discharge for the three spring locations differs by only 5 percent from the observed total.

Evapotranspiration was also simulated in White River Valley and was about 8,500 acre-ft/yr. This additional discharge accounts for the difference between the simulated inflow and that estimated by Alan H. Welch and James M. Thomas (U.S. Geological Survey, written commun., 1986). ET was not considered in their geochemical analysis of flow in the White River subregion.

Outflow from the White River Valley area southward was estimated by Welch and Thomas to be about

13,000 acre-ft/yr. The model simulates outflow of about 17,000 acre-ft/yr into the middle section of the White River subregion, primarily as flow through the lower model layer (fig. 27). From this area southward the boundaries delineated from the simulations are considerably different from those delineated by Eakin (1966). The western boundary in the simulation extends south from the Grant Range through the Groom and Pintwater Ranges to the vicinity of the Las Vegas Valley shear zone (figs. 21A and 27) and corresponds with the eastern boundaries of the Death Valley region. The boundary in the area of the shear zone is not precisely defined because, in the simulation, some water from the Sheep and Las Vegas Ranges and the Tikaboo drainage area (fig. 27) was simulated as flowing southward toward Las Vegas Valley.

The eastern boundary in the simulation extends eastward to the Indian Peak Range in Utah. Thus, recharge from the Wilson Creek Range and White Rock Mountains was simulated as flowing in a southwestward direction (fig. 27). A zone of high computed transmissivities immediately to the south of these mountain ranges extends into the White River subregion toward Pahrnatag Valley (fig. 19B) and allows a flow path westward for recharge from these mountain ranges (fig. 27). Southward flow toward the Meadow Valley Wash area is inhibited by what may be buried igneous intrusive rocks associated with the Pioche mineral belt (fig. 21A) described by Stewart and others (1977), although other factors may influence the low computed transmissivities. A subsurface magnetic high (fig. 23) beneath the Delamar and Mormon Mountains (figs. 23 and 27) may possibly represent an igneous intrusion, which may also inhibit southward flow to some degree. The low computed transmissivities in the area probably reflect the volcanic and intrusive bodies associated with the transverse crustal boundary that extends all the way to the north end of Death Valley. Consequently, all recharge east of the Delamar Mountains and south of the high-transmissivity zone just to the north of the transverse crustal boundary was simulated not as flow in the White River subregion but rather as flow in the Virgin River subregion.

The boundary of the White River subregion north of the Wilson Creek Range, White Rock Mountains, and Indian Peak Range is uncertain in the simulation (fig. 27). The uncertainty arises because simulated flow boundaries in the upper and lower model layers do not coincide. Also, simulated heads at the north end of Lake Valley are somewhat lower in the upper model layer than observed values indicate; because of this, the gradient in this area extending northward to Spring Valley is rather flat, making it

difficult to place the location of the boundary. East of Lake Valley, the boundary, particularly in the upper model layer, becomes even more obscure. Flow boundaries between the Bonneville and Colorado River regions are different, thus making it difficult to determine the amount of recharge reaching the White River subregion in the simulation from the area of the Indian Peak Range in Utah.

The major flow path for water from the eastern section of the White River subregion follows a southwest-trending high-transmissivity zone in the simulation that creates a conduit for water to flow through Lake and Dry Lake Valleys southward through Delamar Valley (figs. 19B and 27), and eventually into the southern end of Pahrnatag Valley near where the Pahrnatag Valley springs discharge. Alan H. Welch and James M. Thomas (U.S. Geological Survey, written commun., 1986) estimated that about 35,000 acre-ft/yr recharges their middle section of the White River flow system (modified from Eakin's original delineation) with principal contributors to the west being recharge from the Grant and Quinn Canyon Ranges, where the estimated annual recharge is 10,000 acre-ft. According to Welch and Thomas, mountain ranges contributing recharge from the east are the Egan and Schell Creek Ranges where 14,000 acre-ft is estimated to recharge the flow system each year; additional recharge was simulated from areas farther to the east.

About 25,000 acre-ft/yr of recharge was simulated to enter the White River subregion from the Wilson Creek Range, White Rock Mountains, and Indian Peak Range (southern part of The Needles). An additional 5,500 acre-ft/yr of water was simulated to discharge at Panaca springs near Panaca. This spring lies on the northern border of a band of high computed transmissivities that trend to the southwest (figs. 19B, 27, and 28). The springs may be the result of westward flowing water that is blocked by volcanic or other crystalline rock south of the springs, or perhaps might be associated with the regional lineaments in the area (figs. 21A and 23). According to Rush and Eakin (1963), as much as 8,500 acre-ft/yr is discharged as ET from Lake Valley where the water table is fairly shallow. Because simulated heads in the upper model layer are low in this area, ET was simulated primarily in the north end of Lake Valley north of the border between the Colorado River and the Bonneville regions. In the simulation, only 300 acre-ft/yr was discharged by ET in the Colorado River region part of Lake Valley, and may account for some excess of simulated flow to the lower part of the White River subregion.

Discharge along the axis of the central part of the White River subregion occurs in Pahrnatag Valley, where spring discharge has been measured at 26,000

acre-ft/yr from regional springs between Hiko and Alamo (fig. 28). However, springflow in the simulations was only 22,000 acre-ft/yr; an additional 4,000 acre-ft/yr was simulated as ET in the valley. Eakin (1963) estimated that about 25,000 acre-ft/yr discharges from Pahrnatag Valley by ET, which he considered was from spring discharge.

Simulated flow from Pahrnatag Valley is southward into the lower section of the White River subregion (fig. 27). Deep flow in the lower model layer becomes increasingly complicated at this point. Much debate has centered around the role that the Sheep Range and Spring Mountains play in the White River flow system defined by Eakin (1966). The geochemical model presented by Alan H. Welch and James M. Thomas (U.S. Geological Survey, written commun., 1986) deviates substantially from the results of the flow simulations described here in the lower section of the subregion. Welch and Thomas estimated that 17,000 acre-ft/yr flows from the central section of their White River flow system to their lower section. Approximately 6,000 acre-ft/yr from the middle section was directed toward Ash Meadows in the Death Valley region, as first suggested by Winograd and Friedman (1972). However, in the simulations, flow from the middle to lower section of the White River subregion was 36,000 acre-ft/yr. Some of this flow was simulated from Tikaboo Valley, which is a drainage area for the Groom, Pahrnatag, Timpahute, and northern Desert Ranges (fig. 27). As much as 9,000 acre-ft/yr of recharge from these ranges and perhaps from as far north as the Quinn Canyon Range was simulated as flowing beneath Tikaboo Valley. Some of the 9,000 acre-ft/yr of flow in the Tikaboo drainage area was simulated as entering the main area of flow toward Muddy River springs at the north end of the Sheep Range (figs. 27 and 28). Part of the simulated flow in the Tikaboo drainage area continues to move southward, where small amounts of recharge from the Pintwater and southern Desert Ranges is added to the flow. From this point, flow is more eastward, so that at the southern end of the Las Vegas Range, much of the water in the simulations flows southward, but part continues eastward toward the Virgin River subregion, in spite of Precambrian rocks exposed in the Las Vegas Range which may inhibit eastward flow. About 8,000 acre-ft/yr of flow in the lower model layer was simulated as flowing from the lower section of the White River subregion toward the Las Vegas subregion (fig. 27). Flow from the Tikaboo drainage area and recharge in the Sheep and Las Vegas Ranges contribute to this southward flow. Much of the water is funneled southward through a 10-mi-wide section just south of the Las Vegas Range (figs. 21A and 27).

Flow that did not enter the Las Vegas subregion was simulated as continuing in an eastward direction toward the Virgin River subregion.

Alan H. Welch and James M. Thomas (U.S. Geological Survey, written commun., 1986) estimated on the basis of geochemistry that recharge into the lower section of the White River subregion is mainly from the Sheep and Delamar Ranges and from the Meadow Valley Wash area to the east (fig. 27). They also estimated small amounts of recharge from the Pahrnatag and Pahroc Ranges. Rush (1964, p. 24) indicated that as much as 8,000 acre-ft/yr may leave the Meadow Valley Wash area and flow toward the Muddy River springs area. Welch and Thomas used this estimate in their isotopic budgets of water discharging from Muddy River springs. The simulations suggest that ground water in the Meadow Valley Wash area is part of the Virgin River subregion and discharges to the Muddy River. Thomas (U.S. Geological Survey, oral commun., 1987) suggested that water from Meadow Valley Wash area is needed to balance the isotopic budget for the Muddy River springs.

Discharge from the lower model layer at the Muddy River springs is 35,000 acre-ft/yr, which is about 1,000 acre-ft/yr less than the reported spring discharge estimates (Eakin, 1964, p. 14). Previous reports propose no underflow from this area eastward or southward toward the Virgin River. However, about 24,000 acre-ft/yr of underflow was simulated toward the Virgin River subregion in excess of the 35,000 acre-ft/yr that was simulated as discharging from the springs; this is a substantial departure from estimates in previous studies. Geologic evidence indicates that basement rock is shallow, inhibiting significant flow from bypassing the Muddy River springs to areas farther east (Michael D. Dettinger, U.S. Geological Survey, oral commun., 1987).

Precambrian rocks that were thrust up and are now exposed in the Las Vegas Range, and the possible low-permeability barrier along the Las Vegas Valley shear zone, were not explicitly included in the delineation of the flow regions. In the vicinity of the Las Vegas Valley shear zone and Las Vegas Range, however, computed transmissivities in the lower model layer were very low, except immediately south of the Sheep and Las Vegas Ranges (fig. 19B). Flow was diverted around these low-transmissivity areas in the simulations. About 8,000 acre-ft/yr was simulated as leaving the White River subregion to the Las Vegas subregion between the south end of the Sheep and Las Vegas Ranges and the Las Vegas Valley shear zone (see section on Las Vegas subregion for more details).

The inclusion of ET in budgets for the White River subregion, together with the complexity of the flow

within this hydrogeologically complex area, makes deuterium balances extremely difficult to evaluate. Knowledge of the degree of mixing between waters of different origin and the effect ET has on the overall balance is essential in evaluating representative deuterium levels in water along the course of this subregion. Because some major differences exist between the geochemical model of a White River flow system presented by Alan H. Welch and James M. Thomas (U.S. Geological Survey, written commun., 1986) and the simulation results presented here, further understanding is needed to better delineate the strengths and weaknesses of each model.

Water from the Muddy River springs contains a mean deuterium content of -97 permil (Alan H. Welch and James M. Thomas, U.S. Geological Survey, written commun., 1986). Deuterium in water entering the lower section of the White River subregion from Pahranagat Valley was reported by Welch and Thomas to be -107 permil. Sources of much heavier water (less negative reported values) are necessary for the deuterium budget to balance with respect to the mixed water that discharges at Muddy River springs. Among the sources they considered, only water from the Sheep Range and Meadow Valley Wash area are "heavier" than water that discharges at the Muddy River springs area. Welch and Thomas found that incorporating Meadow Valley Wash water (-88 permil) into the geochemical model was important. Water recharging the White River subregion from the Tikaboo drainage area, as simulated during this study, may also be fairly heavy, perhaps on the order of -95 to -100 permil, and may negate the need to simulate additional water from the Meadow Valley Wash area.

Unanswered questions at this time pertain to deuterium levels in the recharge water from the Wilson Creek Range, White Rock Mountains, and Indian Peak Range. If the chemical characteristics of water recharged from these mountain ranges are similar to that found at Panaca (-106 permil), the deuterium budget is thrown off even further. If the deuterium concentrations of water recharged from these mountain ranges are more representative of water found near Caliente (-89 permil), the deuterium budget may work out better, but this seems unlikely. Flow from the Tikaboo drainage area seems to make the water somewhat heavier with respect to deuterium concentrations at the Muddy River springs area; however, the deuterium concentration of flow into the lower section of the White River subregion from the north is the critical factor in determining whether the simulation results presented here would fit the geochemical model of the White River flow system as described by Alan H. Welch and James M. Thomas (U.S. Geological

Survey, written commun., 1986). How much (if any) water from Long Valley reaches the lower section of the White River subregion? Is mixing complete along the length of the subregion? What effect does ET have on the overall deuterium levels of deep flow? It is obvious that many different approaches can be taken to better understand the ground-water flow patterns of this subregion. The results presented here are no more than an alternative approach in handling a complex hydrogeologic area. Many questions have arisen as to the behavior of ground-water flow and the factors influencing the flow. Many additional data are needed to further answer these perplexing questions attached to this complex area.

VIRGIN RIVER SUBREGION

Recharge to the Virgin River subregion originates primarily from three mountain ranges in Utah—the Bull Valley, Pine Valley, and Beaver Dam Mountains, which supply 64,000 of the estimated 73,000 acre-ft/yr of the recharge to the subregion (fig. 28). Of the total from the three ranges, 45,000 acre-ft/yr was simulated as downward leakage into the lower model layer and 19,000 acre-ft/yr was simulated as flow through the upper model layer. The general direction of flow was southward beneath Beaver Dam Wash. The remaining recharge of about 9,000 acre-ft/yr was primarily from the Clover and Mormon Mountains in Nevada (fig. 28).

About 24,000 acre-ft/yr of underflow was simulated from the White River subregion (table 3). Approximately 3,000 acre-ft/yr of this amount was simulated as flow toward the Virgin River south of the Muddy River springs area (fig. 28). About 1,000 acre-ft/yr was simulated as discharge at Rogers Spring (fig. 28) in the lower Moapa Valley just west of the Overton Arm of Lake Mead.

Low computed transmissivities that are prevalent in much of the northern part of the subregion reflect the influence of volcanic and intrusive rocks associated with the transverse crustal boundary and the Pioche mineral belt, which extend through the northern half of the subregion (fig. 21A). Only in the area of Beaver Dam Wash are computed transmissivities high, creating a north-south conduit for ground-water flow in the simulation (fig. 19B). Beaver Dam Wash also lies to the east of the aeromagnetic ridge (fig. 21A) that may be associated with low-permeability basement or intrusive rocks. Higher computed transmissivities along the Beaver Dam Wash have caused recharge to be routed from the north through a region two cell widths (10 mi) wide. The 64,000 acre-ft/yr was simu-

lated to flow to the Virgin River. Upward hydraulic gradients, perhaps caused by the terminating carbonate rocks, are known to result in a significant amount of seepage into the Virgin River. Glancy and Van Denburgh (1969, p. 36) estimated that 50,000 acre-ft/yr of ground water discharges into the Virgin River near Mesquite, near the Nevada-Utah border. These authors suggested that the seepage is flow through carbonate rocks. Simulated ground-water discharge to the Virgin River totals 30,000 acre-ft/yr at this location (one cell); however, an additional 18,000 acre-ft/yr was simulated as ground-water discharge along a reach of the Virgin River between Mesquite and the northern tip of Overton Arm. Simulated ground-water discharge to the Virgin River is separated from discharge by ET and head-dependent boundaries in table 3 for clarification.

Much of the flow in the Meadow Valley Wash area was simulated in the upper model layer rather than in the lower layer, owing to the much lower computed transmissivities in the lower layer through much of the flow area (figs. 19B and 27). Much of the flow simulated in the upper layer either is discharged as ET in the lower Moapa Valley or enters the Virgin River. Total simulated ET in the Moapa Valley area was 16,000 acre-ft/yr. Rush (1968b, p. 35) estimated ET in the area to be 14,000 acre-ft/yr and did not include ET due to spring discharge.

Total simulated discharge in the Virgin River subregion was 96,000 acre-ft/yr, with 48,000 acre-ft/yr simulated as discharge to the Virgin River and 16,000 acre-ft/yr simulated as ET (table 3). Another 32,000 acre-ft/yr was simulated as discharge to the upper end of the Overton Arm of Lake Mead. No additional ground-water discharge was simulated south of this point. Seismicity studies by Anderson and Laney (1975) indicate that, from Lake Mead to the north end of Overton Arm, low-permeability Cenozoic evaporite beds and fine-grained clastic sediments impede ground-water flow to the Overton Arm area from the north or west. Rogers Spring is the only significant discharge in the area. Simulated steady-state discharge from Rogers Spring is 1,000 acre-ft/yr. Simulated flow through the lower model layer shows no flow in the vicinity of Overton Arm. Upper layer transmissivities in this stretch of the Virgin River subregion are also fairly low (fig. 18A). The simulated ground-water budget for the Virgin River subregion is listed in table 3.

The simulation of 32,000 acre-ft/yr entering Overton Arm from the Virgin River in excess of water budgets presented in earlier investigations may indicate one of five things:

1. Either the estimates of recharge from the

mountain ranges of Utah are too high, or the flow path may be southeastward toward the Virgin River in Utah rather than southwestward. Sandberg and Sultz (1985) estimated that between 25,000 and 35,000 acre-ft/yr may seep into streams along the entire reach of the Virgin River northeast of the carbonate-rock province. Much of the simulated 32,000 acre-ft/yr seeping into the Virgin River along the Nevada Utah border may actually be seeping into the river in Utah outside the study area.

2. Simulated heads in this subregion may be much different from actual head values. No deep head data exist east of the Muddy River springs area. Consequently, actual heads may be considerably different from those simulated in the lower model layer, and flow paths could be different from those described in this report.

3. It is possible that recharge from the Wilson Creek Range, White Rock Mountains, and Indian Peak Range could flow northward toward the Great Salt Lake (although limited water-level data do not support this) rather than into the White River subregion. Also, ground water from the Tikaboo drainage area could flow either toward Las Vegas or to Ash Meadows, which would essentially make the White River subregion identical to the flow system by Eakin (1966) and modified by others.

4. Simulated ET in the Escalante Desert and Lake Valley and simulated spring discharge at Panaca are lower than estimates in previously published reports. If simulated results were made to more closely match the reported estimates, southward flow would decrease by about 12,000 acre-ft/yr.

5. The 32,000 acre-ft/yr derived from model simulations might be representative of the volume of flow discharging into the Virgin River near Overton or at the north end of Lake Mead.

LAS VEGAS SUBREGION

The Las Vegas subregion is one of the most densely populated areas in the province, and water resources are vitally important to this arid region. Recharge enters the Las Vegas subregion primarily from the Spring Mountains to the west. Total recharge to Las Vegas Valley, which makes up most of the subregion, has been estimated by several investigators. Maxey and Jameson (1948) estimated that recharge to Las Vegas Valley from adjacent mountain ranges was from 30,000 to 35,000 acre-ft/yr; Malmberg (1965) estimated it at 25,000 acre-ft/yr, Harrill (1976) estimated it at about 30,000 acre-ft/yr, and Morgan and Dettinger (in press) estimated 32,000 acre-ft/yr. These authors

reported that all or nearly all the recharge was from the Spring Mountains.

For this study, recharge to Las Vegas Valley was simulated as 28,000 acre-ft/yr, of which 20,000 acre-ft/yr originates from the Spring Mountains to the west and 8,000 acre-ft/yr enters the subregion from the White River subregion through an area just south of the Sheep and Las Vegas Ranges. Recharge from the Spring Mountains was simulated as flowing only through the upper model layer to Las Vegas Valley. The more shallow flow path may be attributed to the low computed transmissivities in the lower model layer. The low computed transmissivities were needed to create a ground-water mound in the upper model layer beneath the Spring Mountains, and the low transmissivities may be related to low-permeability intrusive or basement rocks, inferred from a large aeromagnetic source body beneath the southern end of the Spring Mountains, that may inhibit downward flow (fig. 23). Recharge from the White River subregion entering the Las Vegas subregion was simulated in the lower model layer. The source of flow in the lower model layer may be recharge from as far north as the Quinn Canyon Range (fig. 27), where deuterium levels are about -106 permil (James M. Thomas, U.S. Geological Survey, oral commun., 1986).

Water underlying Las Vegas Valley has an average deuterium content of -100 permil; some areas are as low as -104 permil (James M. Thomas, U.S. Geological Survey, written commun., 1986). Local recharge from the Spring Mountains and Sheep Range generally have deuterium levels of -98 and -95 permil, respectively; thus, water underlying Las Vegas Valley may be a mixture from different sources. Alternatively, Michael D. Dettinger (U.S. Geological Survey, oral commun., 1986) suggested that ground water in Las Vegas Valley may originate from higher altitudes in the Spring Mountains, where deuterium levels are expected to be lighter (-100 to -110 permil).

Discharge from the Las Vegas subregion was simulated as ET within the Las Vegas Valley and included some spring flow. Model simulations assumed pre-development conditions in Las Vegas Valley and did not include ground-water withdrawals (in excess of 60,000 acre-ft/yr, fig. 8) which have affected ground-water flow patterns and discharge in the valley since about 1920. About 23,000 acre-ft/yr was simulated as ET with an additional 5,000 acre-ft/yr simulated as underflow to Lake Mead (fig. 28, table 3). Harrill (1976, p. 50) estimated that about 1,200 acre-ft/yr left the upper basin-fill deposits near the northeast corner of the valley as underflow to carbonate rocks. More recently, Morgan and Dettinger (in press) increased this estimate to about 2,000 acre-ft/yr on the basis of

flow through all basin-fill deposits. Thus, the 5,000 acre-ft/yr of underflow in the simulations might represent the flow through both the basin-fill deposits and the underlying carbonate rocks.

Decreasing transmissivities along the Las Vegas Valley shear zone and along the thrust fault on the western slope of the Las Vegas Range resulted in a decrease in flow from the White River subregion to about 4,000 acre-ft/yr. Increasing transmissivities in the Las Vegas Range but keeping the low transmissivities along the shear zone resulted in almost no flow from the White River subregion into the Las Vegas subregion. Increasing transmissivities along the Las Vegas Range may be reasonable because the Precambrian rocks exposed in the range may be thin and thus not act as a barrier to flow. The simulation also resulted in an increase in flow to the Overton Arm area and caused an abrupt increase in simulated discharge at Rogers Spring. The increase in flow in the Overton Arm area seems unrealistic because of the low permeability of the evaporite beds and fine-grained deposits in the area. Higher discharge rates were also simulated at the Muddy River springs as well as increased ET in the Moapa Valley area.

Equipotential lines in the lower model layer were shifted westward and recharge from the Spring Mountains to the Las Vegas subregion increased when transmissivities along the Las Vegas Valley shear zone and the Las Vegas Range were decreased to near zero. However, flow to Ash Meadows was reduced in the simulation but not flow to Pahrump Valley (fig. 26). Flow to both Pahrump Valley and Ash Meadows was reduced when transmissivities along the shear zone were near zero while transmissivities along the Las Vegas Range were increased. In this simulation, all the recharge to the Las Vegas subregion was from the Spring Mountains. Water budgets for both Pahrump Valley and Ash Meadows in the simulation were less than the estimated water budgets. Thus, for this simulation to be reasonable, recharge in the Spring Mountains must be considerably more than was used in the simulations.

Another possibility, but one that could not be adequately simulated, is that the Las Vegas Valley shear zone is a conduit for flow along its axis and a barrier to flow across it. If this is true, it may be possible to divert flow along the west side of the Sheep Range (White River subregion) and (or) recharge from the Spring Mountains toward the Ash Meadows flow system. However, simulations aimed at redirecting flow from the White River subregion away from the Las Vegas subregion to Ash Meadows negatively affected water budgets in the White River, Las Vegas, and Virgin River subregions. Attempts made at captur-

ing additional recharge from the Spring Mountains for the Las Vegas subregion affected water budgets in the Death Valley region.

BONNEVILLE REGION

The Bonneville region covers an area of approximately 38,000 mi² in the northeastern part of the carbonate-rock province and occupies 41 percent of the entire study area, making it the largest of the five flow regions (fig. 23). For the most part, few data are available on flow through the carbonate rocks. This fact should be kept in mind when evaluating the model results presented in this section.

RECHARGE

Recharge to the Bonneville region is believed to be widespread and considerably greater than in the other four flow regions. The eastern boundary of the flow region is along mountain ranges that supply large quantities of water to both the southeastern Great Salt Lake area and the Sevier Desert area (fig. 29). The remaining principal recharge areas are within the easternmost fault-block mountains in Nevada that make up the western border of the region. Total recharge from the mountain blocks to the Bonneville region is estimated to be approximately 904,000 acre-ft/yr.

DISCHARGE

Unlike the Colorado River region, where regional spring discharge and seepage to the Virgin River represents the largest part of the total discharge, discharge in the Bonneville region is mostly by ET. Evapotranspiration represents about 85 percent (775,000 acre-ft/yr) of the total simulated discharge (fig. 29, table 4). Regional springs account for only 7 percent (64,000 acre-ft/yr) of the total discharge in the simulations, and discharge to Utah Lake and the Great Salt Lake make up the remaining 8 percent. Most of the central part of the region is occupied by three deserts where ground water predominantly discharges as ET: the Great Salt Lake Desert in the north, the Sevier Desert in the middle, and the Escalante Desert in the south.

DESCRIPTION OF SUBREGIONS

The Bonneville region was divided into four subregions (fig. 30) on the basis of principal discharge

areas and results of flow directions in both model layers. The subregions are (1) Sevier-Escalante subregion, (2) Fish Springs subregion, (3) Steptoe subregion, and (4) Great Salt Lake subregion. Discussions of these subregions do not include every valley within the region, but only those areas directly affecting the flow either by significant recharge or by geologic features that may influence flow.

SEVIER-ESCALANTE SUBREGION

The Sevier-Escalante subregion is characterized by high recharge and locally high ET (fig. 29). The combined estimate of annual recharge from the Pavant Range-Tushar Mountains to the east and the Markagunt Plateau-Kolob Terrace highland to the south is 213,000 acre-ft, making this the highest recharge area within the entire region. About 70,000 acre-ft/yr was simulated as downward flow from the upper model layer to the lower layer in the vicinity of the Tushar Mountains and Pavant Range and about 46,000 acre-ft/yr in the vicinity of the Markagunt-Kolob highland.

In the simulations, recharge from the Markagunt-Kolob highland flows north and northwestward to discharge areas in the Escalante Desert, Parawan Valley, and Milford area, and as far north as Sevier Lake. Aside from flow in the upper model layer from the mountain ranges to adjacent valleys, flow was also simulated in the lower model layer from this southern recharge area to the Escalante Desert northward to the Milford area, where much of the flow in the lower model layer moves upward into the upper layer and is discharged as ET (fig. 30). Mower and Cordova (1974) estimated that 16,000 of the 33,000 acre-ft/yr discharging from the Milford area by ET prior to large ground-water withdrawals was from flow through consolidated rocks. Their estimate was determined by taking the difference between estimated recharge and discharge. More recently, James L. Mason (U.S. Geological Survey, written commun., 1986) estimated the discharge by ET as 30,000 acre-ft/yr from model simulations. Evapotranspiration in the Milford area in these simulations was about 38,000 acre-ft/yr, considerably higher than the 30,000 acre-ft/yr simulated by Mason, and is probably related to differences in the estimates of recharge in the area. Mason estimated recharge through model calibration, whereas this report uses recharge estimates from reconnaissance reports for Utah. The remainder of flow through the lower model layer from the Markagunt-Kolob highland, about 5,000 acre-ft/yr, is toward the Sevier Lake area where it is simulated as upward flow into the upper model layer and then discharged by ET.

EXPLANATION

17 Generalized area of recharge—Number is estimated recharge in thousands of acre-feet per year

18 Generalized area of discharge—Number is simulated evapotranspiration in thousands of acre-feet per year

14 Regional spring and simulated discharge—Number is simulated discharge in thousands of acre-feet per year

— Boundary of carbonate-rock province study area

--- Simulated boundary of Bonneville region—Dashed where approximately located

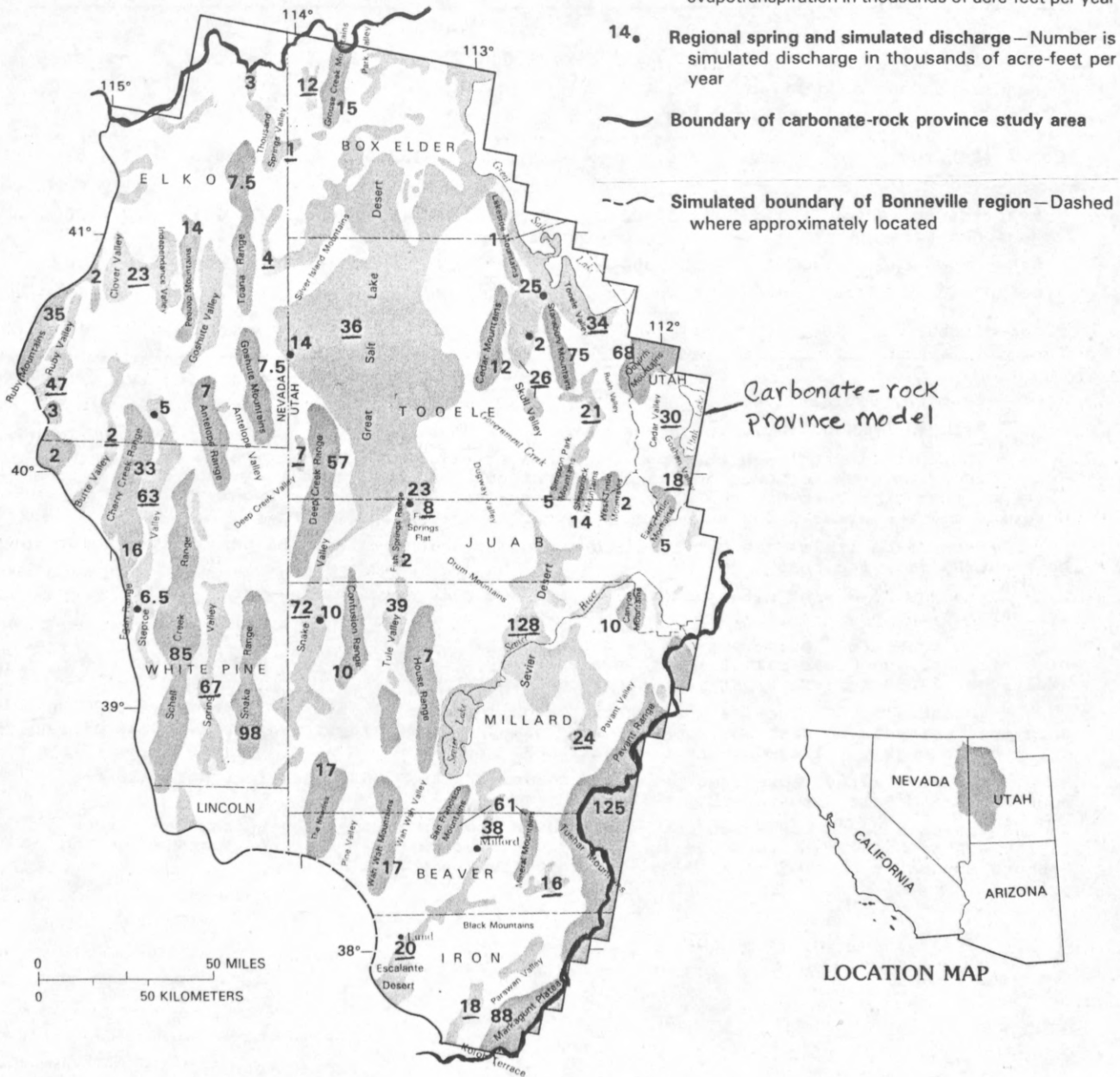


FIGURE 29.--Areas of estimated recharge, simulated regional spring discharge, and simulated evapotranspiration in Bonneville Region.

TABLE 4.--Simulated ground-water flow budgets, Bonneville region, in acre-feet per year

	Sevier- Escalante subregion	Fish Springs subregion	Steptoe subregion	Great Salt Lake subregion	Bonneville region
Recharge					
Mountain blocks	315,000	222,000	183,000	183,000	903,000
Head-dependent boundaries	^a 1,000	0	0	0	1,000
Subsurface inflow	^b 14,000	13,000	0	^c 6,000	(d)
Total recharge	330,000	235,000	183,000	189,000	904,000
Discharge					
Evapotranspiration	265,000	186,000	154,000	170,000	775,000
Regional springs	0	33,000	26,000	5,000	64,000
Head-dependent boundaries	^e 51,000	0	0	^f 14,000	5,000
Subsurface outflow	^g 14,000	^h 16,000	ⁱ 3,000	0	(d)
Total discharge	330,000	235,000	183,000	189,000	904,000

^a From the Sevier River.

^b From Wah Wah Valley through the upper model layer.

^c Includes flow through the upper model layer of 1,000 acre-feet per year from the Toana Range and Goshute Mountains, and flow through the lower model layer of 2,000 acre-feet per year from Deep Creek Valley; 1,000 acre-feet per year from Dugway Valley-Government Creek area; 2,000 acre-feet per year from Fish Springs Flat.

^d Subsurface inflow and outflow is between subregions within the Bonneville region not between the five regions.

^e Seepage to Sevier River and Sevier Lake where it is discharged as evapotranspiration.

^f Includes 6,000 acre-feet per year of seepage to Utah Lake, 6,000 acre-feet per year of outflow to the Great Salt Lake at Tooele Valley through the upper model layer. An additional 2,000 acre-feet per year enters elsewhere.

^g Includes 5,000 acre-feet per year through lower model layer to Tule Valley; 8,000 acre-feet per year to Fish Springs Flat through upper model layer region; 1,000 acre-feet per year to Dugway Valley-Government Creek area.

^h Includes 14,000 acre-feet per year to Sevier Lake; 2,000 acre-feet per year to southern Great Salt Lake Desert.

ⁱ Includes 2,000 acre-feet per year through the lower model layer from Deep Creek Valley to the Great Salt Lake Desert; 1,000 acre-feet per year from the Toana Range and Goshute Mountains through upper model layer to the Great Salt Lake Desert.

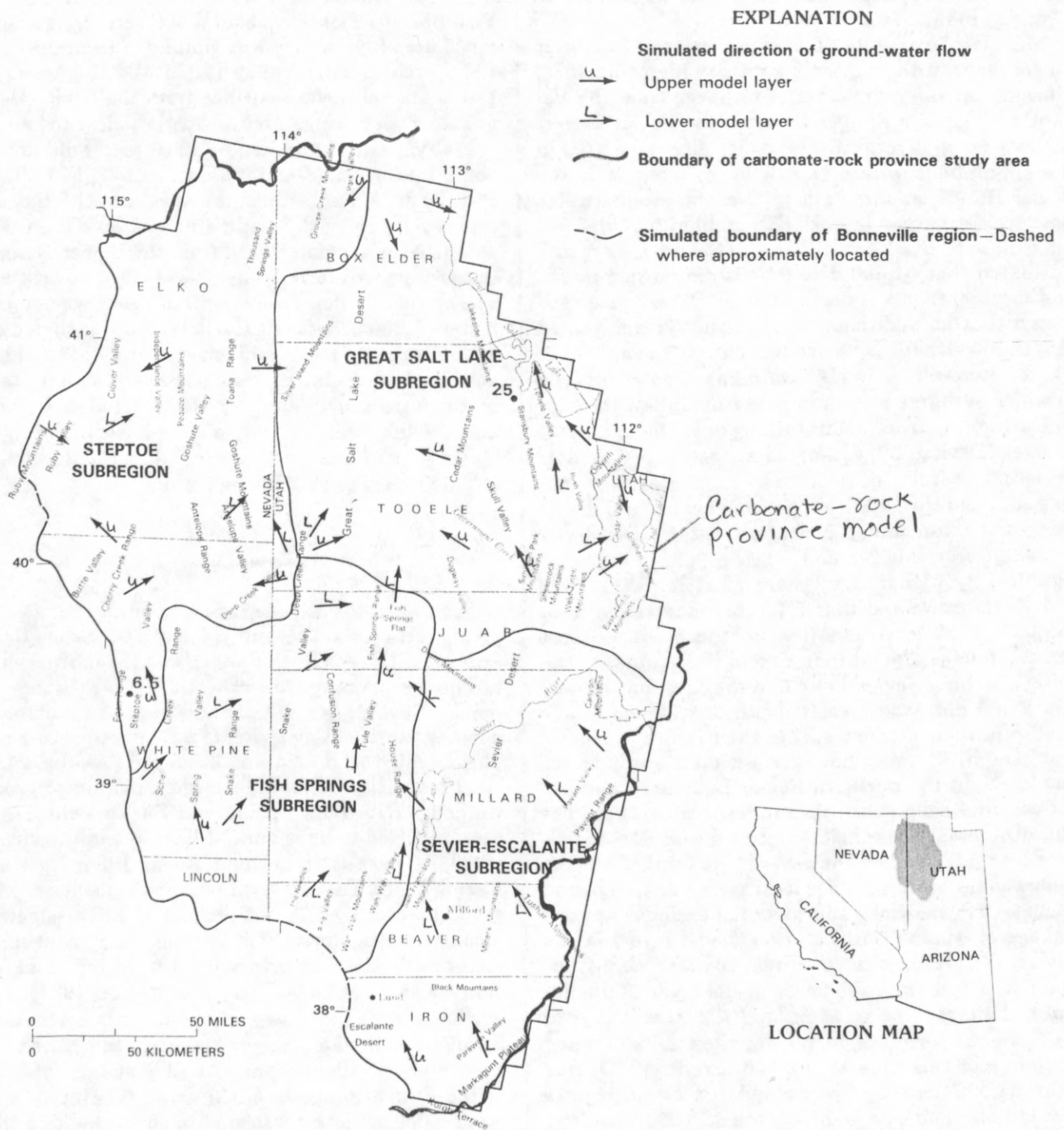


FIGURE 30.--Area boundaries and simulated ground-water flow directions in Bonneville region.

Mason simulated about 9,000 acre-ft/yr flowing through consolidated rocks from the Markagunt-Kolob highland to the Sevier Lake area.

In general, computed transmissivities of the lower model layer in the Sevier Desert are high (fig. 19B), allowing for large amounts of recharge from the Pavant and Tushar Ranges to reach the Sevier Desert without much diversion. The major discharge area in the simulations within the Bonneville region is the Sevier Desert, as large amounts of the ground-water flow are discharged here as ET. Holmes (1984) simulated flow in the basin fill in the Sevier Desert and estimated that 61,600 acre-ft/yr is discharged by ET and local springs within the Sevier Desert. He estimated that an additional 3,600 acre-ft/yr discharged into the Sevier River where it eventually evaporated. These discharge estimates were based on conditions in which recharge was estimated from inflow through the alluvium from mountain ranges to the east. Holmes (1984, p. 27) estimated almost 57,000 acre-ft/yr as inflow from the east. The remaining recharge was supplied through leakage from canals and reservoirs and unconsumed irrigation water. Discharge estimates from Mower and Feltis (1968, p. 52) were significantly higher than those of Holmes. Mower and Feltis estimated that ET rates may range from 135,000 to 175,000 acre-ft/yr in the Sevier Desert alone. Holmes argued that, due to the salinity of the water reaching Sevier Lake and the fact that Mower and Feltis did not consider depth to water or water quality in their estimates, that their figure is considerably high. Holmes, however, estimated only losses due to ET in the northern Sevier Lake area and did not consider deep subsurface inflow. Holmes did not find it necessary to consider subsurface inflow to balance his water budget, however. The total ET in the simulations (which includes local spring discharge and seepage to Sevier Lake and River but excludes upward leakage of water from the lower model layer) in the Sevier Desert area was about 104,000 acre-ft/yr. Simulated flow from the lower model layer to the upper model layer was an additional 75,000 acre-ft/yr in the Sevier Desert area, increasing the total simulated discharge of this area to 179,000 acre-ft/yr. Of this total, 51,000 acre-ft/yr was simulated as seepage to Sevier Lake and Sevier River and 128,000 acre-ft/yr was simulated as direct ET from the surrounding area (fig. 29). Discharge in the Sevier Desert is highly sensitive to the amount of recharge in the Pavant Range and Tushar Mountains used in the simulation.

Simulated outflow from the Sevier Desert area is small. Low computed transmissivities in the vicinity of the Deep Creek-Tintic belt (fig. 21A, no. 9) across the southern Great Salt Lake Desert limits flow in

the simulation to the north from the Sevier Desert (fig. 30). Simulated flows from the Sevier Desert to Fish Springs Flat was about 8,000 acre-ft/yr. Another 5,000 acre-ft/yr of flow was simulated from the Sevier Lake area to Tule Valley (table 4). Holmes (1984) estimated subsurface outflow from the Sevier Desert to both Fish Springs Flat and Tule Valley to be 8,800 acre-ft/yr. Gates and Kruer (1981, p. 27) did not pinpoint the origin of water flowing to Tule Valley or Fish Springs Flat, although several possibilities were discussed. They did estimate that less than 5,000 acre-ft/yr moves northward from the Sevier Desert to the vicinity of the Dugway-Government Creek area. The simulated flow following that route was approximately 1,000 acre-ft/yr. Carlton (1985) included only a part of Sevier Lake in his model, and his results did not clearly pinpoint the role of Sevier Lake (in terms of it being a source or sink). He concluded, however, that the lake was probably a sink, but simulating the lake as a source did not greatly affect the flow budget of Tule Valley or Fish Springs Flat.

FISH SPRINGS SUBREGION

From west to east, the major mountain ranges supplying recharge in this subregion are the Schell Creek, Snake, and Deep Creek Ranges and the northern part of The Needles (fig. 33). The Deep Creek Range lies north of the Snake Range, and both are part of the north-south-trending string of metamorphic core complexes which tend to inhibit eastward flow (fig. 21B).

Three valleys discharge large amounts of ground water by ET. Both Spring and Snake Valleys have been reported to have annual ET rates in the vicinity of 70,000 acre-ft (Hood and Rush, 1965; Rush and Kazmi, 1965). Tule Valley discharges considerably less ground water by ET, but estimates differ somewhat among investigators. Fish Springs, a regional spring area or collection of springs in Fish Springs Flat, discharges at about 26,000 acre-ft/yr (Gates, 1984).

Flow through the lower model layer is northeast at Spring and Snake Valleys (fig. 30). Simulated flow from Spring Valley to Snake Valley at the north end of the Snake Range is 6,000 acre-ft/yr (fig. 30); another 5,000 acre-ft/yr was simulated as shallower flow in the upper model layer. Simulated ET in Spring Valley was 67,000 acre-ft/yr, slightly less than the 70,000 acre-ft/yr estimated by Rush and Kazmi (1965, table 7). Simulated ET in Snake Valley was about 72,000 acre-ft/yr and is within the range of values estimated in the literature. Simulated ET areas in northern Snake Valley are continuous with ET in the southern Great Salt Lake Desert. Hood and Rush

(1965) estimated ET in Snake Valley to be about 80,000 acre-ft/yr for a similar area. Gates and Kruer (1981) and Carlton (1985) estimated only 65,000 acre-ft/yr for much of the same area. Because a significant amount of ET is discharged from the flow system in the southern Great Salt Lake Desert, however, discrepancies in the literature of as much as 10,000-15,000 acre-ft/yr could be expected. Underflow of about 6,000 acre-ft/yr from Spring Valley to Snake Valley was simulated around the north end of the metamorphic core complex (fig. 23) in the Snake Range into Snake Valley where it was discharged as ET. By increasing the computed transmissivities in the lower model layer in the vicinity of the Snake Range, underflow to Snake Valley also increased. This increased underflow, in turn, increased the amount of ET simulated in Snake Valley and decreased the total simulated ET in Spring Valley. This suggests that the proportions of ET discharged from these valleys are controlled by the permeability of the metamorphic core complex in the Snake Range, which is thought to be quite low.

East of Snake Valley, flow is simulated almost due north (fig. 30). Available head data suggest that recharge from The Needles and the Wah Wah Range flows northward toward either Tule Valley or Sevier Lake. Although head data from shallow wells show a slight gradient from southern Sevier Lake to northern Wah Wah Valley, limited head data from deep wells suggest a northward direction that almost parallels Sevier Lake. Carlton (1985) estimated the amount of flow from Wah Wah Valley to Tule Valley to be 26,000 acre-ft/yr. He also estimated that as much as 15,000 acre-ft/yr discharges to the southern Sevier Lake area in the Sevier-Escalante subregion.

Present model results of this area were sensitive to the amount of ET simulated at Tule Valley. Previous reports vary quite considerably as to the amount of water discharging by ET from Tule Valley. Gates and Kruer (1981, table 7) estimated an annual ET rate of 32,000 acre-ft. Carlton (1985, table 7) simulated only 19,500 acre-ft/yr. Evapotranspiration in Tule Valley was simulated in this study at about 39,000 acre-ft/yr. Because local recharge is not sufficient to supply the large amount of ET from Tule Valley, some flow must come from outside the immediate drainage area. About 15,000 acre-ft/yr was simulated in the lower model layer as flowing from Wah Wah Valley to Tule Valley. In addition, an upward head gradient was simulated between the two model layers beneath Tule Valley and northward to Fish Springs Flat. About 14,000 acre-ft/yr of water was also simulated as flowing through the upper model layer from Wah Wah Valley northward to Sevier Lake

in the Sevier-Escalante subregion (table 4). However, some of this flow was derived from recharge in the San Francisco Mountains south of Sevier Lake.

Springs at Fish Springs Flat discharge at an annual rate of 26,000 acre-ft (Gates, 1984). Recharge from local mountain ranges is only about 4,000 acre-ft/yr; thus, the primary source of water must flow from distant source areas (fig. 30). Fish Springs Flat acts as a sink for flow in the lower model layer. Simulated flow to Fish Springs Flat originates in the Deep Creek Range to the west, Snake Valley to the southwest, Tule Valley to the south, and the Sevier Desert to the southeast. Flow north from Fish Springs Flat is inhibited by low computed transmissivities in the lower model layer perhaps associated with the Deep Creek-Tintic Belt (figs. 19B and 21B). Low computed transmissivities in the upper model layer in the vicinity of the Great Salt Lake Desert inhibit shallower flow north of Fish Springs Flat as well (fig. 19A).

Approximately 25,000 acre-ft/yr was simulated as flowing from the southern Deep Creek Range eastward toward Fish Springs (fig. 30), with an additional 14,000 acre-ft/yr from Snake Valley. However, about 24,000 acre-ft/yr was simulated as ET in the extreme southern Great Salt Lake Desert, thus only about 15,000 acre-ft/yr was simulated to flow eastward toward Fish Springs Flat.

Previous investigations as to the total amount of ET discharging from the southern Great Salt Lake Desert are not conclusive. Because Snake Valley includes a part of the playa, no separate estimate of ET for just the playa and vicinity has been reported. Carlton (1985, p. 75) simulated 24,500 acre-ft/yr of ET in northern Snake Valley, which includes a part of the playa area.

Additional flows to Fish Springs Flat in the simulation include 6,000 acre-ft/yr directly from Snake Valley, 8,000 acre-ft/yr from the northern Sevier Desert, and 4,000 acre-ft/yr from Tule Valley (fig. 30 and table 4). The amount entering Fish Springs Flat from Tule Valley is in sharp contrast to the 25,500 acre-ft/yr estimated by Carlton (1985). Major differences in the total ET discharging from Tule Valley and the incorporation of the Deep Creek Range probably account for much of this discrepancy. Gates and Kruer (1981) suggested that flow from the Deep Creek Range does supply a large part of the discharge from Fish Springs. Their estimates are based in part on the carbon-14 dating of water from the Fish Springs, which indicated that the water discharging from the springs was between 12,000 and 14,000 years old, and estimates of transmissivities and hydraulic gradients in the area. Computed transmissivities in the

vicinity of the Deep Creek Range are within the range estimated by Gates and Kruer (1981).

Determining the actual amount of water discharging from the Fish Springs area is complicated due to a significant amount of ET in the vicinity of the springs (fig. 29). Simulated ET at Fish Springs Flat was 8,000 acre-ft/yr, which is identical to the estimate of Bolke and Sumsion (1978). The springs were simulated as discharging at an annual rate of about 23,000 acre-ft, leaving only about 2,000 acre-ft/yr, which flows northward from Fish Springs Flat into the southern Great Salt Lake Desert (fig. 30). Gates (1984) suggested that flow northward out of Fish Springs Flat was negligible (about 0.1 acre-ft/yr). Because the spring discharge is 3,000 acre-ft/yr lower than observed rates, the actual amount of underflow to the southern Great Salt Lake Desert could be closer to the estimate by Gates.

STEPTOE SUBREGION

Computed transmissivities in both model layers in the Steptoe subregion are fairly low except in Ruby Valley; thus, simulated flow is quite small throughout much of the area (figs. 19 and 30). Three shallow-flow regions are simulated in the upper model layer within the Steptoe subregion (fig. 22). Only small amounts of leakage to and from the lower model layer were simulated in each of the shallow-flow regions.

Little is known concerning the nature of the flow in the Steptoe subregion, although Eakin and others (1951) suggested that the consolidated Paleozoic rocks in this subregion are probably poorly permeable and that flows through these rocks are probably small. Estimated total recharge from mountain ranges in this subregion totals about 193,000 acre-ft/yr (fig. 29). Reconnaissance reports for much of this area indicate that virtually all the ET in these closed basins originates from recharge to the adjacent mountain blocks.

Virtually all the recharge in mountain ranges simulated in the Steptoe subregion is consumed by ET within adjacent valleys. According to reconnaissance reports, Steptoe Valley has the largest reported ET of 70,000 acre-ft/yr (Eakin and others, 1967) in the Steptoe subregion. Ruby Valley is the next highest at 53,000 acre-ft/yr, followed by the Clover and Independence Valleys area, having an estimated ET of 30,000 acre-ft/yr (Eakin and others, 1976, table 7). Evapotranspiration in northern Butte Valley has been reported to be about 7,000 acre-ft/yr (Glancy, 1968), while for Goshute Valley, at the north end of the area, ET is about 10,000 acre-ft/yr (Eakin and others, 1976, table 7). In Deep Creek Valley, reported ET values

range from 15,000 acre-ft/yr (Hood and Waddell, 1969, p. 23) to 12,000 acre-ft/yr (Gates and Kruer, 1981). Total reported estimated ET in the Steptoe subregion is about 185,000 acre-ft/year (compare to table 4). Much of the remaining discharge is attributed to a few regional springs and outflow to the Great Salt Lake subregion.

Evapotranspiration for the Steptoe subregion was about 154,000 acre-ft/yr in the simulations (fig. 29 and table 4), 15 percent less than the previously reported estimates. However, ET in the simulations is separate from regional spring discharge, whereas reported estimates are often combined, so the difference between simulated and reported estimates of ET may be less than 3 percent. Spring discharge in the model simulations was about 26,000 acre-ft/yr. Although the total reported estimates are similar to the simulations, some significant differences do exist. For instance, the amount of ET simulated in northern Butte Valley is considerably less than the amount reported by Glancy (1968). This difference is attributed in part to the large size of the model cells and to the computed heads being below the estimated land surface in the model cells that correspond to northern Butte Valley. Deep Creek Valley also has computed heads far below the estimate of land surface, resulting in a simulated ET of 7,000 acre-ft/yr, about half of the reported estimate. The simulation of less ET in this valley may be due to low computed transmissivities in surrounding model cells that result in less flow to the valley. In the simulations, flow from the Deep Creek Range was primarily to the east, north, and northeast toward the Great Salt Lake Desert rather than westward into Deep Creek Valley (fig. 30). Flow simulated into the Great Salt Lake Desert from the Deep Creek Range may therefore be somewhat high.

Only small quantities of ground-water flow were simulated in the lower model layer over most of the northern part of the Steptoe subregion, except perhaps locally. Simulated downward flow to the lower model layer is mostly from the Ruby Mountains or alluvial fans adjacent to the Ruby Mountains and represents almost one-third of the total inflow to the lower model layer in the Steptoe subregion. High computed transmissivities, moderately high vertical leakance values, and a northeastward hydraulic gradient are responsible for the simulation of this flow in the lower model layer. About 8,000 acre-ft/yr was simulated as flow in the lower model layer in the vicinity of Ruby Valley, of which 2,000 acre-ft/yr flows northward into Clover Valley and another 5,000 acre-ft/yr flows northeast into Independence Valley (fig. 30). The Clover-Independence Valley area acts as a sink in which most of this flow moves upward into the upper model layer

and discharges as ET. Flow in the lower model layer beneath Clover and Independence Valleys was simulated to be almost due east toward Goshute Valley, although the flow is less than 1,000 acre-ft/yr.

A steep hydraulic gradient was simulated in both model layers near the Utah-Nevada border between the Deep Creek Range and the northern boundary of the province (figs. 22 and 23). The steep gradient is also present in the observed head data (Thomas and others, 1986). A band of generally lower transmissivities was computed in the corresponding model cells (fig. 19) in response to the steep hydraulic gradients. This band is more discernible in the upper model layer (fig. 19A) as it is more discontinuous in the lower model layer (fig. 19B). The discontinuous band in the lower model layer is related to how the computed transmissivity values were categorized. Many of the computed transmissivity values for cells in this area are actually near to the 0.006 ft²/s value. The low computed transmissivities in this area may be related to low-permeability rocks that are exposed near the surface and are probably more continuous at depth (see fig. 23). At any rate, the steep hydraulic gradient reflects a change in the ability of the rocks to transmit water and results in the simulation of little flow from eastern Nevada toward the Great Salt Lake Desert. The amount of flow entering the Great Salt Lake subregion from the upper model layer from the Steptoe subregion was about 1,000 acre-ft/yr, primarily from the Toana Range and the Goshute Mountains. The amount of flow entering the Great Salt Lake subregion through the lower model layer was about 2,000 acre-ft/yr, with most of this entering just north of the Deep Creek Range.

Flow in the lower model layer was simulated in the area of Blue Lake springs (also called Big Salt springs), which is located east of the steep hydraulic gradient and near the Great Salt Lake Desert (figs. 21B and 29). This area could have been included in the Great Salt Lake subregion, but because little ground water was simulated as flowing to the desert it was included in the Steptoe subregion. Discharge to this spring area was simulated to be about 14,000 acre-ft/yr (fig. 29), which is somewhat less than the observed discharge of 19,000 acre-ft/yr (Gates and Kruer, 1981, p. 18). In the simulations, flow to the Blue Lake springs in the lower model layer was from (1) Deep Creek Range, which accounted for 7,000 acre-ft/yr, (2) Goshute Mountains and Toana Range, which accounted for 6,000 acre-ft/yr, and (3) Antelope Range, which accounted for 1,000 acre-ft/yr.

Other smaller regional springs are located near the edge of Steptoe Valley—Campbells embayment located in the southwest part of the valley and Curry-McDer-

mitt springs located at the northern end of the valley (figs. 11 and 29). The origin of water discharging at these locations is probably more localized than water discharging at Blue Lake springs. However, it is possible that some water discharging at Campbells embayment may originate from recharge in mountains adjacent to Butte and Long Valleys, as discussed in the section about the White River subregion of the Colorado River region. Several other springs that discharge in the Steptoe subregion are found in Thousand Springs Valley and northern Butte Valley. Although ground-water flow through carbonate rocks may supply these springs, the springs were not considered regional because of their presumed short flow paths.

GREAT SALT LAKE SUBREGION

The Great Salt Lake subregion within the Bonneville region is primarily a discharge area, except for localized areas with high recharge from mountain ranges within the subregion, such as ranges adjacent to Tooele, Rush, and Skull Valleys south of the Great Salt Lake and northwest of Utah Lake and Park Valley in the northwest corner of Utah (fig. 29). Flow in the lower model layer was simulated in the Oquirrh and Stansbury Mountains and extending to the eastern margin of the province (figs. 29 and 30). However, for the most part, little flow was simulated in the lower model layer in the Great Salt Lake subregion. Except for a small area north of Tooele Valley, only small amounts of ground-water discharge were simulated into the Great Salt Lake (fig. 30 and table 4). Recharge from direct precipitation onto the salt flats adjacent to the lake and in the Great Salt Lake Desert, although significant (Gates, 1984, estimated 52,000 acre-ft/yr), was omitted from the simulations because most of the precipitation that falls on these areas was assumed to be local flow, as the water does not travel far before it is discharged by ET.

Discharge from the eastern part of the Great Salt Lake subregion is primarily by ET, although several small regional springs are located in the subregion. Simulated ground-water flow directions vary widely in the upper model layer in the area surrounding Utah Lake, as shown in figure 30. Southwest of the Oquirrh Mountains, flow is south and eastward toward Utah Lake. Hood and others (1969, p. 23) reported similar findings. In northern Rush Valley, ground-water flow in the upper model layer is northward toward Tooele Valley and northwest from Tooele and Skull Valleys. The direction of flow in the lower model layer is similar to that simulated in the upper layer

(fig. 30). North of the East Tintic Mountains and southeast of the Oquirrh Mountains, flow was simulated northwest toward the Great Salt Lake Desert, but the amounts are small. Flow in the lower model layer to the Great Salt Lake Desert from areas east of the Cedar Mountains was also simulated to be small.

Discharge from the Great Salt Lake subregion in areas east of the Cedar Mountains is primarily by ET (fig. 29). Estimates of ET for valleys east of the Cedar Mountains have been reported as follows: Skull Valley—30,000 acre-ft/yr (Hood and Waddell, 1968); Tooele Valley—23,000 acre-ft/yr (Razem and Steiger, 1981, p. 16); Goshen Valley—27,000 acre-ft/yr (Cordova, 1970); Rush Valley—27,000 acre-ft/yr (Hood and others, 1969, p. 28); and Cedar Valley—27,000 acre-ft/yr (Eakin and others, 1976, table 8). Total ET simulated during this study for these valleys differs by more than 10 percent in Tooele, Cedar, and Goshen Valleys. In Tooele Valley, ET in the simulations may be high due to boundary effects to the east in the Oquirrh Mountains as northward flow is not allowed, but rather is routed westward toward Tooele Valley. In Cedar and Goshen Valleys, general-head boundaries are included as part of the valley; thus, the conductance value at the boundary directly affects the amount of ET simulated in the valleys and also the amount of water leaking into Utah Lake. The rate of leakage into Utah Lake has not been estimated from areas west of the Jordan River (fig. 5), although such occurrence of leakage into Utah Lake has been suggested by Cordova and Subitzky (1965, p. 23). Only 6,000 acre-ft/yr was simulated as discharge to Utah Lake from areas to the west while about 48,000 acre-ft/yr was simulated as ET in Cedar and Goshen Valleys.

Ground-water flow into the Great Salt Lake was simulated in an area north of Tooele Valley through the upper model layer (fig. 30). Discharge into the Great Salt Lake was simulated to be 6,000 acre-ft/yr, 5,000 acre-ft/yr of which is at Tooele Valley. Razem and Steiger (1981, p. 17) estimated about 3,000 acre-ft/yr of ground water discharging into the Great Salt Lake from Tooele Valley. Razem and Steiger did not indicate what effect pumping (28,000 acre-ft/yr) from Tooele Valley has on the amount of discharge into the Great Salt Lake.

Overall, the Great Salt Lake Desert subregion is characterized by computed transmissivities that are moderately high in the lower model layer and generally low in the upper model layer (fig. 19), low flow rates, and high ET. Gates (1984, table 1) estimated that the amount of ET from the Great Salt Lake Desert is approximately 30,000 to 40,000 acre-ft/yr if precipitation onto the salt flats is not included. Total discharge simulated as ET was 36,000 acre-ft/yr, with

only minor amounts of outflow simulated at the boundary with the Great Salt Lake (about 1,000 acre-ft/yr). Lowest heads in both model layers were in the south-central part of the Great Salt Lake Desert and along the margins of the Great Salt Lake (fig. 18). The depression-shaped equipotential in the Great Salt Lake Desert is caused by ET in the central part of the desert; and because the heads in the area are near 4,250 ft in altitude, small changes in head affect the way the 4,250-ft contour is drawn.

Flow through the lower model layer into the Great Salt Lake Desert was generally limited from areas to the south and southwest and was about 5,000 acre-ft/yr (note c in table 4). Gates (1984) also proposed that subsurface outflow from Deep Creek and Snake Valleys was by deep flow (3,000 and 22,000 acre-ft/yr, respectively), although he assumed that most of the 22,000 acre-ft/yr was flowing from Snake Valley toward Fish Springs Flat.

Flow through the upper model layer into the Great Salt Lake Desert within the Great Salt Lake subregion was simulated to be about 32,000 acre-ft/yr. Gates (1984) reported that inflow to the desert through the basin-fill deposits was about 26,000 acre-ft/yr, mostly from Park Valley, the Dugway Valley-Government Creek area, and Snake Valley.

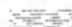
RAILROAD VALLEY REGION

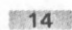
The Railroad Valley region occupies an area of 6,250 mi², making it the smallest of the five regions delineated from flow in the lower model layer (fig. 23). The basin is surrounded by 11 mountain ranges and encloses two others, as shown in figure 31. Most of these mountain ranges supply varying amounts of recharge. Total recharge to the basin is approximately 121,000 acre-ft/yr, the smallest amount of recharge for any of the five regions.

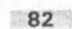
Ground-water discharge is primarily by ET. Van Denburgh and Rush (1974) estimated about 80,000 acre-ft/yr as being discharged by ET in Railroad Valley alone. Eakin (1960) estimated ET in Newark Valley at 16,000 acre-ft/yr. Regional spring discharge is about 19,000 acre-ft/yr, of which discharge at Duckwater springs accounts for 11,000 acre-ft/yr (Van Denburgh and Rush, 1974).

Flow through the lower model layer in the Railroad Valley region was simulated to be about 36,000 acre-ft/yr or 30 percent of the estimated annual recharge to the region (fig. 31). Flow into the lower model layer is from downward leakage through the upper model layer in the White Pine Range (8,500 acre-ft/yr), Pancake Range (9,000 acre-ft/yr), Grant

EXPLANATION


 Approximate extent of Cortez Rift—Also referred to as Oregon-Nevada lineament


 Generalized area of recharge—Number is estimated recharge in thousands of acre-feet per year


 Generalized area of discharge—Number is simulated evapotranspiration in thousands of acre-feet per year

2. Regional spring and simulated discharge—Number is discharge in thousands of acre-feet per year

Simulated direction of ground-water flow

 Upper model layer

 Lower model layer

 Simulated boundary of Railroad Valley region—Dashed where approximately located

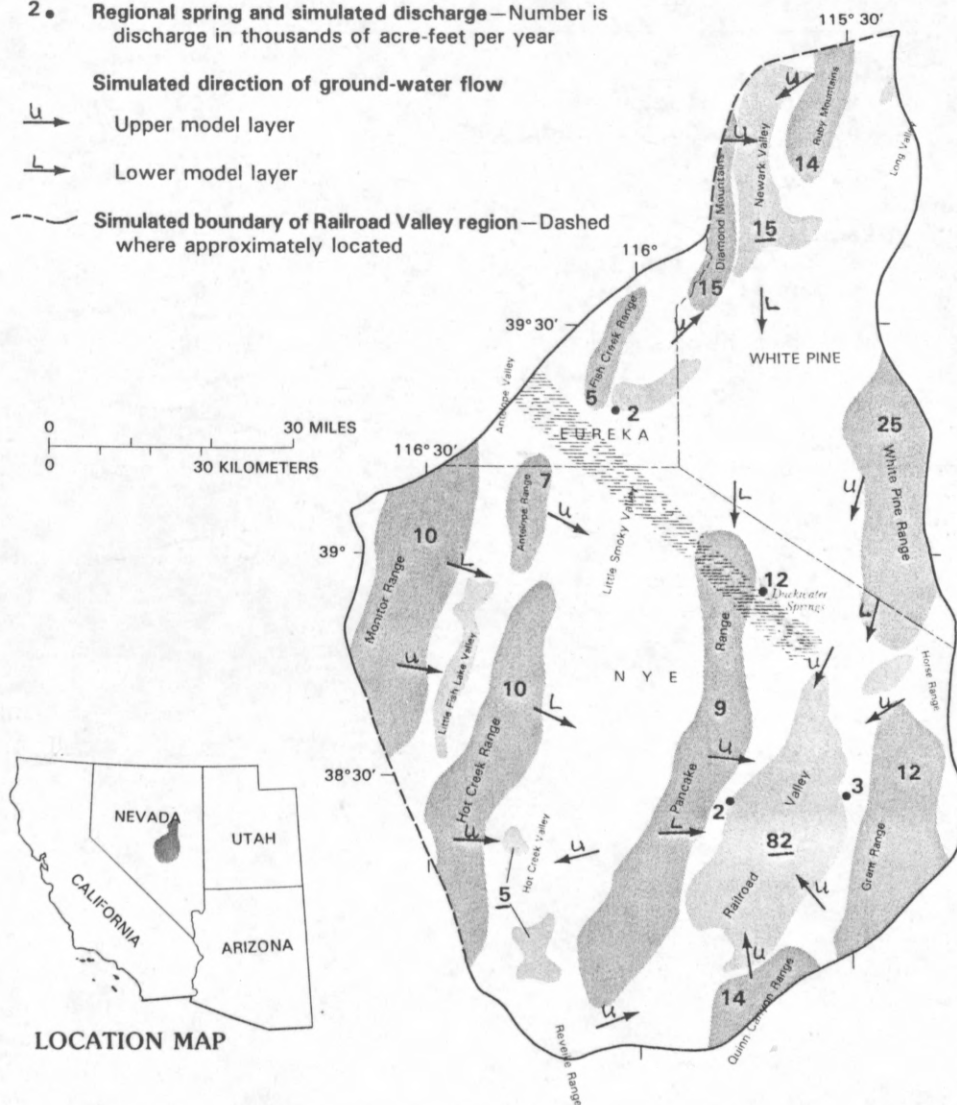


FIGURE 31.--Areas of estimated recharge and simulated regional spring discharge and evapotranspiration; approximate extent of the Cortez rift; and simulated flow directions for both upper and lower model layers for Railroad Valley region.

TABLE 5.--Simulated ground-water flow budget,
Railroad Valley region, in acre-feet per year

Recharge	
Mountain blocks	121,000
Head-dependent boundaries	0

Total recharge	121,000
Discharge	
Evapotranspiration	102,000
Regional springs	19,000

Total discharge	121,000

Range (2,700 acre-ft/yr), and Newark Valley (15,000 acre-ft/yr).

About 102,000 acre-ft/yr was simulated as ET in the entire region. Of this amount, 82,000 acre-ft/yr was simulated as ET in Railroad Valley, the terminal sink for the Railroad Valley region (fig. 31). The remaining 20,000 acre-ft/yr of ET was simulated in Newark and Hot Creek Valleys.

Flow in the lower model layer beneath Monitor, Hot Creek, and Antelope Ranges was to the southeast toward Railroad Valley, a pattern that is consistent with the results of test drilling described by Dinwiddie and Schroder (1971). The amount of this flow is about 9,000 acre-ft/yr. Flow elsewhere was also simulated as converging toward Railroad Valley. Flow through the lower model layer into Railroad Valley was about 37,000 acre-ft/yr. About 17,000 acre-ft/yr was simulated as discharging to regional springs while the remaining 20,000 acre-ft/yr was simulated as leakage into the upper model layer, where it was discharged by ET.

Flow in the upper model layer was generally from the mountain ranges to the adjacent valleys. About 62,000 acre-ft/yr was simulated as flow through the upper model layer into Railroad Valley, where it was discharged by ET. The amounts of flow in the upper layer from mountains adjacent to Little Fish Lake, Hot Creek, and Little Smoky Valleys (fig. 31) to Railroad Valley were similar to those estimated by Eakin and others (1951), Eakin (1960), Rush and Everett (1966b), and Fiero (1968), and was about 6,000 acre-ft/yr. Flow from the Fish Creek Range was toward Newark Valley as well as from parts of the Diamond and Ruby Mountains.

Blankennagel and Weir (1973, p. B20) suggested that at least 1,000 acre-ft/yr of ground water flows from Railroad Valley into adjoining Kawich Valley to the south, which is part of the Death Valley region. However, no flow was simulated out of the Railroad Valley from either model layer to the south (fig. 31 and table 5).

Only 3,000 of the 12,000 acre-ft/yr that was simulated as discharge from Duckwater Springs was from the nearby source areas in the Pancake Range and the White Pine Range (fig. 31). Changing the transmissivity in the lower model layer between Newark Valley and Duckwater springs markedly changed spring discharge. When transmissivities between these two places were decreased to less than 0.05 ft²/s, discharge at Duckwater springs was solely from water recharged in nearby mountain ranges, and simulated ET in Newark Valley was well above the values estimated by Eakin (1960). However, when transmissivities were increased in the lower model layer to nearly

1.0 ft²/s between Newark Valley and Duckwater springs, spring discharge increased to nearly 12,000 acre-ft/yr, and ET in Newark Valley was reduced from nearly 23,000 acre-ft/yr to 15,000 acre-ft/yr, which is close to the 16,000 acre-ft/yr reported by Eakin. Thus, on the basis of model results, some of the discharge at Duckwater springs was from downward leakage into the lower model layer in the vicinity of Newark Valley. All flow in the upper model layer at the north end of the Railroad Valley region was toward Newark Valley (fig. 31).

The occurrence of Duckwater springs may be related in part to the Cortez rift, also referred to as the Oregon-Nevada lineament (fig. 21B), which in figure 31 is shown as extending in a northwest line just south of the spring. Aeromagnetic data along with topographic expression, local hydraulic gradients, and thermal springs suggest that the Cortez rift may extend farther southeast into Railroad Valley than has been previously published. Computed transmissivities along the rift are generally low (fig. 19B), and might reflect low-permeability intrusive rocks at depth, especially at the western end of the region. These intrusive rocks may create barriers along parts of the rift and not at other places, because the rocks seem to be discontinuous. Flow in the lower model layer was simulated across the rift only in the vicinity of the White Pine Range, where 7,000 acre-ft/yr was simulated as flowing toward Railroad Valley.

To test the possible impact on flow caused by the low transmissivities along the rift, transmissivities in the lower model layer were increased along the rift to match values of the surrounding cells. In this simulation, southward flow through the lower layer increased from 7,000 to nearly 20,000 acre-ft/yr and ET in Newark Valley decreased significantly while ET in Railroad Valley approached 95,000 acre-ft/yr.

Reducing transmissivities in cells along the rift in the lower model layer to values of 0.0001 ft²/s, including areas within the White Pine Range, resulted in flow being split into two subregions. In this simulation, heads north of the rift were raised and a steep gradient was simulated across the rift. North of the rift, the hydraulic gradient was eastward toward the Colorado River region. ET in Newark Valley increased to over 20,000 acre-ft/yr, while ET in Railroad Valley decreased to about 70,000 acre-ft/yr.

Flow across the Cortez rift is probably not completely inhibited, but rather may be directed to areas of higher transmissivities such as the zone simulated along the eastern side of Railroad Valley.

The part of the Humboldt River drainage basin (Eakin and Lamke, 1966) which is discussed in this section is referred to as the Upper Humboldt River region and is approximately 7,300 mi² (fig. 23). Boundaries of the region are shown in figure 32 and should not be confused with the upper basin described by Eakin and Lamke, which includes the entire drainage area of the Humboldt River east of Palisade (fig. 32).

The Upper Humboldt River region is unlike the other four regions in that the volume of surface water flowing through the Humboldt River and its tributaries far exceeds the water that recharges to the ground-water flow system. This discussion deals solely with those interactions of surface and ground water that directly affect the model simulations, either by removal or addition of water. Discussion will concern (1) the net amount of water exchanged between the upper and lower model layers and the head-dependent cells representing the Humboldt River, and (2) the amount of ET that is attributed to ground-water discharge in the vicinity of the Humboldt River.

Recharge from source areas within the bounds of the Upper Humboldt River region was estimated to be about 150,000 acre-ft/yr (fig. 32 and table 6). Surface water from outside the modeled area enters the Humboldt River and its tributaries from the north (Eakin and Lamke, 1966). Thus, head-dependent boundaries were used to represent the Humboldt River and its major tributaries and allow for either recharge from the Humboldt River or discharge to it, depending on the relation of heads in the upper model layer to the river stages assigned to the Humboldt River.

Evapotranspiration rates associated with surface water within the entire Humboldt River drainage basin are in the millions of acre-feet per year (Eakin and Lamke, 1966), but neither streamflows nor ET associated with streams were simulated in the model because such processes represent local flow.

Most of the valleys south of the Humboldt River have been described in previous reports (Eakin, 1961, 1962; Rush and Everett, 1964, 1966a). Discharge from these areas is primarily through ET. The total estimated ET from northern Monitor, Kobeh, Antelope, Diamond, Huntington, Grass, Crescent, Pine, and Boulder Valleys is about 102,000 acre-ft/yr. Evapotranspiration simulated during this study for each of the valleys (fig. 36) is similar to those reported estimates except for Kobeh Valley, which has a simulated value 50 percent less than the estimate reported by Rush and Everett (1964). The discrepancy between

simulated and estimated ET in Kobeh Valley might be justified if the location of the southern boundary is too far to the north. Estimated recharge from only the eastern half of the Toiyabe Range was used in the model simulations. If the estimated recharge is too low, then the boundary between the Death Valley region and the Upper Humboldt River region may move southward, allowing for more recharge from the Monitor Range into Monitor and Kobeh Valleys. Perhaps the boundary between the two regions should be moved southward by adjusting transmissivities near the boundary. Another possible explanation is that the Cortez rift (fig. 32), which lies along the northern and western borders of Kobeh Valley, may impede ground-water flow from the north and west just enough to lower the computed heads in Kobeh Valley and lower the ET, while still allowing significant flow to Diamond Valley.

Eakin (1962, p. 18) estimated that if underflow from Kobeh Valley to Diamond Valley did occur, it was very small. Therefore, if all the simulated underflow leaving Kobeh Valley discharges as ET in Kobeh Valley instead of leaving the valley, then the total simulated ET would differ from the estimated rate of Rush and Everett (1964) by only 10 percent. Simulated ET in Diamond Valley was 40,000 acre-ft/yr, considerably higher than the reported estimates of Eakin (1962, table 6) or Harrill (1968, p. 34), who estimated 23,000 and 30,000 acre-ft/yr, respectively. Thus, the seemingly high values of simulated underflow between Kobeh and Diamond Valleys suggest that the calibrated transmissivities between Kobeh and Diamond Valleys may also be high.

ET in Huntington Valley and associated areas north of Diamond Valley was simulated at 20,000 acre-ft/yr, about 3,000 acre-ft/yr greater than reported by Rush and Everett (1966a). The amount of simulated underflow from Diamond Valley to Huntington Valley was about 5,900 acre-ft/yr of which about 3,600 acre-ft/yr was simulated as flow in the upper model layer and 2,300 acre-ft/yr in the lower model layer.

Simulated flow in much of the remaining areas is generally toward the Humboldt River (fig. 32), but amounts are small. Evapotranspiration and ground-water discharge through general-head boundaries along the Humboldt River upstream (northeast) from Elko was simulated to be about 69,000 acre-ft/yr. About 17,000 acre-ft/yr was simulated as recharge from the Humboldt River along the same reach (table 6). Thus, the net discharge was about 52,000 acre-ft/yr. Much of the discharge in the simulation originated in the Ruby Mountains, East Humboldt Range, and recharge areas north of the Humboldt River.

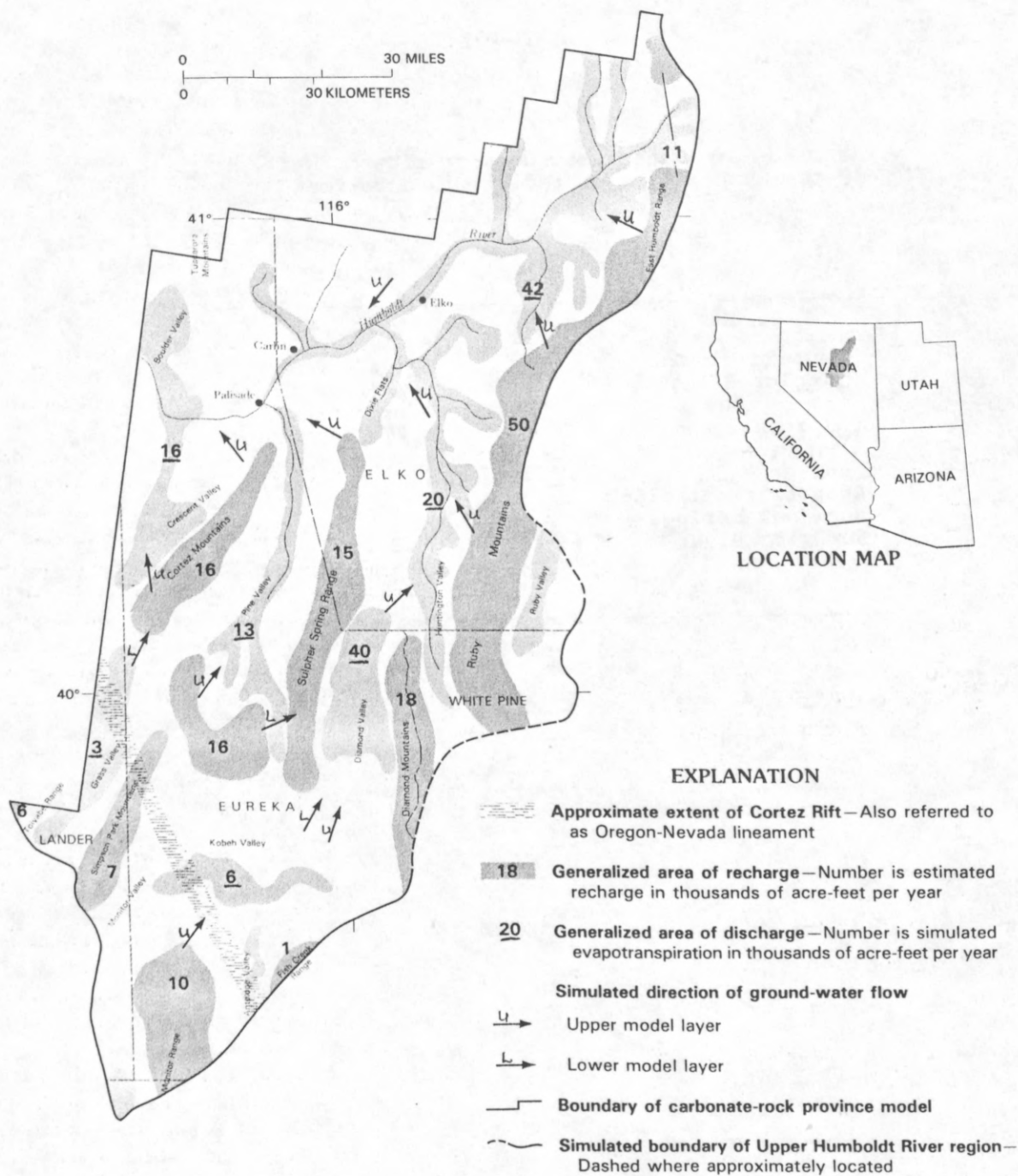


FIGURE 32.--Areas of estimated recharge and simulated evapotranspiration, approximate extent of Cortez rift, and simulated flow directions of Upper Humboldt River region in relation to Humboldt River drainage basin.

TABLE 6.--Simulated ground-water flow budget,
Upper Humboldt River region, in acre-feet
per year

Recharge	
Mountain blocks	150,000
Humboldt River	17,000

Total recharge	167,000
Discharge	
Evapotranspiration	140,000
Regional springs	0
Humboldt River	27,000

Total discharge	167,000

Eakin and Lamke (1966) used stream gaging along the Humboldt River and its tributaries to determine surface-water inflow and outflow along selected reaches of the river. According to them, the river between Elko and Palisade, a distance of about 30 mi, gains about 14,000 acre-ft/yr. This increase is not associated with inflow from tributaries and therefore must be from ground-water discharge. Ground-water discharge along the same reach of the river was simulated at 27,000 acre-ft/yr. Much of this discharge into the Humboldt River is from the Ruby Mountains. For the most part, computed transmissivities within the lower model layer are low in this area, but are still greater than those of the upper model layer (fig. 19). These lower values may be related to the thinning of carbonate rocks and more abundant transitional assemblage of rocks near the western edge of the miogeosyncline. The transitional assemblage consists predominantly of volcanic, clastic, and intrusive rocks that may have a lower permeability than the carbonate rocks. However, because even shallow water-level data are sparse in the area, computed transmissivities may differ significantly than those that actually exist.

SUMMARY AND CONCLUSIONS

Ground-water flow in an area dominated by basin-fill and carbonate-rock aquifers in western Utah and eastern Nevada and small parts of Arizona, California, and Idaho was studied as part of the U.S. Geological Survey Great Basin Regional Aquifer-System Analysis project. The area studied is referred to as the carbonate-rock province and is geologically complex. Rocks range in age from Precambrian to Holocene, and the history of the area includes many episodes of sedimentation, volcanic activity, and tectonic deformation by both compressional and extensional forces. By 1984, the population of the study area had increased fivefold since World War II. Expected continued population increases and water-resources demands have resulted in a desire for a three-dimensional conceptual flow model of the carbonate-rock province. The model incorporated all available information. The present physiography of the province is the result of block faulting caused by extensional forces that began about 20 million years ago and is characterized by north- to northeast-trending mountain ranges separated by intervening valleys partly filled with deposits eroded from adjacent mountains. The mountain ranges rise from 1,000 to more than 7,000 ft above the adjacent valleys.

Shallow ground-water reservoirs are the basin-fill deposits, which supply most of the water pumped from

wells. Thick sequences of Paleozoic carbonate rocks underlie much of the study area and are also significant ground-water reservoirs. Most of the large springs in the province issue from carbonate rocks or from basin fill overlying or adjacent to carbonate rocks. The other types of consolidated rocks (except for the fractured welded tuffs and basalts) and fine-grained basin-fill deposits generally transmit small quantities of water and act as low-permeability barriers to ground-water flow.

The source of ground water in the province is precipitation that falls primarily on the higher mountain ranges. About 3 percent of the precipitation is estimated to recharge ground water, but this percentage does not include recharge that travels a short distance before it is discharged locally. Most of the ground-water discharge is by evapotranspiration in the low parts of the many valleys or along rivers and streams. Some ground water also discharges to springs. Numerous springs are discharge points of ground water that originated in the adjacent mountains while at others, the ground water originated in distant mountains and traveled long distances beneath valleys and perhaps beneath other mountain ranges.

Ground-water flow in the province was conceptualized as relatively shallow flow primarily through basin-fill deposits and adjacent mountain ranges superimposed over deeper flow through primarily carbonate rocks. A three-dimensional ground-water flow model was used to simulate this concept of ground-water flow in the province. The province was divided into cells 5 mi wide and 7.5 mi long. Two model layers were used to simulate relatively shallow and deep flow. The upper layer was used to simulate flow primarily through basin-fill deposits and adjacent mountain ranges to depths of several thousand feet. The lower model layer was used to simulate the concept of deep flow beneath the basin fill and mountain ranges, presumably through carbonate rocks. The actual depth of deep flow in the province is unknown, but the carbonate rocks may be as much as 30,000 ft thick, and fresh water has been detected to depths of as much as 10,000 ft.

Several simplifying assumptions were necessary in the simulation and conceptualization of the flow regions: (1) Fractures and solution openings in consolidated rocks could be represented as a porous medium on a regional scale. (2) Darcy's Law is applicable to flow through the fractures and solution openings and in a geologically complex area where numerous abrupt lithologic changes are caused by innumerable faults, several shear zones, intrusive rocks, and ancient volcanoes. (3) Steady-state conditions exist in the province in which estimates of present-day recharge (oc-

curing in the mountain ranges) is assumed equal to estimates of the discharge (prior to withdrawals). (4) Areal distribution of discharge is known as well as amount of discharge from regional springs. (5) Horizontal transmissivity was homogeneous and isotropic in each model cell. Although the assumptions are probably valid for parts of the study area, the validity of each assumption is not known for the entire area. Therefore, the results of the simulations should be considered as conceptual and interpreted with caution.

Assumptions about the available data were used in addition to the general assumptions. Recharge in the province was assumed to be known and was estimated from numerous reports. Recharge was also assumed to occur only in the mountains except for the areas underlying rivers and lakes, which were assumed as head-dependent flow boundaries that could either recharge or discharge ground water. The areal distribution of discharge by evapotranspiration was assumed to be known and was assumed to be the discharge from the upper model layer. The distribution and amount of discharge by regional springs was assumed to be known and was mostly from the lower layer.

Transmissivity values in both model layers and vertical leakance values between layers were adjusted during repeated simulations until simulated water levels in both model layers approximated general water-level trends that were interpolated and extrapolated from measured water levels, and areas of simulated discharge approximated areas of known evapotranspiration. Transmissivity values were computed and refined on the basis of general water-level trends, distribution and amount of recharge, and the distribution and amount of discharge.

Magnitude of the computed transmissivity and leakance values were dependent on the amount of recharge and water-level trends used in the simulations because the model assumed steady-state conditions. Increasing recharge in the simulations resulted in a corresponding increase in discharge and a proportional increase in the computed transmissivity and vertical leakance values. Estimates of recharge are only rough approximations and could be off by 100 percent or more. Thus, the magnitude of the computed transmissivity and leakance values by simulations include an uncertainty equal to the uncertainty of the estimated recharge.

Another limitation of the computed transmissivity values is that the values are based on limited water-level data, particularly for the lower model layer. Transmissivity and vertical leakance values could be changed by at least an order of magnitude in areas of no data and the model results might still be reasonable

with respect to areas of known water-level trends and places of discharge. The simulated transmissivity and vertical leakance values may also change more gradually than might be expected, because the water-level data were smoothed by interpolation and extrapolation from known points and were averaged over a large cell area. Thus, the computed transmissivity and vertical leakance values include large uncertainties.

Computed transmissivity values in the upper model layer varied more than those of the lower model layer (fig. 19). This probably reflects greater fluctuations in water levels in the upper layer due to more available data. The greater variation of transmissivity values in the upper model layer may also result from applying all the recharge in model cells that correspond to mountains instead of including the adjacent cells that correspond to the alluvial fans and valleys, or to highly variable thicknesses of permeable rock that is reflected in differing thicknesses of model cells.

In the upper model layer, the simulated flow in the eastern part of the province was generally from south to north toward the Great Salt Lake Desert (Bonneville region). In the northwest part of the province, simulated flow was north toward the Humboldt River. In the southern half of the province, simulated flow was from north to south toward either Death Valley or the Virgin River (tributary to the Colorado River). Simulated flow in the lower model layer was not always in the same direction as that simulated in the upper model layer, and in some instances flow was simulated in opposite directions.

Only one of several extensive east-west-trending lineaments could be correlated with a marked change in the simulated water levels as well as observed water-level trends. The lineament, called the transverse crustal boundary, extends across southern Nevada. It marks the southern extent of Cenozoic volcanism in the province, is delineated by a considerable southward decrease in the altitude of the valley floors and a marked change in gravity, and is associated with left-lateral shears at several places.

The lack of correlation of marked changes in simulated water levels and transmissivity values, as well as observed water-level trends across other lineaments north of the transverse crustal boundary, might be due to normal faults disrupting the lineaments as the lineaments may be older in age than the normal faults. However, several regional springs are located near the lineaments, which indicates that the lineaments may influence regional ground-water flow to some degree.

The direction of simulated flow in the upper model layer was generally away from or around outcrop areas of intrusive rocks, ancient volcanoes, Precambrian and

Cambrian basement rocks, and fine-grained basin-fill deposits. Only small amounts of water were simulated as moving through such areas. Most simulated flow in the lower model layer was diverted around inferred hydrologic low-permeability barriers as determined from aeromagnetic anomalies. Thus, limited water-level data and known discharge points used in the simulation may generally reflect both surface and deep structures.

Only five flow regions were simulated in the lower model layer and were delineated on the basis of flux through each model cell. The five deep-flow regions were named after the terminal discharge point in each region, even though little ground water was simulated to discharge at the terminal discharge points: (1) Death Valley, (2) Colorado River, (3) Bonneville (includes the Great Salt Lake and Great Salt Lake Desert), (4) Railroad Valley, and (5) Upper Humboldt River. Superimposed over the deep-flow regions are 17 shallow-flow regions delineated from the simulation of flow in the upper model layer. These shallow-flow regions approximately coincide with the delineations of flow systems from topography, water-level data, discharge areas, and water budgets.

A total of about 1.6 million acre-ft/yr was simulated as recharge to the model layers. Table 7 summarizes the simulated recharge and discharge within each of the five deep-flow regions and includes flow within the overlying shallow-flow regions. Recharge to local flow (less than the area of a model cell) was not considered in the study, but if included, the estimated recharge would be considerably more.

Recharge to the Death Valley region was simulated to be about 165,000 acre-ft/yr or 10 percent of the total simulated recharge to the entire modeled area. Major recharge areas included the Springs Mountains west of Las Vegas and the Toiyabe Range north of Tonopah in central Nevada. Discharge was simulated as mostly evapotranspiration (122,000 acre-ft/yr). Simulated regional spring discharge was 20,000 acre-ft/yr at Ash Meadows. Another 23,000 acre-ft/yr was simulated as discharge in Death Valley and included both regional spring discharge and evapotranspiration.

Recharge in the Colorado River region was simulated to be about 249,000 acre-ft/yr or 15 percent of the total simulated recharge to the entire modeled area. The greatest simulated discharge in the Colorado River region was to regional springs (about 106,000 acre-ft/yr); simulated evapotranspiration was 58,000 acre-ft/yr and leakage to the Virgin River and vicinity was another 85,000 acre-ft/yr.

The Bonneville region in western Utah was the largest of the delineated flow regions. About 904,000 acre-ft/yr, more than 50 percent of the total simu-

lated recharge to the entire modeled area, was estimated as recharge in this region. Most of the simulated discharge was by evapotranspiration and was about 775,000 acre-ft/yr. Simulated discharge from regional springs accounted for only 7 percent of the simulated discharge in the region. Only ground-water flow north of Tooele Valley was simulated to discharge to the Great Salt Lake; otherwise ground-water discharge to the lake was simulated only in the areas surrounding the lake.

The Railroad Valley region is areally the smallest. Simulated recharge was about 121,000 acre-ft/yr, or about 7 percent of the total simulated recharge for the modeled area. About 85 percent of the simulated discharge was by evapotranspiration, primarily in Railroad Valley. In the northern half of the region, simulated flow in the upper model layer was toward Newark Valley. In Newark Valley, simulations indicated that flow in the upper model layer leaked downward into the lower model layer and discharged at Duckwater Springs, located at the north end of Railroad Valley.

The Upper Humboldt River region is a part of the Humboldt River drainage basin. Simulated recharge was about 167,000 acre-ft/yr, of which 17,000 acre-ft/yr was simulated as recharge from the Humboldt River. Simulated evapotranspiration was about 140,000 acre-ft/yr and is much less than the total estimates reported by other investigators that include evapotranspiration along the Humboldt River and its tributaries. About 27,000 acre-ft/yr was simulated as discharge to the Humboldt River between Elko and Palisade, Nev.

Conclusions of this study can be grouped into three categories: (1) results that are in general agreement with hypotheses found in the literature; (2) results which are either basically new ideas, or further development of ideas that have been presented by previous investigators but not fully expanded upon; and (3) results which differ from hypotheses presented in the literature.

Model results that are in agreement with current hypotheses concerning the hydrogeology of the carbonate-rock province are many. The major ones are as follows:

1. Ground water discharging from springs at Ash Meadows and Death Valley has its origin from multiple sources.
2. The Death Valley region is further divided into two individual flow subregions (or subsystems) by a north-south barrier through the western half of Pahute Mesa.
3. The White River subregion, part of the Colorado River region, is generally long and narrow and ex-

TABLE 7.--Simulated ground-water flow budgets of the five deep-flow regions,
in acre-feet per year

	Death Valley	Colorado River	Bonneville	Railroad Valley	Upper Humboldt River	Total within the modeled area
Recharge						
Mountain blocks	165,000	249,000	903,000	121,000	150,000	1,588,000
Head dependent boundaries	0	0	1,000	0	17,000	18,000
	-----	-----	-----	-----	-----	-----
Total recharge	165,000	249,000	904,000	121,000	167,000	1,606,000
Discharge						
Evapotranspiration	122,000	58,000	775,000	102,000	140,000	1,197,000
Regional springs	20,000	106,000	64,000	19,000	0	209,000
Seepage to lakes, rivers	0	48,000	65,000	0	27,000	140,000
Other boundaries	23,000	37,000	0	0	0	60,000
	-----	-----	-----	-----	-----	-----
Total discharge	165,000	249,000	904,000	121,000	167,000	1,606,000

tends from Butte Valley in the north to Lake Mead in the south.

4. Ground water discharging from the Muddy River springs, which is within the Colorado River region, is from multiple source areas and likely is isotopically diverse.

5. Ground water discharging at Fish Springs in Utah, which is within the Bonneville region, also has multiple source areas, but the primary source was simulated as the Deep Creek Range.

6. Little ground water discharges to the Great Salt Lake; rather, most is discharged in the Great Salt Lake Desert.

7. Railroad Valley is the terminus for ground-water flow within the Railroad Valley region, which encompasses valleys to the north and east of Railroad Valley.

Results dealing with new ideas or expanding on those ideas briefly discussed or results discussing controversial topics are extensive. The major conclusions include the following:

1. The northern boundary of the simulated Death Valley region extends northward beyond Cactus and Sarcobatus Flats. Recharge from the southern Monitor and Hot Creek Ranges might provide some flow to the Ash Meadows and Pahute Mesa-Oasis Valley flow systems.

2. Deep flow into Las Vegas Valley may be only from areas to the north (White River subregion). Recharge from the Spring Mountains to Las Vegas Valley occurs primarily in the upper model layer representing shallow flow, probably not more than 1,000 ft.

3. Recharge in mountain ranges in southwestern Utah may supply water that flows through carbonate rocks southward toward the Virgin River subregion, within the Colorado River region, where it is discharged to the river.

4. Deep flow from recharge areas in the Pavant Range and Tushar Mountains is toward the Sevier Desert, within the Bonneville region, where it is discharged as evapotranspiration in the vicinity of the Sevier River and Sevier Lake.

5. Discharge at Blue Lake springs, within the Bonneville region, may be primarily from the Deep Creek Range with lesser amounts from the Toana Range, Goshute Mountains, and the Antelope Range.

6. A discontinuous north-south-trending chain of metamorphic core complexes and low-permeability intrusive bodies that extends from the Grouse Creek Range near the Idaho border southward through the Toana, Deep Creek, and Snake Ranges may inhibit the eastward flow of ground water into the eastern half of the Bonneville region.

7. Discharge at Duckwater springs may be primarily from Newark Valley.

8. Evapotranspiration of ground water discharging from the upper Humboldt River region was simulated to be about 52,000 acre-ft/yr, and is small compared to the total estimated evapotranspiration along the river reported by other investigators.

The following results do not disregard results by other investigators but rather offer alternative explanations to the complex hydrogeology of the Great Basin:

1. The eastern boundary of the Ash Meadows flow system defined by previous investigators may be about 30 mi west of the Sheep Range in the Reville, Groom, and Pintwater or perhaps the Desert Ranges rather than in Pahrnagat Valley and the Sheep Range as suggested in previous studies.

2. The southern Hot Creek Range, perhaps the Monitor Range, and even the Pahute Mesa-Oasis Valley flow system may supply water to the springs discharging at Ash Meadows in the Death Valley region.

3. Ground-water flow to Las Vegas Valley may not be only from the Spring Mountains but also from deep flow from the Sheep Range and Tikaboo drainage basin, which includes areas as far north as the Grant Range. About 8,000 acre-ft/yr was simulated as ground-water flow from the north.

4. Ground-water flow in the White River sub-region, within the Colorado River region, was simulated from as far east as Utah. Recharge from the Wilson Creek Range, White Rock Mountains, and Indian Peak Range was simulated as draining into a highly transmissive zone in the lower model layer representing deep flow, then flowing southwest through Dry Lake Valley into the southern part of the White River subregion just south of Pahrnagat Valley.

Many of the above-mentioned differences result from varying interpretations of sparse hydrologic information throughout much of the area, in particular the uncertainty in the amount of recharge, and from the many assumptions used to simulate ground-water flow regions. As the demand for water increases in the study area, more detailed information that may or may not resolve these uncertainties needs to be collected.

REFERENCES CITED

- Anderson, R.E., and Laney, R.L., 1975, The influence of late Cenozoic stratigraphy on distribution of impoundment-related seismicity at Lake Mead, Nevada-Arizona: U.S. Geological Survey Journal of Research, v. 3, no. 3, p. 333-343.
- Arnold, Ted, 1984, Water-level and water-quality changes in Great Salt Lake, Utah, 1847-1983: U.S. Geological Survey Circular 913, 22 p.
- Bedinger, M.S., Harrill, J.R., and Thomas, J.M., 1984, Maps showing ground-water units and withdrawal, Basin and Range

- province, Nevada: U.S. Geological Survey Water-Resources Investigations Report 83-4119-A, 10 p., 2 plates.
- Bedinger, M.S., Sargent, K.A., and Langer, W.H., 1989, Studies of geology and hydrology in the Basin and Range province, southwestern United States, for isolation of high-level radioactive waste—Characterization of the Death Valley region, Nevada and California: U.S. Geological Survey Professional Paper 1370-F, 49 p.
- 1990, Studies of geology and hydrology in the Basin and Range province, southwestern United States, for isolation of high-level radioactive waste—Characterization of the Bonneville region, Utah and Nevada: U.S. Geological Survey Professional Paper 1370-G, 38 p.
- Blankennagel, R.K., and Weir, J.E., Jr., 1973, Geohydrology of the eastern part of Pahute Mesa, Nevada Test Site, Nye County, Nevada: U.S. Geological Survey Professional Paper 712-B, 35 p.
- Bolke, E.L., and Sumsion, C.T., 1978, Hydrologic reconnaissance of the Fish Springs Flat area, Tooele, Juab, and Millard Counties, Utah: Utah Department of Natural Resources Technical Publication 64, 30 p.
- Brenner, I.S., 1974, A surge of maritime tropical air—Gulf of California to the southwestern United States: *Monthly Weather Review*, v. 102, p. 375-389.
- Bunch, R.L., and Harrill, J.R., 1984, Compilation of selected hydrologic data from the MX missile-siting investigation, east-central Nevada and western Utah: U.S. Geological Survey Open-File Report 84-702, 123 p.
- Carlton, S.M., 1985, Fish Springs multibasin flow system, Nevada and Utah: Reno, University of Nevada, M.S. thesis., 78 p.
- Carpenter, Everett, 1915, Ground water in southeastern Nevada: U.S. Geological Survey Water-Supply Paper 365, 86 p.
- Carr, W.J., 1984, Regional structural setting of Yucca Mountain, southwestern Nevada, and late Cenozoic rates of tectonic activity in part of the southwestern Great Basin, Nevada and California: U.S. Geological Survey Open-File Report 84-854, 114 p.
- Claassen, H.C., 1983, Sources and mechanisms of recharge for ground water in the west-central Amargosa Desert, Nevada—A geochemical interpretation: U.S. Geological Survey Open-File Report 83-542, 66 p.
- Coney, P.J., 1980, Cordilleran metamorphic core complexes—An overview, in Crittenden, M.D., Jr., Coney, P.J., and Davis, G.K., eds., *Cordilleran metamorphic core complexes: Geological Society of America Memoir 153*, p. 7-31.
- Cordova, R.M., 1970, Ground-water conditions in southern Utah Valley and Goshen Valley, Utah: Utah Department of Natural Resources Technical Publication 28, 72 p.
- Cordova, R.M., and Subitzky, Seymour, 1965, Ground water in northern Utah Valley, Utah—A progress report for the period 1948-63: Utah State Engineer Technical Publication 11, 41 p.
- Dinwiddie, G.A., and Schroder, L.J., 1971, Summary of hydraulic testing in and chemical analyses of water samples from deep exploratory holes in Little Fish Lake, Monitor, Hot Creek, and Little Smoky Valleys, Nevada: U.S. Geological Survey Report USGS-474-90, 70 p. [Available only from National Technical Information Service, U.S. Department of Commerce, Springfield, VA 22161.]
- Eakin, T.E., 1960, Ground-water appraisal of Newark Valley, White Pine County, Nevada: Nevada Department of Conservation and Natural Resources, Ground-Water Resources-Reconnaissance Report 1, 33 p.
- 1961, Ground-water appraisal of Pine Valley, Eureka and Elko Counties, Nevada: Nevada Department of Conservation and Natural Resources, Ground-Water Resources-Reconnaissance Report 2, 41 p.
- 1962, Ground-water appraisal of Diamond Valley, Eureka and Elko Counties, Nevada: Nevada Department of Conservation and Natural Resources, Ground-Water Resources-Reconnaissance Report 6, 60 p.
- 1963, Ground-water appraisal of Pahrangat and Pahroc Valleys, Lincoln and Nye Counties, Nevada: Nevada Department of Conservation and Natural Resources, Ground-Water Resources-Reconnaissance Report 21, 36 p.
- 1964, Ground-water appraisal of Coyote Spring and Kane Spring Valleys and Muddy River Springs area, Lincoln and Clark Counties, Nevada: Nevada Department of Conservation and Natural Resources, Ground-Water Resources-Reconnaissance Report 25, 40 p.
- 1966, A regional interbasin ground-water system in the White River area, southeastern Nevada: Nevada Department of Conservation and Natural Resources, Water Resource Bulletin 33, 21 p.
- Eakin, T.E., Hughes, J.L., and Moore, D.O., 1967, Water-resources appraisal of Steptoe Valley, White Pine and Elko Counties, Nevada: Nevada Department of Conservation and Natural Resources, Water Resources-Reconnaissance Report 42, 48 p.
- Eakin, T.E., and Lamke, R.D., 1966, Hydraulic reconnaissance of the Humboldt River Basin, Nevada: Nevada Department of Conservation and Natural Resources, Water Resources Bulletin 32, 107 p.
- Eakin, T.E., Maxey, G.B., Robinson, T.W., Fredericks, J.C., and Loeltz, O.J., 1951, Contributions to the hydrology of eastern Nevada: Nevada State Engineer, Water Resources Bulletin 12, 171 p.
- Eakin, T.E., and Moore, D.O., 1964, Uniformity of discharge of Muddy River Springs, southeastern Nevada, and relation to interbasin movement of ground water, in *Geological Survey Research 1964*: U.S. Geological Survey Professional Paper 501-D, p. D171-D176.
- Eakin, T.E., Price, Don, and Harrill, J.R., 1976, Summary appraisals of the Nation's ground-water resources—Great Basin region: U.S. Geological Survey Professional Paper 813-G, 37 p.
- Eakin, T.E., Schoff, S.L., and Cohen, Phillip, 1963, Regional hydrology of a part of southern Nevada—A reconnaissance: U.S. Geological Survey Open-File Report TEI-833, 40 p.
- Eakin, T.E., and Winograd, I.J., 1965, Interbasin movement of ground water in south-central Nevada—Some implications, in *Abstracts for 1964: Geological Society of America Special Paper 82*, p. 52.
- Eaton, G.P., 1975, Characteristics of a transverse crustal boundary in the Basin and Range province of southern Nevada: *Geological Society of America Abstracts with Programs*, v. 7, no. 7, p. 1062.
- Eaton, G.P., Wahl, R.R., Prostka, H.J., Mabey, D.R., and Kleinkopf, M.D., 1978, Regional gravity and tectonic patterns: Their relation to late Cenozoic epeirogeny and lateral spreading in the western Cordillera, in Smith, R.B., and Eaton, G.P., eds., *Cenozoic tectonics and regional geophysics of the western Cordillera: Geological Society of America Memoir 152*, p. 51-92.
- Ekren, E.B., Bucknam, R.C., Carr, W.J., Dixon, G.L., and Quinlivan, W.D., 1976, East-trending structural lineaments in central Nevada: U.S. Geological Survey Professional Paper 986, 16 p.
- Ekren, E.B., Orkild, P.P., Sargent, K.A., and Dixon, G.L., 1977, Geologic map of the Tertiary rocks, Lincoln County, Nevada: U.S. Geological Survey Miscellaneous Investigations Series Map I-1041, scale 1:250,000.
- Fiero, G.W., Jr., 1968, Regional ground-water flow systems of central Nevada: University of Nevada, Desert Research Institute, Miscellaneous Report 5, 213 p.
- Frisbie, H.R., La Camera, R.J., Riek, M.M., and Wood, D.B., 1985,

- Water resources data, Nevada, water year 1984: U.S. Geological Survey Water-Data Report NV-84-1, 247 p.
- Gates, J.S., 1984, Hydrogeology of northwestern Utah and adjacent parts of Idaho and Nevada: Utah Geologic Association Publication 13, p. 239-248.
- Gates, J.S., and Krueger, S.A., 1981, Hydrologic reconnaissance of the southern Great Salt Lake Desert and summary of the hydrology of west-central Utah: Utah Department of Natural Resources Technical Publication 71, 55 p.
- Glancy, P.A., 1968, Water-resources appraisal of Butte Valley, Elko and White Pine Counties, Nevada: Nevada Division of Water Resources, Reconnaissance Report 49, 50 p.
- Glancy, P.A., and Van Denburgh, A.S., 1969, Water-resources appraisal of the Lower Virgin River Valley area, Nevada, Arizona, and Utah: Nevada Division of Water Resources, Reconnaissance Report 51, 87 p.
- Hardman, George, 1936, Nevada precipitation and acreages of land by rainfall zones: University of Nevada-Reno, Agriculture Experiment Station mimeograph paper, 10 p.
- , 1965, Nevada precipitation map: University of Nevada-Reno, Agriculture Experiment Station.
- Harrill, J.R., 1968, Hydrologic response to irrigation pumping in Diamond Valley, Eureka and Elko Counties, Nevada, 1950-65: Nevada Department of Conservation and Natural Resources, Water Resources Bulletin 35, 85 p.
- , 1976, Pumping and ground-water storage depletion in Las Vegas Valley, Nevada, 1955-74: Nevada Division of Water Resources, Bulletin 44, 70 p.
- , 1986, Ground-water storage depletion in Pahrump Valley, Nevada-California, 1962-75: U.S. Geological Survey Water-Supply Paper 2279, 53 p.
- Harrill, J.R., Gates, J.S., and Thomas, J.M., 1988, Major ground-water flow systems in the Great Basin region of Nevada, Utah, and adjacent states: U.S. Geological Survey Hydrologic Investigations Atlas HA-694-C.
- Harrill, J.R., Welch, A.H., Prudic, D.E., Thomas, J.M., Carman, R.L., Plume, R.W., Gates, J.S., and Mason, J.L., 1983, Aquifer systems in the Great Basin region of Nevada, Utah, and adjacent states—A study plan: U.S. Geological Survey Open-File Report 82-445, 49 p.
- Hess, J.W., and Mifflin, M.D., 1978, A feasibility study of water production from deep carbonate aquifers in Nevada: University of Nevada, Desert Research Institute Publication 41054, 125 p.
- Hildenbrand, T.G., and Kucks, R.P., 1982, A description of colored gravity maps of the Basin and Range province, southwestern United States: U.S. Geological Survey Open-File Report 82-500, 18 p.
- Hintze, L.F., 1973, Geologic map of Utah: Utah Geologic and Mineralogical Survey, scale 1:500,000.
- Holmes, W.R., 1984, Ground-water hydrology and projected effects of ground-water withdrawals in the Sevier Desert, Utah: Utah Department of Natural Resources Technical Publication 79, 54 p.
- Hood, J.W., and Price, Don, 1970, Hydrologic reconnaissance of Grouse Creek Valley, Box Elder County, Utah: Utah Department of Natural Resources Technical Publication 29, 54 p.
- Hood, J.W., Price, Don, and Waddell, K.M., 1969, Hydrologic reconnaissance of Rush Valley, Tooele County, Utah: Utah Department of Natural Resources Technical Publication 23, 63 p.
- Hood, J.W., and Rush, F.E., 1965, Water-resources appraisal of the Snake Valley area, Utah and Nevada: Nevada Department of Conservation and Natural Resources, Water Resources-Reconnaissance Report 34, 43 p.
- Hood, J.W., and Waddell, K.M., 1968, Hydrologic reconnaissance of Skull Valley, Tooele County, Utah: Utah Department of Natural Resources Technical Publication 18, 54 p.
- , 1969, Hydrologic reconnaissance of Deep Creek Valley, Tooele and Juab Counties, Utah, and Elko and White Pine Counties, Nevada: Utah Department of Natural Resources Technical Publication 24, 54 p.
- Houghton, J.G., 1967, Characteristics of rainfall in the Great Basin: University of Nevada Desert Research Institute, 205 p.
- Hubbs, C.L., and Miller, R.R., 1948, The Great Basin with emphasis on glacial and postglacial times, II—The zoological evidence: University of Utah Bulletin, v. 36, no. 20, p. 17-166.
- Hunt, C.B., and Robinson, T.W., 1960, Possible interbasin circulation of ground water in the southern part of the Great Basin: U.S. Geological Survey Professional Paper 400-B, p. 273-274.
- Hunt, C.B., Robinson, T.W., Bowles, W.A., and Washburn, A.L., 1966, Hydrologic basin, Death Valley, California: U.S. Geological Survey Professional Paper 494-B, 138 p.
- Jones, B.F., 1982, Mineralogy of fine grained alluvium from borehole U11G, expl. 1, northern Frenchman Flat area, Nevada Test Site: U.S. Geological Survey Open-File Report 82-765, 10 p.
- Kohler, M.A., Nordenson, T.J., and Baker, D.R., 1959, Evaporation maps for the United States: U.S. Department of Commerce, Weather Bureau Technical Paper 37, 13 p.
- Loeltz, O.J., 1960, Source of water issuing from springs in Ash Meadows Valley, Nye County, Nevada [abs.]: Geological Society of America Bulletin, v. 71, no. 12, part 2, p. 1917-1918.
- Lohman, S.W., 1972, Ground-water hydraulics: U.S. Geological Survey Professional Paper 708, 70 p.
- Malmberg, G.T., 1965, Available water supply of the Las Vegas ground-water basin, Nevada: U.S. Geological Survey Water-Supply Paper 1780, 116 p.
- Maxey, G.B., and Eakin, T.E., 1949, Ground water in White River Valley, White Pine, Nye, and Lincoln Counties, Nevada: Nevada State Engineer, Water Resources Bulletin 8, 59 p.
- Maxey, G.B., and Jameson, C.H., 1948, Geology and water resources of Las Vegas, Pahrump, and Indian Springs Valleys, Clark and Nye Counties, Nevada: Nevada State Engineer, Water Resources Bulletin 5, 292 p.
- McDonald, M.G., and Harbaugh, A.W., 1984, A modular three-dimensional finite-difference ground-water flow model: U.S. Geological Survey Open-File Report 83-875, 528 p.
- Meinzer, O.E., 1917, Geology and water resources of Big Smoky, Clayton, and Alkali Spring Valleys, Nevada: U.S. Geological Survey Water-Supply Paper 423, 167 p.
- Mendenhall, W.C., 1909, Some desert watering places in southeastern California and southwestern Nevada: U.S. Geological Survey Water-Supply Paper 224, 86 p.
- Mifflin, M.D., 1968, Delineation of ground-water flow systems in Nevada: University of Nevada, Desert Research Institute Technical Report H-W 4, 112 p.
- Mifflin, M.D., and Hess, J.W., 1979, Regional carbonate flow systems in Nevada, in Back, William, and Stephenson, D.A., eds., Contemporary hydrogeology, the George Burke Maxey memorial volume: Journal of Hydrology, v. 43, p. 217-237.
- Miller, G.A., 1977, Appraisal of the water resources of Death Valley, California-Nevada: U.S. Geological Survey Open-File Report 77-728, 68 p.
- Morgan, D.S., and Dettinger, M.D., (in press), Ground-water conditions in Las Vegas Valley, Clark County, Nevada—Part II, Geohydrology and simulation of ground-water flow: U.S. Geological Survey Open-File Report 90-179.
- Mower, R.W., and Cordova, R.M., 1974, Water resources of the Milford area, Utah, with special emphasis on ground water: Utah Department of Natural Resources Technical Publication

- 43, 105 p.
- Mower, R.W., and Feltis, R.D., 1968, Ground-water hydrology of the Sevier Desert, Utah: U.S. Geological Survey Water-Supply Paper 1854, 75 p.
- Nolan, T.B., 1943, The Basin and Range province in Utah, Nevada, and California: U.S. Geological Survey Professional Paper 197-D, 55 p.
- Plume, R.W., 1984, Use of aeromagnetic data to help define some properties of a carbonate-rock aquifer system in eastern Nevada: Geological Society of America, Abstracts with Programs, v. 16, no. 6, p. 624.
- Plume, R.W., and Carlton, S.M., 1988, Hydrogeology of the Great Basin region of Nevada, Utah, and adjacent states: U.S. Geological Survey Hydrologic Investigations Atlas HA-694-A.
- Rantz, S.E., 1972, Mean annual precipitation in California region: U.S. Geological Survey Open-File Map, scale 1:1,000,000.
- Razem, A.C., and Steiger, J.I., 1981, Ground-water conditions in Tooele Valley, Utah, 1976-78: Utah Department of Natural Resources Technical Publication 69, 95 p.
- ReMillard, M.D., Andersen, G.C., Birdwell, G.A., and Sandberg, G.W., 1986, Water resources data, Utah, water year 1985: U.S. Geological Survey Water-Data Report UT-85-1, 412 p.
- Remson, Irwin, Hornberger, G.M., and Molz, F.J., 1971, Numerical methods in subsurface hydrology: New York, Wiley-Interscience, 389 p.
- Roberts, R.J., 1964, Economic geology, mineral and water resources of Nevada: U.S. 88th Congress, 2d session, Senate Document 87, p. 39-48.
- 1966, Metallogenic provinces and mineral belts in Nevada, in AIME Pacific Southwest Mineral Industry Conference, Sparks, Nevada, 1965, Papers, part A: Nevada Bureau of Mines Report 13, p. 47-52.
- Rosenau, J.C., and Faulkner, G.L., 1974, An index to springs of Florida: Florida Department of Natural Resources, Bureau of Geology Map Series 63, 1 sheet.
- Rowan, L.C., and Wetlaufer, P.H., 1981, Relation between regional lineament systems and structural zones in Nevada: American Association of Petroleum Geologists Bulletin, v. 65, no. 8, p. 1414-1432.
- Rowley, P.D., Lipman, P.W., Mehnert, H.H., Lindsey, D.A., and Anderson, J.J., 1978, Blue Ribbon lineament, an east-trending structural zone within the Pioche Mineral Belt of southwestern Utah and eastern Nevada: U.S. Geological Survey Journal of Research, v. 6, no. 2, p. 175-192.
- Rush, F.E., 1964, Ground-water appraisal of the Meadow Valley area, Lincoln and Clark Counties, Nevada: Nevada Department of Conservation and Natural Resources, Ground-Water Resources-Reconnaissance Report 27, 43 p.
- 1968a, Water-resources appraisal of Thousand Springs Valley, Elko County, Nevada: Nevada Division of Water Resources, Reconnaissance Report 47, 61 p.
- 1968b, Water-resources appraisal of the Lower Moapa-Lake Mead area, Clark County, Nevada: Nevada Division of Water Resources, Reconnaissance Report 50, 66 p.
- 1968c, Index of hydrographic areas in Nevada: Nevada Division of Water Resources, Information Report 6, 38 p.
- 1970, Regional ground-water systems in the Nevada Test Site area, Nye, Lincoln, and Clark Counties, Nevada: Nevada Division of Water Resources, Reconnaissance Report 54, 25 p.
- 1974, Static ground-water levels of Nevada: Nevada Division of Water Resources map, scale 1:750,000, 1 sheet.
- Rush, F.E., and Eakin, T.E., 1963, Ground-water appraisal of Lake Valley in Lincoln and White Pine Counties, Nevada: Nevada Department of Conservation and Natural Resources, Ground-Water Resources-Reconnaissance Report 24, 29 p.
- Rush, F.E., and Everett D.E., 1964, Ground-water appraisal of Monitor, Antelope, and Kobeh Valleys, Nevada: Nevada Department of Conservation and Natural Resources, Ground-Water Resources-Reconnaissance Report 30, 42 p.
- 1966a, Water-resources appraisal of the Huntington Valley area, Elko and White Pine Counties, Nevada: Nevada Department of Conservation and Natural Resources, Water Resources-Reconnaissance Report 35, 37 p.
- 1966b, Water-resources appraisal of Little Fish Lake, Hot Creek, and Little Smoky Valleys, Nevada: Nevada Department of Conservation and Natural Resources, Water Resources-Reconnaissance Report 38, 38 p.
- Rush, F.E., and Kazmi, S.A.T., 1965, Water resources appraisal of Spring Valley, White Pine and Lincoln Counties, Nevada: Nevada Department of Conservation and Natural Resources, Water Resources-Reconnaissance Report 33, 36 p.
- Salts, R.W., 1984, A description of colored gravity and terrain maps of the southwestern Cordillera: U.S. Geological Survey Open-File Report 84-95, 16 p.
- Sandberg, G.W., and Sultz, L.G., 1985, Reconnaissance of the quality of surface water in the Upper Virgin River Basin, Utah, Arizona, and Nevada, 1981-82: Utah Department of Natural Resources Technical Publication 83, 69 p.
- Shane, D.R., and Stewart, J.H., 1976, Ore deposits as related to tectonics and magnetism, Nevada and Utah: American Institute of Metallurgical and Petroleum Engineers Transactions, v. 260, p. 225-232.
- Stewart, J.H., 1980, Geology of Nevada—A discussion to accompany the geologic map of Nevada: Nevada Bureau of Mines and Geology Special Publication 4, 136 p.
- Stewart, J.H., and Carlson, J.E., 1978, Geologic map of Nevada: U.S. Geological Survey, scale 1:500,000.
- Stewart, J.H., Moore, W.J., and Zietz, Isidore, 1977, East-west patterns of Cenozoic igneous rocks, aeromagnetic anomalies, and mineral deposits, Nevada and Utah: Geological Society of America Bulletin, v. 88, p. 67-77.
- Stewart, J.H., Walker, G.W., and Kleinhampl, F.J., 1975, Oregon-Nevada lineament: Geology, v. 3, no. 5, p. 265-268.
- Sumsion, C.T., and others, 1976, Ground-water conditions in Utah, spring of 1976: Utah Division of Water Resources Cooperative Investigations Report 15, 69 p.
- Thomas, J.M., Mason, J.L., and Crabtree, J.D., 1986, Ground-water levels in the Great Basin of Nevada, Utah, and adjacent states: U.S. Geological Survey Hydrologic Investigations Atlas HA-694-B.
- U.S. Bureau of the Census, 1913, Population—1910, v. 3: Washington, D.C., U.S. Government Printing Office.
- 1922, Census of population—1922, v. 3: Washington, D.C., U.S. Government Printing Office.
- 1952, Census of population—1950, v. 2, part 28: Washington, D.C., U.S. Government Printing Office.
- 1983, Census of population—1980, v. 1, chapter A, part 1: Washington, D.C., U.S. Government Printing Office.
- U.S. Department of Commerce, 1985, Provisional estimates of the population of counties—July 1, 1984: Bureau of the Census, Current Population Reports, Local Population Estimates, Series P-26, no. 84-52C, 23 p.
- U.S. Weather Bureau, 1963, Normal annual precipitation, normal May-September precipitation, 1931-1960, State of Utah: Utah State Engineer map, scale 1:500,000.
- 1965, Mean annual precipitation, 1930-57, State of Idaho: U.S. Soil Conservation Service in cooperation with the U.S. Weather Bureau.
- Van Denburgh, A.S., and Rush, F.E., 1974, Water resources appraisal of Railroad and Penoyer Valleys, east-central Nevada:

- Nevada Division of Water Resources, Reconnaissance Report 60, 61 p.
- Waddell, R.K., 1982, Two-dimensional steady-state model of ground-water flow, Nevada Test Site and vicinity, Nevada-California: U.S. Geological Survey Water-Resources Investigations Report 82-4085, 72 p.
- Waddell, R.K., Robison, J.H., and Blankennagel, R.K., 1984, Hydrology of Yucca Mountain and vicinity, Nevada-California—Investigative results through mid-1983: U.S. Geological Survey Water-Resources Investigations Report 84-4267, 72 p.
- Watson, Phil, Sinclair, Peter, and Waggoner, Ray, 1976, Quantitative evaluation of a method for estimating recharge to the desert basins of Nevada: *Journal of Hydrology*, v. 31, p. 335-357.
- Welch, A.H., and Thomas, J.M., 1984, Aqueous geochemistry and isotope hydrology of the White River system, eastern Nevada: *Geological Society of America Abstracts with Programs*, v. 16, no. 6, p. 689.
- Wernicke, Brian, Guth, P.L., and Axen, G.J., 1984, Tertiary extension in the Sevier thrust belt of southern Nevada: 97th Annual Meeting, Geological Society of America, Reno, Nev., November 1984, Field-Trip Guidebook, v. 4, p. 473-510.
- Williamson, A.L., Prudic, D.E., and Swain, L.A., 1989, Ground-water flow in the Central Valley, California: U.S. Geological Survey Professional Paper 1401-D, 127 p.
- Winograd, I.J., 1962, Interbasin movement of ground water at the Nevada Test Site, Nevada, in *Short papers in geology, hydrology, and topography*: U.S. Geological Survey Professional Paper 450-C, p. 108-111.
- 1963, A summary of the ground-water hydrology of the area between the Las Vegas Valley and the Amargosa Desert, Nevada, with special reference to the effects of possible new withdrawals of ground water: U.S. Geological Survey Open-File Report TEI-840, 79 p.
- 1971, Hydrogeology of ash-flow tuff: A preliminary statement: *Water Resources Research*, v. 7, no. 4, p. 994-1006.
- Winograd, I.J., and Eakin, T.E., 1965, Interbasin movement of ground-water in south-central Nevada—The evidence, in *Abstracts for 1964*: Geological Society of America Special Paper 82, p. 227.
- Winograd, I.J., and Friedman, Irving, 1972, Deuterium as a tracer of regional ground-water flow, southern Great Basin, Nevada and California: *Geological Society of America Bulletin*, v. 83, no. 12, p. 3691-3708.
- Winograd, I.J., and Pearson, F.J., Jr., 1976, Carbon 14 anomaly in a regional carbonate aquifer: Possible evidence for megascale channeling, south-central Great Basin: *Water Resources Research*, v. 12, no. 6, p. 1125-1143.
- Winograd, I.J., and Szabo, B.J., 1986, Water-table decline in the south-central Great Basin during the Quaternary period: Implications for toxic-waste disposal: U.S. Geological Survey Open-File Report 85-697, 18 p.
- Winograd, I.J., and Thordarson, William, 1968, Structural control of ground-water movement in miogeosynclinal rocks of south-central Nevada, in Eckel, E.B., ed., *Nevada Test Site: Geological Society of America Memoir 110*, p. 35-48.
- 1975, Hydrogeologic and hydrochemical framework, south-central Great Basin, Nevada-California, with special reference to the Nevada Test Site: U.S. Geological Survey Professional Paper 712-C, 126 p.

USGS LIBRARY-RESTON



3 1818 00069787 8